Large deviations for the local time of a jump diffusion with two sided reflections

Giovanni Zoroddu

A Thesis

in

The Department

of

Mathematics and Statistics

Presented in Partial Fulfillment of the Requirements

for the Degree of Master of Arts (Mathematics) at

Concordia University

Montreal, Quebec, Canada

August 2018

©Giovanni Zoroddu, 2018

CONCORDIA UNIVERSITY

School of Graduate Studies

This is to certify that the thesis prepared

By: Giovanni Zoroddu

Entitled: Large deviations for the local time of a jump diffusion with two sided reflections

and submitted in partial fulfillment of the requirements for the degree of

Master of Arts (Mathematics)

complies with the regulations of the University and meets the accepted standards with respect to originality and quality.

Signed by the final Examining Committee:

_____ Chair

Dr. Cody Hyndman

_____ Examiner

Dr. Xiaowen Zhou

_____ Supervisor

Dr. Lea Popovic

Approved by _____

Chair of Department or Graduate Program Director

_____ 2018 _____

Dean of Faculty

Abstract

Let X be a jump diffusion, then its reflection at the boundaries 0 and $b > 0$ forms the process V. The amount by which V must reflect to stay within its boundaries is added to a process called the local time. This thesis establishes a large deviation principle for the local time of a reflected jump diffusion. Upon generalizing the notion of the local time to an additive functional, we establish the desired result through a Markov process argument. By applying Ito's formula to a suitably chosen process M and in proving that M is a martingale, we find its associated integro-differential equation. M can then be used to find the limiting behavior of the cumulant generating function which allows the large deviation principle to be established by means of the Gärtner-Ellis theorem. These theoretical results are then illustrated with two specific examples. We first find analytical results for these examples and then test them in a Monte Carlo simulation study and by numerically solving the integro-differential equation.

Acknowledgements

This thesis would not have been possible without the help of Dr. Lea Popovic. Her patience and thoroughness in answering all my questions, no matter how small, have been invaluable at every stage of this process. I am truly grateful for her guidance throughout this degree.

I would also like to thank the other committee members, Dr. Cody Hyndman and Dr. Xiaowen Zhou, for taking time out of their schedules to be on the examinations committee. Their feedback has been greatly appreciated.

I am indebted to my parents whose never ending support and encouragement has allowed me to keep pursuing my dreams. They believed in me at the toughest times and continue to be a source of inspiration. Finally, I thank Luzia, with whom I have shared all the ups and downs of the last two years. She is my motivation, my best friend and the other half of my life.

Contents

List of Figures

List of Tables

Chapter 1

Introduction

1.1 Motivation

A diffusion process can be thought of as a strong Markov process, where common intuition restates this as a process in which the past cannot help in predicting the future. As our central object of study, we will be considering jump diffusions with jumps of bounded variation. The paths of this process will be reflected at two boundaries and the resulting process will be studied.

In 1961, A.V. Skorokhod proposed taking an Itô diffusion and reflecting it at a single boundary. In his original papers [23, 24], he studied the paths of such a process, proved its existence and uniqueness and derived an equation for the solution. Since then, solving stochastic differential equations with reflecting boundaries has become ubiquitous with the label of a Skorokhod problem.

For the purposes of this thesis, we are concerned with reflections at two boundaries of a single càdlàg process in $\mathbb{R}$. In this light, we formally present the Skorokhod problem as shown in [1]:

Given a càdlàg process $\{X(t)\}$ and continuous, non-decreasing and adapted processes $\{L(t)\}$ and $\{U(t)\}$, we say the triple $(\{V(t)\}, \{L(t)\}, \{U(t)\})$ of processes is the solution to the **Skorokhod problem** on $[0, b]$ if

$$V(t) = V(0) + X(t) + L(t) - U(t) \in [0, b]$$

for all t and

$$\int_0^\infty V(t)dL(t) = 0 \text{ and } \int_0^\infty (b - V(t))dU(t) = 0.$$

Existence and uniqueness follow from the general work of [17].

It is important to note that we will not be studying solutions to the Skorokhod problem, rather we will be primarily concerned with the boundary local time of the reflected process V. In 1948 [16], P. Lévy introduced Brownian local time, which can be intuitively thought of as the amount of time spent by a Brownian motion at a certain level in space. When we consider reflected processes, the boundary local time comes to represent the amount that must be added in order to make the process reflect. The local time is a process in its own right for which we will study its large deviation behavior.

The theory of large deviations was unified by Varadhan in 1966 [25], previously having been used as sparse techniques in insurance mathematics. The central question asked by the theory relates to the asymptotic rate of decay for probabilities of rare events. An event is rare if it deviates from its mean in excess of what the central limit theorem purports, that is, a *large* deviation. Traditionally, the sequences were independent and identically distributed but due to R. S. Ellis and J. Gärtner [6, 8], the theory was extended to include Markovian processes for which a suitable limit to the cumulant generating function could be established.

The main result of the present thesis extends the previous works related to large deviations for the boundary local time of reflected processes in [7, 11, 1]. The first reference provided an explicit form for the rate function of a reflected standard Brownian motion and the second and third references establish a large deviation principle for reflected diffusions and reflected Lévy processes, respectively. They employ the Markov process argument which we use for reflected jump diffusions.

Reflected processes have a number of applications whenever one assumes a certain capacity, either minimal or maximal inherent in a model. One need not think too long to imagine a context with some finite capacity to it, such as a queue with a maximum length, networks with a finite buffer or when monetary authorities attempt to target specific zones for macroeconomic purposes. A list of references to such models are provided in the introductions to the above mentioned articles. From a practitioner's perspective, we are primarily concerned

with the probability of a rare overflow or underflow event occurring.

1.2 Thesis Outline

This thesis is structured into four main components and a conclusion. After considering the present introduction:

Chapter 2 lists those mathematical preliminaries that were considered most relevant to the following chapters, either as a direct application or to build up the theory behind some of the topics. An effort was made to be as efficient in this as possible, oftentimes choosing a less general presentation in favor of direct applicability.

Chapter 3 is the main portion of this thesis. It begins by setting up the model and then presents some small computational results necessary for the following sections. We then present the main proof followed by some analytical considerations and conclude the section with the result implied by this thesis' title. The last part of the chapter presents examples for which analytical solutions may be reached. We use these solutions in the following chapter as a way to verify the simulations.

Finally, Chapter 4 puts the theory into practice. Two algorithms are studied as possible practical implementations of the previous chapter's theoretical results. One algorithm achieves the results through a Monte Carlo simulation and the other by numerically solving the integro-differential equation of Chapter 3. We then consider the same examples mentioned in the previous chapter to study the effectiveness of the algorithms in computing the correct results.

Chapter 2

Mathematical Preliminaries

2.1 Stochastic Analysis

Stochastic analysis allows for a theory of integration to be defined with respect to stochastic processes. In doing so a calculus on stochastic processes can be developed similar to the more traditional calculus. In this section, we collect a list of classic definitions and results which will serve as the foundations for the analysis conducted in Chapter 3. Much of what is written here can be found in [20], albeit in greater generality. The second subsection lists some topics that play less of a background role and for which a bit more care in their exposition was deemed necessary.

2.1.1 Preliminaries for Stochastic Analysis

Throughout this thesis, we will assume a complete probability space $(\Omega, \mathcal{F}, \mathbb{P})$, where Ω is the sample space, $\mathcal{F}$ is the filtration and $\mathbb{P}$ is the probability measure. We say that a stochastic process X on $(\Omega, \mathcal{F}, \mathbb{P})$ is **adapted** if $X(t) \in \mathcal{F}_t$ and a random variable $\tau : \Omega \to [0, \infty]$ is a **stopping time** if the event $\{\tau \leq t\} \in \mathcal{F}_t$, for every t.

Finally, we refer to a stochastic process X as being **càdlàg** if it has sample paths which are right continuous, with left limits or as being **càglàd** if the sample paths are left continuous, with right limits. The notation $\mathcal{P}$ denotes the set of all partitions on $[0, t]$, where $0 = t_0 < t_1 < ... < t_{n-1} < t_n = t$, with $\{t_i\}_{i=1,...,n}$ denoting a partition on the interval $[0, t]$. We begin

in familiar territory, with a discussion of the continuous time martingale.

Definition 2.1.1. A real-valued, adapted process $M = (M(t))_{0\leq t<\infty}$ is called a **martingale** with respect to $(\mathcal{F}_t)_{0\leq t\leq\infty}$ if

(i) $\mathbb{E}[|M(t)|] < \infty$, and

(ii) if $s \leq t$, then $\mathbb{E}[M(t)|\mathcal{F}_s] = M(s)$, a.s.

This process allows one to establish the future expectation as the current state of the process. As an immediate consequence of the martingale property, we may establish the following two properties:

(i) $\mathbb{E}[M(t)] = \mathbb{E}[\mathbb{E}[M(t)|\mathcal{F}_0]] = \mathbb{E}[M(0)]$;

(ii) if $M(t) - M(0)$ is a martingale then so is $M(t)$.

Definition 2.1.2. An adapted, càdlàg process Y is a **local martingale** if there exists a sequence of increasing stopping times, τ_n, with $\lim_{n\to\infty} \tau_n = \infty$ a.s. such that $Y(t \wedge \tau_n)\mathbf{1}_{\{\tau_n>0\}}$ is a martingale for each n.

Clearly any martingale is always a local martingale, but the converse is not true in general. A local martingale generalizes the notion of the martingale to processes that exhibit the martingale property just at stopping times. We state the following two lemmas for use later.

Lemma 2.1.1. *The sum of two local martingales is a local martingale.*

Lemma 2.1.2. *Every bounded local martingale is a martingale.*

Definition 2.1.3. Let $A = (A(t))_{t\geq 0}$ be a càdlag process and let $\mathcal{P}$ denote the set of all partitions on $[0, \infty)$. A is called a **finite variation process** if for almost all paths of A, $\sup_{\mathcal{P}} \sum_{i=0}^{n-1} |A(t_{i+1}) - A(t_i)| < \infty$.

The term $\sup_{\mathcal{P}} \sum_{i=0}^{n-1} |A(t_{i+1}) - A(t_i)|$ is the *total variation* of the process. Clearly Brownian motion, which is nowhere differentiable due to its self similarity on every time interval, does not satisfy this property. However, the Poisson process which has finitely many jumps on any finite time interval and is constant otherwise, does.

The sum of finite variation processes on $[0,t]$ is of finite variation. To show this, consider càdlàg processes A, B, then for $A+B$,

$$\begin{aligned}\sup_{\mathcal{P}} \sum_{i=0}^{n-1} |(A+B)(t_{i+1}) - (A+B)(t_i)| &= \sup_{\mathcal{P}} \sum_{i=0}^{n-1} |A(t_{i+1}) - A(t_i) + B(t_{i+1}) - B(t_i)| \\ &\leq \sup_{\mathcal{P}} \sum_{i=0}^{n-1} |A(t_{i+1}) - A(t_i)| + |B(t_{i+1}) - B(t_i)| \\ &< \infty\end{aligned}$$

This idea of finite variation paths would be required to define a stochastic integral in terms of the Riemann-Stieltjes integral, so that the sums converge. As many random processes are not of finite variation, the Riemann-Stieltjes integral is a poor candidate for the stochastic integral.

Definition 2.1.4. Let A be an adapted finite variation process and Y a local martingale, then we call X a **semimartingale** if it can be decomposed as $X = Y + A$.

The semimartingale is introduced as it encompasses a sufficiently large class of processes from which a good integrator may be chosen for the purposes of defining a stochastic integral.

Lemma 2.1.3. *Let X, Y be two semimartingales. Then $X+Y$ and XY are semimartingales.*

Definition 2.1.5. Let X be a semimartingale. For a partition $\{t_i\}$, we define the **quadratic variation** of X as

$$[X]_t = \lim_{\max |t_{i+1} - t_i| \to 0} \sum_{i=0}^{n-1} (X(t_{i+1}) - X(t_i))^2,$$

where the limit is in probability.

Definition 2.1.6. Let X and Y be semimartingales. For a partition $\{t_i\}$, we define the **quadratic covariation** of X and Y as

$$[X,Y]_t = \lim_{\max |t_{i+1} - t_i| \to 0} \sum_{i=0}^{n-1} (X(t_{i+1}) - X(t_i))(Y(t_{i+1}) - Y(t_i)),$$

where the limit is in probability.

These last two definitions provide another way of measuring the variation in a process or between two processes. They give a sense of how controlled the process is, in the sense that if the total variation is unbounded, the sum of the differences squared may be finite and provide some useful information as to the dispersion of the process. But if it is not, then the process is truly unbounded in its fluctuations.

Definition 2.1.7. A process $H = (H(t))_{t\geq 0}$ is said to be **predictable** if H is measurable with respect to the smallest $\sigma-$algebra generated by all adapted processes with càglàd paths.

Being measurable with respect to càglàd paths means that the process' current value is known from the information just before the current time. For example, since standard Brownian motion is continuous in time we may establish that $W(t) = \lim_{s\to t-} W(s)$, and so it is a predictable process. Since one cannot know when a Poisson process will jump, it is not a predictable process.

Definition 2.1.8. Let H be an adapted predictable process and let X be a semimartingale. Let $0 = \tau_0^n \leq \tau_1^n \leq ... \leq \tau_k^n < \infty$ be a random partition of finite stopping times with $\lim_{n\to\infty} \sup_k \tau_k^n = \infty$. Then the **stochastic integral** of H with respect to X is

$$\int_0^t H(s-)dX(s) = \lim_{\sup_k |\tau_{k+1}^n - \tau_k^n| \to 0} \sum_{i=0}^{n-1} H(\tau_i^n)(X(t\wedge\tau_{i+1}^n) - X(t\wedge\tau_i^n)),$$

where the limit is in probability.

Having the limit converge in probability ensures that as the partition gets smaller, the probability of all paths whose sum does not converge, tends to zero. This allows for processes with paths of unbounded variation to have a well defined integral.

To conclude this subsection, we present the following quick lemma which will be useful later.

Lemma 2.1.4. *Let B be a standard Brownian motion, then every local martingale Y has a representation $Y(t) = Y(0) + \int_0^t H(s)dB(s)$, where H is predictable.*

2.1.2 Definitions and Results

Ito's Two Dimensional Formula

We present the following theorem as the two dimensional version of the more general d-dimensional Itô formula. It will prove to be the starting point in establishing the large deviation result.

Theorem 2.1.1. ***(Itô's formula)*** *Let X_1 and X_2 be two semimartingales, and let $f : \mathbb{R}^2 \to \mathbb{R}$ have twice continuously differentiable partial derivatives in space and once in time. Then $f(t, X_1, X_2)$ is a semimartingale and the following formula holds:*

$$\begin{aligned} f(t, X_1(t), X_2(t)) - f(0, X_1(0), X_2(0)) \\ &= \int_0^t \dot{f}(s-, X_1(s-), X_2(s-))ds \\ &+ \sum_{i=1}^{2} \int_0^t f_i(s-, X_1(s-), X_2(s-))dX^{(c,i)}(s) \\ &+ \frac{1}{2} \sum_{1 \le i,j \le 2} \int_0^t f_{i,j}(s-, X_1(s-), X_2(s-))d[X^i, X^j]_s^c \\ &+ \sum_{0<s\le t} [f(s, X_1(s), X_2(s)) - f(s-, X_1(s-), X_2(s-))] \end{aligned}$$

where the superscript c denotes the continuous part of the semimartingale.

Itô's formula, or commonly known as the chain rule of stochastic calculus, is a fundamental result in that it allows for a wide range of applications like finding differentials of functions of stochastic processes or finding solutions to stochastic integrals. The application this thesis will be interested in is deriving the conditions under which a certain process is a martingale.

The Compensator

Definition 2.1.9. A finite variation process A with $A_0 = 0$ is of **integrable variation** if the expected total variation is finite.

Definition 2.1.10. Let X be a càdlàg adapted process and let A be a predictable finite variation process, with $A_0 = 0$. We say that A is the **compensator** of X if $X - A$ is a local martingale.

In a sense, subtracting the compensator allows one to remove the drift from a process and be left with a (local) martingale. For the purpose of building intuition, consider the discrete case where X is decomposable into the sum of a martingale M and a predictable process A, that is $X = M + A$.

By the definition of the martingale,

$$\begin{aligned}
&\mathbb{E}[X(n) - A(n)|\mathcal{F}_{n-1}] = \mathbb{E}[M(n)|\mathcal{F}_{n-1}] = M(n-1) = X(n-1) - A(n-1) \\
\iff &A(n) = \mathbb{E}[X(n) - X(n-1)|\mathcal{F}_{n-1}] + A(n-1) \\
\iff &A(n) = \mathbb{E}[X(n) - X(n-1)|\mathcal{F}_{n-1}] + \mathbb{E}[X(n-1) - X(n-2)|\mathcal{F}_{n-2}] + A(n-2) \\
\iff &A(n) = \cdots \\
\iff &A(n) = \sum_{k=1}^{n} \mathbb{E}[X(k) - X(k-1)|\mathcal{F}_{k-1}]
\end{aligned}$$

From this, we may develop a possible way to compute the continuous time compensator by taking the limit of a discretization over ever smaller steps. That is, consider a stochastic partition $0 = \tau_0 \leq \tau_1 \leq \tau_2 \leq ...$ of stopping times with $\lim_{i\to\infty} \tau_i = \infty$. Since, by definition, $X - A$ is a local martingale, we have that $(X(t \wedge \tau_i) - A(t \wedge \tau_i))\, \mathbf{1}_{\{\tau_i > 0\}}$ is a martingale for each i. Therefore,

$$\begin{aligned}
&\mathbf{1}_{\{\tau_{i-1}<t\}}\mathbb{E}[(X(\tau_i) - A(\tau_i))\,|\mathcal{F}_{\tau_{i-1}}] = \mathbf{1}_{\{\tau_{i-1}<t\}}\,(X(\tau_{i-1}) - A(\tau_{i-1})) \\
\iff &\mathbf{1}_{\{\tau_{i-1}<t\}}\mathbb{E}[(X(\tau_i) - X(\tau_{i-1}))\,|\mathcal{F}_{\tau_{i-1}}] + \mathbf{1}_{\{\tau_{i-1}<t\}}A(\tau_{i-1}) = \mathbf{1}_{\{\tau_{i-1}<t\}}A(\tau_i) \\
\iff &... \\
\iff &\sum_{n=1}^{\infty} \mathbf{1}_{\{\tau_{n-1}<t\}}\mathbb{E}[(X(\tau_n) - X(\tau_{n-1}))\,|\mathcal{F}_{\tau_{n-1}}] = \mathbf{1}_{\{\tau_{i-1}<t\}}A(\tau_i)
\end{aligned}$$

Finally, taking the limit as this partition goes to zero, we arrive at the following result.

Theorem 2.1.2. *Let X be a cadlag adapted process with integrable total variation and let*

A be its compensator. Define an increasing stochastic partition $0 = \tau_0 \leq \tau_1 \leq \tau_2 \leq ...$ *with* $\lim_{i\to\infty} \tau_i = \infty$*, then*

$$\lim_{\sup_n |\tau_n - \tau_{n-1}| \to 0} \sum_{n=1}^{\infty} \mathbf{1}_{\{\tau_{n-1} < t\}} \mathbb{E}[X(\tau_n) - X(\tau_{n-1}) | \mathcal{F}_{\tau_{n-1}}] = A.$$

The Local Time

In this thesis, we study the local time at the boundaries of a reflected jump diffusion. Informally, a local time can be thought of as the amount of time a process spends at a certain level in space. When the process being studied is reflected, the boundary local time takes on an additional interpretation in that it comes to represent the amount necessary to push the process in order to keep it within its boundaries. The local time is connected directly to the occupation measure, which we define first. The following definitions may be found in [2].

Definition 2.1.11. Let X be a semimartingale, for every $t > 0$, the **occupation measure** on the time interval $[0, t]$ is the measure μ_t given for every measurable function $f : \mathbb{R} \to [0, \infty)$ by

$$\int_{\mathbb{R}} f(x)\mu_t(dx) = \int_0^t f(X(s))ds.$$

The occupation measure is quite general. However, we may specify a particular density for it, namely $L^x(t)$, which we define below.

Definition 2.1.12. The **local time** $L^x(t)$ is defined as

$$L^x(t) = \lim_{\varepsilon \to 0+} \frac{1}{2\varepsilon} \int_0^t \mathbf{1}_{\{|X(s)-x|<\varepsilon\}} ds$$

uniformly on compact intervals of time, for every $x \in \mathbb{R}$.

By consequence of being uniformly compact, we see the property that the local time is continuous in t. This definition illustrates two other important properties, that the local time is nondecreasing, cumulating strictly when $|X(s) - x| < \varepsilon$, and how it represents the amount of time the process X spends in that vanishing neighborhood of x. Furthermore, we see the connection between the occupation measure and the local time through the *occupation*

density formula,

$$\int_0^t f(X(s))ds = \int_{\mathbb{R}} f(x)L^x(t)dx$$

which holds for all measurable bounded functions $f \geq 0$.

Going forward, we will be studying the local times at the upper and lower boundaries of a reflected process. In this context, it will be convenient to denote each local time uniquely. Therefore, throughout the remainder of the thesis, we denote the local time at the lower boundary of 0 as $L^0(t) = L(t)$ and the local time at the upper boundary of $b > 0$ as $L^b(t) = U(t)$.

We conclude with a final definition reproduced from [1], which will allow us to generalize the main result of this thesis from that of a local time to an occupation time from which the local times may be derived.

Definition 2.1.13. The process $\Lambda = (\Lambda(t) : t \geq 0)$ is an **additive functional** of X if it can be represented as $\Lambda(t) = g_t(X(u) : 0 \leq u \leq t)$ where

$$g_{t+s}(X(u) : 0 \leq u \leq t+s) = g_s(X(u) : 0 \leq u \leq s) + g_t(X(s+u) : 0 \leq u \leq t).$$

Note that the *occupation time* $\int_0^t f(X(s))ds$ is an additive functional since by a change of variables

$$\begin{aligned}\int_0^s f(X(u))du + \int_0^t f(X(s+u))du &= \int_0^s f(X(u))du + \int_s^{t+s} f(X(u))du \\ &= \int_0^{t+s} f(X(u))du.\end{aligned}$$

2.2 Large Deviations

The study of large deviations is concerned with the rate at which probabilities of rare events decay. Naturally, if we consider the probability that a process deviates from its mean by more than a *normal* amount for a prolonged period of time, we would expect this quantity to go to zero. The question large deviations theory asks is, at what rate does this happen?

To make the concept of *normal* a little more precise, we know that by the Ergodic

theorem that the $\lim_{t\to\infty} \frac{1}{t}\int_0^t F(V(s))ds = \int_{\mathbb{R}} F(v)\pi(dv)$, where π is the stationary distribution for some ergodic process V. That is, for large t, $\frac{1}{t}\int_0^t F(V(s))ds$ is well approximated by its expected value. Furthermore, by the Functional Central Limit theorem $\lim_{t\to\infty} \frac{1}{\sigma\sqrt{t}}\left(\int_0^t F(V(s))ds - \int_{\mathbb{R}} F(v)\pi(dv)\right) = G(t)$ where $G(t)$ is a standard Gaussian process. From this we may see that $\int_0^t F(V(s))ds$ deviates from its mean by an amount of order $\sqrt{t}$, where deviations smaller than $\sqrt{t}$ can be described by its variance, σ^2. These deviations are considered normal and deviations in excess of $\sqrt{t}$ are considered *large*.

Most of what follows in this subsection may be found in [13, 5].

2.2.1 Preliminaries for Large Deviations

In this short subsection, we simply list some elementary facts that will be useful in our discussion for Chapter 3. For the remainder of the thesis, we denote the domain of a function f as $\mathcal{D}_f$.

Definition 2.2.1. A set C is **convex** if for any $x, y \in C$ and any $0 \leq \alpha \leq 1$, we have

$$\alpha x + (1-\alpha)y \in C.$$

Definition 2.2.2. A function $f : \mathbb{R} \to \mathbb{R}$ is **convex** if the domain of f is a convex set and if for all $x, y \in \mathcal{D}_f$, and α with $0 \leq \alpha \leq 1$, we have

$$f(\alpha x + (1-\alpha)y) \leq \alpha f(x) + (1-\alpha)f(y).$$

Definition 2.2.3. The **c-level set** of a function $f : \mathbb{R} \to \mathbb{R}$ is defined as $\{x \in \mathcal{D}_f : f(x) = c\}$.

Definition 2.2.4. A function $f : \mathbb{R} \to [-\infty, \infty]$ is **lower semi-continuous** if either of the following is satisfied:

(i) if it has closed level sets.

(ii) $\liminf_{n\to\infty} f(x_n) \geq f(x)$ for all x_n and x such that $x_n \to x$ in $\mathbb{R}$.

Theorem 2.2.1. ***(Heine-Borel)*** *A closed and bounded set is compact.*

Theorem 2.2.2. ***(Holder's Inequality)*** *For random variables X, Y let $0 < r < s$ then* $\mathbb{E}[|X|^r] \leq (\mathbb{E}[|X^s|])^{\frac{r}{s}}$.

2.2.2 Definitions and Results

Large deviations theory hinges on two main definitions, that of the rate function and establishing what it means to satisfy a large deviation principle (LDP). From these two definitions, the theory attempts to compile and establish results for various types of sequences, how to ascertain when an LDP is satisfied and at which rate of decay.

Definition 2.2.5. The function $I : \mathbb{R} \to [0, \infty]$ is called a **good rate function** if

(1) $I \not\equiv \infty$;

(2) I is lower semi-continuous;

(3) I has compact level sets.

We note that if I has compact level sets then it surely has closed level sets and so condition (3) implies (2). We state it to distinguish between a good rate function and a rate function, where the latter simply has closed level sets.

When we consider deviations in excess of $\sqrt{t}$, their probability will tend toward zero. The rate function helps one quantify the rate of decay related to the probability of a large deviation. For example, if we consider $a > \int_{\mathbb{R}} F(v)\pi(dv)$ and deviations are of size t, then if we can establish that $\lim_{t\to\infty} \frac{1}{t} \log \mathbb{P}(\int_0^t F(V(s))ds > at) = -I_{F,t}(a)$, where I is the rate function, we may see that $\mathbb{P}(\int_0^t F(V(s))ds > at) = e^{-tI_{F,t}(a)+o(t)}$ and so the decay is exponential in t. The following definition broadens the scope of this idea.

Definition 2.2.6. A sequence of probability measures (P_t) on $\mathbb{R}$ is said to satisfy the **large deviation principle** with rate t and with good rate function I if

(1) $\limsup_{t\to\infty} \frac{1}{t} \log P_t(C) \leq -\inf_{x\in C} I(x) \qquad \forall C \subset \mathbb{R}$ closed;

(2) $\liminf_{t\to\infty} \frac{1}{t} \log\ P_t(O) \geq -\inf_{x\in O} I(x) \qquad \forall O \subset \mathbb{R}$ open.

Theorem 2.2.3. *Let (P_t) satisfy the large deviation principle. Then the associated rate function I is unique.*

We move immediately to a discussion of the Gärtner-Ellis theorem as this is what will allow us to establish a large deviation principle. Going forward we make the following assumptions:

(1) $\lim_{t\to\infty} \frac{1}{t} \log \mathbb{E}[e^{\theta\Lambda(t)}] = \psi(\theta) \in [-\infty, \infty]$ exists;

(2) $0 \in \text{int}(\mathcal{D}_\psi)$, with $\mathcal{D}_\psi = \{\theta \in \mathbb{R} : \psi(\theta) < \infty\}$, i.e. the domain of $\psi(\theta)$.

The Gärtner-Ellis theorem helps establish a large deviation principle by knowing the limiting behavior of the cumulant generating function. This quantity arises in the proof of the upper bound for the LDP after an exponential Chebyshev inequality, which ultimately leads to the identification of the rate function as the Legendre transform of $\psi(\theta)$. If a large deviation principle is to be satisfied, then the lower bound must also result in the same rate function which is confirmed by tilting the probability measure $P_t(O)$ and so we present the Legendre transform next.

Definition 2.2.7. Let ψ^* denote the **Legendre transform** of ψ, then for $x \in \mathbb{R}$,

$$\psi^*(x) = \sup_{\theta\in\mathbb{R}} [\theta x - \psi(\theta)].$$

The fact that $\psi^*(x)$ is a good rate function can be verified by checking the conditions of the definition in turn. We offer a quick sketch, but full details may be found in [5, 13]. Non-negativity is assured by setting $\theta = 0$ and noting that $\psi^*(x) \geq -\psi(0) = 0$. Lower semi-continuity can be checked by directly applying the second definition provided. This assures we have closed level sets. Bounded level sets are shown by noting that ψ is continuous in a $\delta-$neighborhood around 0 so $\sup_{\theta\in(-\delta,\delta)} \psi(\theta) = c \implies \psi^*(x) \geq \delta|x| - c$. Finally, $\psi^* \not\equiv \infty$ since there exists an x_0 for which $\psi(\theta) \geq x_0\theta$ for all $\theta \in \mathbb{R} \implies \psi^*(x_0) = 0$.

Theorem 2.2.4. ***(Gärtner-Ellis Theorem)*** *If ψ satisfies:*

(1) ψ is lower semi-continuous on $\mathbb{R}$,

(2) ψ is differentiable on int($\mathcal{D}_\psi$),

(3) either $D_\psi = \mathbb{R}$ or $\lim_{\theta \to \partial \mathcal{D}_\psi : \theta \in \mathcal{D}_\psi} |\nabla \psi(\theta)| = \infty$,

then (P_t) satisfies a large deviation principle on $\mathbb{R}$ with rate t and rate function ψ^*.

Trying to directly compute the rate function using a probability density might prove to be intractable in many situations. Although the Gärtner-Ellis theorem was developed as an extension from the i.i.d. cases to those of moderate dependence, like Markovian sequences, it can also serve as a general indirect way to satisfy the large deviation principle.

2.3 Description of a Jump Diffusion

By the end of this section we would like to culminate to an understanding of the jump diffusion model. Before doing so, we briefly introduce the Lévy process as it will help in describing some of the details necessary to get a better grasp of a jump diffusion. Many of the definitions of the first subsection are fully developed in [15], while the second subsection can be found mostly in [20, 18, 19].

2.3.1 The Lévy Process

Brownian motion is a continuous process of unbounded variation and the Poisson process is a non-decreasing jump process of finite variation. Yet, it is commonly known that they are both cases of a more general process with cadlag paths, starting at the origin and with stationary independent increments, the Lévy process.

Definition 2.3.1. A process $X = \{X(t)\}_{t \geq 0}$, defined on a probability space $(\Omega, \mathcal{F}, \mathbb{P})$, is said to be a **Lévy process** if it posses the following properties:

(1) The paths of X are $\mathbb{P}$-almost surely cadlag.

(2) $\mathbb{P}(X(0) = 0) = 1$.

(3) For $0 \leq s \leq t, X(t) - X(s)$ is equal in distribution to $X(t - s)$.

(4) For $0 \leq s \leq t, X(t) - X(s)$ is independent of $\{X(u) : u \leq s\}$

It is helpful to visualize a Lévy process as a Brownian motion, with jumps dictated by a Poisson process. Of course one can easily extend this idea to a Brownian motion with drift and jumps dictated by a compound Poisson process. Before we do so, we will introduce the Lévy-Khintchine formula which will make this characterization intuitive.

Theorem 2.3.1. ***(Lévy-Khintchine formula for Lévy processes)*** *Suppose that $\mu \in \mathbb{R}, \sigma \in \mathbb{R}$ and ν is a measure on $\mathbb{R}$ such that $\nu(\{0\}) = 0$ and $\int_{\mathbb{R}}(1 \wedge x^2)\nu(dx) < \infty$. From this triple, that is the Lévy triple (μ, σ, ν), define for each $\theta \in \mathbb{R}$,*

$$\Psi(\theta) = i\mu\theta + \frac{1}{2}\sigma^2\theta^2 + \int_{\mathbb{R}}(1 - e^{i\theta x} + i\theta x \mathbf{1}_{\{|x|<1\}})\nu(dx).$$

Then there exists a probability space $(\Omega, \mathcal{F}, \mathbb{P})$ on which a Lévy process is defined having characteristic exponent Ψ.

Put briefly, we may immediately recognize the first two terms as belonging to the exponent of the characteristic function for a normal distribution with mean μ and variance σ^2. As Brownian motion with drift has independent stationary $\mathcal{N}(\mu, \sigma^2)$ increments, we can see these first two terms relate to the continuous part of the Lévy process. On the other hand, the first two terms in the integral belong to the characteristic function of a compound Poisson process, while the last term compensates for a possible measure with infinite jumps in finite time. Since the continuous part and the jump part act independently, we may multiply their respective characteristic functions and see where this characteristic exponent comes from. It is in this sense that a Lévy process may be seen as a Brownian motion, with jumps dictated by a compound Poisson process. As this is not our focus, we will refer the reader to [15] for the computations and further explanations. However, we would like to pay close attention to the measure ν.

Definition 2.3.2. The measure ν on $\mathbb{R}$ defined by $\nu(\{0\}) = 0$ and $\int_{\mathbb{R}}(1 \wedge x^2)\nu(dx) < \infty$ is called the **Lévy measure**.

A more intuitive description of the Lévy measure is that it characterizes the expected number of jumps of a certain size in a small interval of time. For now, of importance to us is the condition $\int_{\mathbb{R}}(1 \wedge x^2)\nu(dx) < \infty$. If we consider $|x| > 1$, intuitively jumps of

absolute size greater than 1, we can see that the expected number of *large* jumps is finite, i.e. $\int_{|x|>1} \nu(dx) < \infty$. The alternative, *small* jumps of size less than 1, only leaves us with the requirement that ν be square integrable, but with possibly infinite jumps on any small interval of time.

Lemma 2.3.1. *For a Lévy measure ν and a process X, if $\int_{|x|\leq 1} |x|\nu(dy) < \infty$ then the jumps of X have bounded variation.*

From this, we may see that the sum of all the jumps of X is an absolutely convergent series and so we may infer that this sum is finite. In Section 3.1, we will require the jump component of our process to be of bounded variation. This will ensure that even for small jumps, we will have finite jump activity.

The Lévy measure provides a way to explain the expected number of jumps of a certain size in an interval, but it does not tell us much about where the jumps occur nor of which size.

Definition 2.3.3. Let $N : [0, \infty) \times \mathbb{R} \to \{0, 1, 2, ...\} \cup \{\infty\}$ with intensity measure ν, then N is called a **Poisson random measure** if

(1) for mutually disjoint $A_1, ..., A_n \in [0, \infty) \times \mathbb{R}$, the variables $N(A_1), ..., N(A_n)$ are independent,

(2) for each $A \in [0, \infty) \times \mathbb{R}, N(A)$ is Poisson distributed with parameter $\nu(A)$,

From this definition we may see that for any set $A \in [0, \infty) \times \mathbb{R}$, the Poisson random measure will count how many instances of the set occur. A may be interpreted as an interval of time and the corresponding size of the jump, thus counting how many jumps of that size will occur in that interval. The resulting set of points counted by the Poisson random measure form the *marked point process* where the distribution of the mark variable is described by the measure ν.

Before we move on to diffusion processes, we introduce some familiar terminology. The Markov property is an important characteristic of diffusions and has even given name to the Markov process argument; the argument this thesis applies to establish the conditions for the martingale that will be used. From such a process we may derive an integro-differential

equation, given by the *infinitesimal generator*, from which a number of analytical conclusions may be reached, most notably the limiting behavior of the cumulant generating function which we will be interested in later.

Definition 2.3.4. The process $X = \{X(t)\}_{t\geq 0}$ posses the **Markov property** if, for each $B \in \mathbb{R}$ and $s, t \geq 0$,

$$\mathbb{P}(X(t+s) \in B|\mathcal{F}_t) = \mathbb{P}(X(t+s) \in B|\sigma(X(t))).$$

Definition 2.3.5. For the stopping time τ, define the sigma algebra

$$\mathcal{F}_\tau \equiv \{A \in \mathcal{F} : A \cap \{\tau \leq t\} \in \mathcal{F}_t \text{ for all } t \geq 0\}.$$

Then, the process X is said to satisfy the **strong Markov property** if, for each stopping time, τ,

$$\mathbb{P}(X(\tau+s) \in B|\mathcal{F}_\tau) = \mathbb{P}(X(\tau+s) \in B|\sigma(X(\tau))) \text{ on } \{\tau < \infty\}.$$

The classic intuition behind the Markov property is that one need only rely on the current time and can safely disregard the history in order to compute probabilities. The strong Markov property takes it one step further in that it specifies the current time can be at a stopping time. The strong Markov property naturally contains the Markov property by setting $\tau = t$.

It is natural to think of a Lévy process as a strong Markov process due to its independent increments, although not a necessary condition, and so we conclude with the following theorem whose proof may be found in [15].

Theorem 2.3.2. *A Lévy processes is a strong Markov process.*

2.3.2 Diffusion Processes

In this section we break the stationarity condition of the Lévy process and introduce the diffusion. This process retains independence of its increments and the strong Markov property, which we will see plays a major role in defining them. We introduce some preliminary

concepts which will be necessary for the existence of the solutions to the discussed stochastic differential equations.

Definition 2.3.6. A function $f : \mathbb{R}^+ \times \mathbb{R}^n \to \mathbb{R}$ is **Lipschitz** if there exists a finite constant k such that

(1) $|f(t,x) - f(t,y)| \leq k|x-y|$, for each $t \in \mathbb{R}^+$, and

(2) $t \mapsto f(t,x)$ is right continuous with left limits, for each $x \in \mathbb{R}^n$.

f is said to be **autonomous** if $f(t,x) = f(x)$, for all $t \geq 0$.

The Lipschitz condition ensures that the coefficient functions of our stochastic differential equations do not become infinitely steep at any point and the autonomous condition will be satisfied as we will be dealing exclusively with time homogeneous equations going forward. We note that if a function is Lipschitz, then it must be continuous.

Theorem 2.3.3. *Let $\boldsymbol{Z} = (Z^1, ..., Z^d)$ be a vector of independent Lévy processes starting at 0, and let (f_j), $1 \leq j \leq d$, be autonomous Lipschitz functions. Let X be a solution of*

$$X(t) = X(0) + \sum_{j=1}^{d} \int_0^t f_j(s-, X(s-)) dZ^j(s).$$

Then X has the strong Markov property.

Definition 2.3.7. An adapted process X with values in $\mathbb{R}$ is a **diffusion** if it has continuous sample paths and if it satisfies the strong Markov property.

Example 2.3.1. A famous example is the Itô diffusion which is the stochastic process X satisfying a stochastic differential equation of the form

$$X(t) = X(0) + \int_0^t \mu(X(s))ds + \int_0^t \sigma(X(s))dB(s)$$

where $B(t)$ is a standard Brownian motion, $\mu : \mathbb{R} \to \mathbb{R}$ and $\sigma : \mathbb{R} \to \mathbb{R}$ satisfying the Lipschitz condition $|\mu(x) - \mu(y)| + |\sigma(x) - \sigma(y)| \leq D|x-y|$ for $x, y \in \mathbb{R}$ and some constant D. We stress that it is time homogeneous, which makes it autonomous and it satisfies the Lipschitz conditions by assumption, so it possesses the strong Markov property.

We note that the quadratic variation of the Itô diffusion is $\int_0^t \sigma^2(X(s))ds$. A short sketch of this proof starts by noting that the problem reduces to finding the quadratic variation of $\int_0^t \sigma(X(s))dB(s)$ for which [20] provides a formula resulting in $\int_0^t \sigma^2(X(s))d[B]_s$ and after applying the identity $d[B]_t = dt$, we arrive at the conclusion.

Definition 2.3.8. A càdlàg process X is a **jump diffusion** if it is the solution to the time homogeneous Lévy stochastic differential equation

$$X(t) = X(0) + \int_0^t \mu(X(s))ds + \int_0^t \sigma(X(s))dB(s) + \int_0^t \int_{\mathcal{M}} \gamma(X(s-), y)p(dy, ds)$$

where $\mu : \mathbb{R} \to \mathbb{R}, \sigma : \mathbb{R} \to \mathbb{R}$ and $\gamma : \mathbb{R} \times \mathbb{R} \to \mathbb{R}$ satisfy the appropriate Lipschitz and linear growth conditions for existence and uniqueness and $p(dy, dt)$ is a random counting measure on $\mathcal{M} \times (0, \infty)$ with intensity measure $\nu(x, dy)$, where the mark space $\mathcal{M}$ is assumed to be a subset of Euclidean space.

It is necessary to generalize the Poisson random measure to a general counting measure in order to account for the state-dependent intensity. That is, the difference between $\nu(x, dy)$ and $\nu(dy)$ from the previous section, is that the intensity measure now depends on the current state of the process, $X(t-)$. Then by definition of the intensity measure, we have that for all bounded and measurable functions $h : \mathcal{M} \to \mathbb{R}$,

$$\int_0^t \int_{\mathcal{M}} h(y)p(dy, ds) - \int_0^t \int_{\mathcal{M}} h(y)\nu(x, dy)ds$$

forms a local martingale [10].

We further assume that we have jumps of bounded variation, $\int_{|y|\leq 1} |y|\nu(x, dy) < \infty$, and that the intensity measure $\nu(x, dy)$ is of the form $\lambda(x)\rho(dy)$ where $\lambda : \mathbb{R} \to \mathbb{R}$ is the arrival rate function for the jumps, satisfying appropriate Lipschitz and linear growth conditions, and ρ is the probability measure on $\mathcal{M}$. Then we may interpret $\int_0^t \int_{\mathcal{M}} \gamma(X(s-), y)p(dy, ds)$ as the sum of the jumps on $(0, t]$ with law $(\lambda(x), \rho(dy), \gamma(x, y))$.

Putting it all together, we may represent our stochastic differential equation as

$$X(t) = X(0) + \int_0^t \mu(X(s))ds + \int_0^t \sigma(X(s))dB(s) + \sum_{0<s\leq t} \Delta X(s)$$

where $\mu(X(t))$ is the drift function, $\sigma(X(t))$ is the volatility function and $\Delta X(s) = X(s) - X(s-) = \gamma(X(s-), y)$ is the jump size, with an arrival rate $\lambda(X(s-))$, and $\rho-$distributed mark variables y.

From this we may see how the Lévy process is a particular case of a jump diffusion with constant coefficient functions. Symmetrically to the previous subsection, we conclude with the following theorem whose result follows from Theorem 2.3.3 as found in [19].

Theorem 2.3.4. *A jump diffusion is a strong Markov process.*

2.4 Simulation Methods

Simulation methods allow one to reach numerical solutions where analytic ones are otherwise intractable. In the first subsection, we summarize how to discretize a stochastic process through the Euler-Maruyama approximation and follow it up with a discussion on the Monte Carlo simulation method to approximate the value of an expectation. A fully detailed account of these techniques may be found in standard textbooks such as [14, 21]. In the following subsection, we revisit some Stochastic Analysis topics which are used to derive the algorithms in Chapter 4, for which we provide as a reference [20].

2.4.1 Approximation Techniques

Euler-Maruyama

In order to simulate a continuous model with a computer that will only accept discrete inputs one must approximate the space. A common technique to do this is the Euler-Maruyama approximation method.

Consider the Itô diffusion on $[0, t]$,

$$X(t) = X(0) + \int_0^t \mu(X(s))ds + \int_0^t \sigma(X(s))dB(s)$$

which may be rewritten in differential form

$$dX(t) = \mu(X(t))dt + \sigma(X(t))dB(t).$$

From this, we see that $X(t) = X(t-) + dX(t)$.

If we divide the time interval $[0, t]$ into N subintervals of equal size $h = \frac{t}{N}$, then we have a discretization $0 = \tau_0 < \tau_1 < \tau_2 < ... < \tau_n < ... < \tau_N = t$ which makes it intuitive to consider $dt = \tau_{n+1} - \tau_n$ and $dB(t) = B(\tau_{n+1}) - B(\tau_n)$. Therefore, we say that the **Euler approximation** to the continuous time stochastic process X satisfies the iterative scheme

$$X_{n+1} = X_n + \mu(X_n)(\tau_{n+1} - \tau_n) + \sigma(X_n)(B(\tau_{n+1}) - B(\tau_n)).$$

Of course we know that Brownian increments are distributed according to the normal distribution with mean 0 and variance $\tau_{n+1} - \tau_n$. If we let $\mathcal{N}$ denote the standard normal random variable, then we may rewrite the Brownian increment as

$$B(\tau_{n+1}) - B(\tau_n) = \sqrt{\tau_{n+1} - \tau_n}\mathcal{N}.$$

There remains an issue of finding the value of $X(\tau)$ should $\tau \in (\tau_n, \tau_{n+1})$, that is, in between the discretization steps. The workaround is to use a linear interpolation scheme,

$$X(\tau) = X(\tau_n) + \frac{\tau - \tau_n}{\tau_{n+1} - \tau_n}(X(\tau_{n+1}) - X(\tau_n)).$$

Monte Carlo

The Monte Carlo method is an effective way to evaluate an expectation when analytically computing it is intractable. It is based on the law of large numbers which roughly states that taking the mean of a large enough sample of i.i.d. random variable will converge to their expected value.

Theorem 2.4.1. ***(Strong Law of Large Numbers)*** *Let $X_1, X_2, ...$ be independent identically distributed random variables. Then*

$$\frac{1}{k}\sum_{i=1}^{k} g(X_i) \to \mathbb{E}[g(X)]$$

with probability 1, as $k \to \infty$.

By repeatedly sampling a distribution, one may evaluate the expectation by simply taking the mean of all the samples. Naturally, the more samples one draws, the higher the accuracy between the sample mean and the actual expectation. Using the central limit theorem for i.i.d. random variables, we may build a confidence interval to see this.

Theorem 2.4.2. ***(Central Limit Theorem)*** *Let $X_1, X_2, ...$ be a sequence of independent identically distributed random variables. Then*

$$\frac{\frac{1}{k}\sum_{i=1}^{k} g(X_i) - \mathbb{E}[g(X)]}{\frac{S}{\sqrt{k}}} \to \mathcal{N}(0,1)$$

in distribution, as $k \to \infty$, where $\mathcal{N}(0,1)$ denotes the standard normal distribution and S denotes the sample standard deviation of the distribution.

From this we may build $(1-\alpha)100\%$ confidence intervals for $\mathbb{E}[g(X)]$, with z being a standard normal random variable, as

$$\left(\frac{1}{k}\sum_{i=1}^{k} g(X_i) - z_{\alpha/2}\frac{S}{\sqrt{k}}, \frac{1}{k}\sum_{i=1}^{k} g(X_i) + z_{\alpha/2}\frac{S}{\sqrt{k}}\right).$$

As we consider $k \to \infty$, we expect the variability around the estimate to tend to zero and so the difference between the estimate and the true expectation should also tend to zero.

2.4.2 Stochastic Analysis Revisited

Stochastic Time Change

Definition 2.4.1. Let $A = (A(t))_{t\geq 0}$ be an adapted, right continuous increasing process. The **change of time** associated with A is the process

$$\tau_t = \inf\{s > 0 : A(s) > t\}.$$

A time change allows for a warping of the time scale in such a way that one stochastic process may take the properties of another. For example, if we consider, $X(t)$ as an inhomogeneous Poisson process with rate $\lambda(t)$, we may want to warp the time scale so as

to result in a process with unit intensity rather than time dependent intensity. We do this by defining an increasing sequence of stopping times $\tau_1 < \tau_2 < ...$ in such a way that $\tau_{i+1} = \inf\{t > \tau_i : \int_{\tau_i}^{t} \lambda(s)ds > \mathcal{E}(1)\}$ where $\mathcal{E}(1)$ is a standard exponential random variable. Essentially, we are stretching out the time where the intensity is very high and compressing the time where the intensity is very low. The new time changed process X_τ, exists on a time scale where the old increments are now unequally spaced to line up with the intensity of the standard Poisson process.

Doob's Optional Sampling Theorem

Definition 2.4.2. A martingale M is said to be **closed** by a random variable Y if $\mathbb{E}[|Y|] < \infty$ and $M(t) = \mathbb{E}[Y|\mathcal{F}_t], 0 \leq t < \infty$.

Theorem 2.4.3. ***(Doob's Optional Sampling Theorem)*** *Let M be a right continuous martingale, which is closed by a random variable $Y = \lim_{t\to\infty} M(t)$. Let τ_1 and τ_2 be two stopping times such that $\tau_1 \leq \tau_2$ a.s. Then $M(\tau_1)$ and $M(\tau_2)$ are integrable and*

$$M(\tau_1) = \mathbb{E}[M(\tau_2)|\mathcal{F}_{\tau_1}] \qquad a.s.$$

If the conditions of the theorem are satisfied, we may calculate the value of the expectation knowing the value of the martingale at the current stopping time. In particular, if we define the stopping time $\tau_1 = 0$ and $\tau_2 = \tau$ then we see that $M(0) = \mathbb{E}[M(\tau)|\mathcal{F}_0]$.

Chapter 3

Main Result

3.1 Model Setup

We begin from where we left off with Section 2.3.2. Assuming $\int_{|y|\leq 1} |y|\nu(x, dy) < \infty$, so that the sum of the jumps are assured to converge absolutely for $t < \infty$, then we have for suitably chosen coefficient functions, a process X that solves the equation,

$$X(t) = X(0) + \int_0^t \mu(X(s))ds + \int_0^t \sigma(X(s))dB(s) + \sum_{0<s\leq t} \Delta X(s),$$

where the triple governing the jump component is $(\lambda(X(s-), \rho(dy), \gamma(X(s-), y))$.

The remainder of this thesis is not focused directly on the jump diffusion but rather the process V generated by reflecting X at the lower boundary of 0 and the upper boundary of $b > 0$. We may imagine $V(t)$, starting at $V(0) \in [0, b]$, following $X(t)$ until it is about to cross either of the two boundaries, call this time $\tau-$. At this point, $X(\tau-)$ may either move continuously or jump. If we are at the lower boundary, the amount $X(\tau) - X(\tau-)$ is then added to a non-decreasing process L, which is then itself added to $V(\tau)$. Likewise, if we were at the upper boundary instead, the amount $X(\tau) - X(\tau-)$ would be added to another non-decreasing process U, which is then subtracted from $V(\tau)$. This then repeats on $[0, t]$, keeping V within the interval $[0, b]$.

Formally, V is defined as the solution to the Skorokhod problem

$$V(t) = V(0) + X(t) + L(t) - U(t) \in [0, b], \qquad \forall t \geq 0$$

where L, U are non-decreasing right-continuous processes such that

$$\int_0^\infty V(t)dL(t) = 0, \qquad \int_0^\infty (b - V(t))dU(t) = 0.$$

In this context, the coefficients of the non-reflected jump diffusion $X(t)$ are understood to depend on the state of $V(t)$ so that

$$X(t) = X(0) + \int_0^t \mu(V(s))ds + \int_0^t \sigma(V(s))dB(s) + \sum_{0<s\leq t} \Delta X(s)$$

where the triple governing the jump component is $(\lambda(V(t-)), \rho(dy), \gamma(V(t-), y))$.

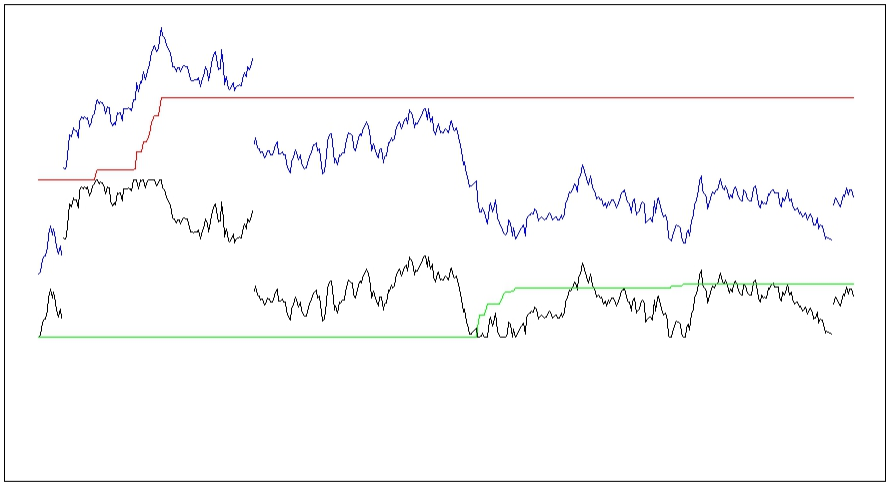

Figure 3.1: Example of a reflected jump diffusion. Black: V, Blue: X, Green: L, Red: U

Intuitively, the process $L(t)$ represents the cumulation of all the reflections necessary to keep $V(t) \geq 0$ on $[0, t]$, called the lower boundary local time. Likewise, $U(t)$ is the cumulation of all the reflections necessary to keep $V(t) \leq b$ and is the upper boundary local time.

This thesis focuses on the practical implementations of the local time at the lower boundary. Therefore, to avoid duplicating the same arguments, we oftentimes perform the calculations for $L(t)$ and note that the same holds for $U(t)$. In this light, the local time at the lower boundary can be computed as follows,

$$\begin{aligned}
L(t) &= \lim_{\varepsilon \to 0+} \frac{1}{2\varepsilon} \int_0^t \mathbf{1}_{\{V(s)<\varepsilon\}} ds \\
&= \lim_{\varepsilon \to 0+} \frac{1}{2\varepsilon} \int_0^t \mathbf{1}_{\{V(s-)+\Delta X(s)<0\}} + \mathbf{1}_{\{V(s-)+\Delta X(s)\in[0,\epsilon)\}} ds \\
&= \int_0^t \mathbf{1}_{\{V(s-)+\Delta X(s)<0\}} ds + \lim_{\varepsilon \to 0+} \frac{1}{2\varepsilon} \int_0^t \mathbf{1}_{\{V(s-)+\Delta X(s)\in[0,\epsilon)\}} ds \\
&= \sum_{0<s\leq t} [-(V(s-) + \Delta X(s))]^+ + L^c(t)
\end{aligned}$$

where the superscript c denotes the continuous part of the local time. The last equality follows from the occupation density formula, which intuitively allows us to slice the integral vertically with respect to time or horizontally with respect to space and arrive at the same result. From this equation, it is evident that $L(t)$ will only increase in the event of a jump below 0 or a continuous crossing below 0. We arrive at the expression $-(V(s-)+\Delta X(s))$ by noting that if there is in fact a jump below 0, $\Delta V(s) = V(s) - V(s-) = \Delta X(s) + \Delta L(s) - \Delta U(s) \implies \Delta L(s) = -(V(s-) + \Delta X(s))$, since $V(s) = \Delta U(s) = 0$. If there is a going to be a continuous crossing, $L(t)$ grows by infinitesimal amounts, which is represented by $L^c(t)$. A similar computation will find that $U(t) = \sum_{0<s\leq t} [(V(t-) + \Delta X(t)) - b]^+ + U^c(t)$.

It is possible to generalize the boundary local times L and U by considering the additive functional $\Lambda(t)$ of the form

$$\Lambda(t) = \int_0^t f(V(s))ds + \sum_{0<s\leq t} \tilde{f}(V(s-), \Delta X(s)) + r_1 L^c(t) + r_2 U^c(t)$$

where r_1 and r_2 are constants. We also assume that the function f is bounded, that $\tilde{f}(x, 0) = 0$, and that

$$\sup_{0\leq x\leq b} \int_{\mathbb{R}} \left|\tilde{f}(x, y)\right| \nu(x, dy) < \infty.$$

Note that L may be recovered from $\Lambda(t)$ by setting $f \equiv 0, \tilde{f} = [-(x + y)]^+, r_1 = 1$ and

$r_2 = 0$ and likewise, U may be recovered by setting $f \equiv 0, \tilde{f} = [(x+y)-b]^+, r_1 = 0$ and $r_2 = 1$.

Finally, we present a notational simplification which will be useful later. Let,

$$r(x,y) = \begin{cases} 0 & x+y \leq 0 \\ x+y & 0 \leq x+y \leq b \\ b & x+y \geq b \end{cases}$$

and we note that $V(s) = r(V(s-), \Delta X(s))$ whenever $\Delta X(s) \neq 0$.

3.2 Preliminary Results

In this section, we introduce a series of lemmas so as to keep the proof of Theorem 3.3.1 from being unnecessarily long. First we show that $V(t)$ and $\Lambda(t)$ are semimartingales as these are necessary conditions to apply Itô's formula. Following that, we compute various quadratic variations and covariations. Finally, we construct the compensator of a process that is used in our exposition later.

3.2.1 $\Lambda(t)$ and $V(t)$ are Semimartingales

Showing that $\Lambda(t)$ and $V(t)$ are semimartingales boils down to decomposing the respective processes into their component parts and showing that the individual terms are either local martingales or finite variation processes. This stems from the fact that the sum of local martingales is itself a local martingale and the sum of finite variation processes is itself a finite variation process. Therefore, when adding all the terms together, it will imply that the sum forms a semimartingale.

Lemma 3.2.1. *$L(t)$ and $U(t)$ are finite variation processes.*

Proof. This is obvious since $L(t)$ and $U(t)$ are non-decreasing processes. □

Lemma 3.2.2. *$X(t)$ is a semimartingale.*

Proof. $X(t)$ may be decomposed into the sum of the following three terms, $\int_0^t \mu(V(s))ds$, $X(0) + \int_0^t \sigma(V(s))dB(s)$ and $\sum_{0<s\leq t} \Delta X(s)$. For the first term, note that

$$\begin{aligned}\sup_{\mathcal{P}} \sum_{i=1}^{n-1} \left| \int_0^{t_{i+1}} \mu(V(s))ds - \int_0^{t_i} \mu(V(s))ds \right| &= \sup_{\mathcal{P}} \sum_{i=1}^{n-1} \left| \int_{t_i}^{t_{i+1}} \mu(V(s))ds \right| \\ &\leq \sup_{\mathcal{P}} \sum_{i=1}^{n-1} \int_{t_i}^{t_{i+1}} |\mu(V(s))|ds \\ &< \infty\end{aligned}$$

since $\mu(x)$ is Lipschitz continuous on a closed interval $[0, b]$ and $V(s)$ is bounded, then $\mu(V(s))$ is bounded. Also, the sum of bounded functions is bounded.

The term $X(0)+\int_0^t \sigma(V(s))dB(s)$ is a continuous term in the Itô diffusion so $\lim_{s\to t-} \sigma(V(s)) = \sigma(V(t))$, making it predictable. Then by Lemma 2.1.4, $X(0) + \int_0^t \sigma(V(s))dB(s)$ is a local martingale.

Finally, the jump part of $X(t)$ is governed by $(\lambda(V(t-)), \rho(dy), \gamma(V(t-), y))$ where we have assumed $\int_{|y|\leq 1} |y|\nu(x, dy) < \infty$. Therefore, the sum of the jumps converges absolutely, and so

$$\sup_{\mathcal{P}} \sum_{i=1}^{n-1} \left| \sum_{0<s\leq t_{i+1}} \Delta X(s) - \sum_{0<s\leq t_i} \Delta X(s) \right| \leq \sup_{\mathcal{P}} \sum_{i=1}^{n-1} \sum_{t_i<s\leq t_{i+1}} |\Delta X(s)| < \infty.$$

This implies $\sum_{0<s\leq t} \Delta X(s)$ must be of finite variation and by consequence $X(t)$ is a semimartingale. □

By the previous two lemmas, we have shown that $V(t)$ is a semimartingale. We are left to show that $\Lambda(t)$ is a semimartingale. To do so we apply the same techniques mentioned above and so summarize it quickly in the following lemma.

Lemma 3.2.3. $\Lambda(t)$ *is a semimartingale.*

Proof. Since we assumed $f(x)$ is bounded, then by the same argument for $\int_0^t \mu(V(s))ds$, we conclude that $\int_0^t f(V(s))ds$ is of finite variation. Again, by assumption we have that $\sup_{0\leq x\leq b} \int_{\mathbb{R}} \left|\tilde{f}(x, y)\right| \nu(x, dy) < \infty$ so $\sum_{0<s\leq t} \tilde{f}(V(s-), \Delta X(s))$ converges absolutely and therefore,

must be of finite variation. By consequence, $\Lambda(t)$ is the sum of finite variation processes making it a semimartingale. $\square$

3.2.2 Computations of $[V]_t^c, [\Lambda]_t^c, [V,\Lambda]_t^c$

Note that for a partition $\{t_i\}$ on $[0,t]$, as $\max|t_{i+1}-t_i| \to 0$ then $L^c(t_{i+1}) - L^c(t_i) \to 0$ and $U^c(t_{i+1}) - U^c(t_i) \to 0$, since they are continuous non-decreasing processes.

$$
\begin{aligned}
[V]_t^c &= \lim_{\max|t_{i+1}-t_i|\to 0} \sum_{i=0}^{n-1} (V^c(t_{i+1}) - V^c(t_i))^2 \\
&= \lim_{\max|t_{i+1}-t_i|\to 0} \sum_{i=0}^{n-1} \left(X^c(t_{i+1}) - X^c(t_i) + L^c(t_{i+1}) - L^c(t_i) - (U^c(t_{i+1})) - U^c(t_i))\right)^2 \\
&= \lim_{\max|t_{i+1}-t_i|\to 0} \sum_{i=0}^{n-1} \Big[(X^c(t_{i+1}) - X^c(t_i))^2 + \left(L^c(t_{i+1}) - L^c(t_i) - (U^c(t_{i+1})) - U^c(t_i))\right)^2 \\
&+2(X^c(t_{i+1}) - X^c(t_i))\left(L^c(t_{i+1}) - L^c(t_i) - (U^c(t_{i+1})) - U^c(t_i))\right)\Big] \\
&= \lim_{\max|t_{i+1}-t_i|\to 0} \sum_{i=0}^{n-1} (X^c(t_{i+1}) - X^c(t_i))^2 \\
&= \int_0^t \sigma^2(V(s))ds
\end{aligned}
$$

The final equality follows from Example 2.3.1 by noting that $X^c(t)$ is just an Itô diffusion. Continuing, we note that

$$
\begin{aligned}
&\lim_{\max|t_{i+1}-t_i|\to 0} \Lambda^c(t_{i+1}) - \Lambda^c(t_i) \\
&= \lim_{\max|t_{i+1}-t_i|\to 0} \int_0^{t_{i+1}} f(V(s))ds + r_1 L^c(t_{i+1}) + r_2 U^c(t_{i+1}) \\
&- \lim_{\max|t_{i+1}-t_i|\to 0} \int_0^{t_i} f(V(s))ds + r_1 L^c(t_i) + r_2 U^c(t_i) \\
&= \lim_{\max|t_{i+1}-t_i|\to 0} \left[\int_{t_i}^{t_{i+1}} f(V(s))ds + r_1(L^c(t_{i+1}) - L^c(t_i)) + r_2(U^c(t_{i+1}) - U^c(t_i))\right] \\
&= 0
\end{aligned}
$$

Consequently,

$$[\Lambda]_t^c = \lim_{\max|t_{i+1}-t_i|\to 0} \sum_{i=0}^{n-1} (\Lambda^c(t_{i+1}) - \Lambda^c(t_i))^2 = 0$$

$$[V,\Lambda]_t^c = \lim_{\max|t_{i+1}-t_i|\to 0} \sum_{i=0}^{n-1} (V^c(t_{i+1}) - V^c(t_i))(\Lambda^c(t_{i+1}) - \Lambda^c(t_i)) = 0$$

3.2.3 Computation of the Compensator

In this subsection we compute that compensator of the process

$$Y(t) = \sum_{0<s\leq t} A(s-)[e^{\theta\tilde{f}(V(s-),\Delta X(s))}u(\theta,V(s)) - u(\theta,V(s-))]$$

where $A(s-) = e^{\theta\Lambda(s-)-\psi(\theta)s-}$, $u(\theta,x)$ is a positive twice differentiable function and $\psi(\theta)$ is a scalar. We eventually use this compensator in the proof of Theorem 3.3.1 to assert that the result of $Y(t)$ less its compensator is a local martingale, however this is immediate by the discussion in Section 2.3.2.

Define an increasing sequence of stopping times $0 = \tau_0 \leq \tau_1 \leq ...$, the compensator of $Y(t)$ is given by

$$\begin{aligned}
&\lim_{\sup_n|\tau_n-\tau_{n-1}|\to 0} \sum_{n=1}^{\infty} \mathbf{1}_{\{\tau_{n-1}<t\}} \mathbb{E}[Y(\tau_n) - Y(\tau_{n-1})|\mathcal{F}_{\tau_{n-1}}] \\
&= \lim_{\sup_n|\tau_n-\tau_{n-1}|\to 0} \sum_{n=1}^{\infty} \mathbf{1}_{\{\tau_{n-1}<t\}} \int_{\mathbb{R}} \sum_{0<s\leq\tau_n} \Big[A(s-)[e^{\theta\tilde{f}(V(s-),y)}u(\theta,V(s)) - u(\theta,V(s-))] \\
&- \sum_{0<s\leq\tau_{n-1}} A(s-)[e^{\theta\tilde{f}(V(s-),y)}u(\theta,V(s)) - u(\theta,V(s-))\Big] \nu(x,dy) \\
&= \lim_{\sup_n|\tau_n-\tau_{n-1}|\to 0} \sum_{n=1}^{\infty} \mathbf{1}_{\{\tau_{n-1}<t\}} \int_{\mathbb{R}} \Big[A(\tau_{n-1})[e^{\theta\tilde{f}(V(\tau_{n-1}),y)}u(\theta,r(V(\tau_{n-1}),y)) \\
&- u(\theta,V(\tau_{n-1}))] + \sum_{0<s\leq\tau_{n-1}} A(s-)[e^{\theta\tilde{f}(V(s-),y)}u(\theta,V(s)) - u(\theta,V(s-))] \\
&- \sum_{0<s\leq\tau_{n-1}} A(s-)[e^{\theta\tilde{f}(V(s-),y)}u(\theta,V(s)) - u(\theta,V(s-))]\Big] \nu(x,dy)
\end{aligned}$$

$$= \lim_{\sup_n |\tau_n - \tau_{n-1}| \to 0} \sum_{n=1}^{\infty} \mathbf{1}_{\{\tau_{n-1} < t\}} \int_{\mathbb{R}} A(\tau_{n-1})[e^{\theta \tilde{f}(V(\tau_{n-1}),y)} u(\theta, r(V(\tau_{n-1}), y))$$
$$- u(\theta, V(\tau_{n-1}))]\nu(x, dy)$$
$$= \int_0^t A(s-) \int_{\mathbb{R}} [e^{\theta \tilde{f}(V(s-),y)} u(\theta, r(V(s-), y)) - u(\theta, V(s-))]\nu(x, dy)ds$$

The last equality follows as a limit of Riemann sums.

3.3 Main Result

In order to arrive at a large deviation result for Λ, we first need to establish the limit of its cumulant generating function from which the Gärtner-Ellis theorem may be applied. This section is split into two subsections. The first is concerned with establishing this limit and the second with finding the rate function from which to establish the large deviation result.

3.3.1 Limit of the Cumulant Generating Function

Using a typical Markov process argument, we are able to establish the limiting behavior of the cumulant generating function. This is done by constructing an appropriate martingale from which the limit is established and deriving the integro-differential equation that may be used to analytically compute the limit.

Theorem 3.3.1. *Fix $\theta \in \mathbb{R}$. Suppose that $\mu(x)$ and $\sigma(x)$ are bounded and*

$$\int_{\mathbb{R}} e^{\theta \tilde{f}(x,y)} \nu(x, dy) < \infty.$$

If there exists a positive twice differentiable function $u(\theta, x) : \mathbb{R} \times [0, b] \to \mathbb{R}$ and a scalar $\psi(\theta)$ such that the pair $(u(\theta, x), \psi(\theta))$ satisfies the integro-differential equation

$$\begin{aligned} 0 =& \mu(x)u_x(\theta, x) + \frac{1}{2}\sigma^2(x)u_{xx}(\theta, x) + (\theta f(x) - \psi(\theta))u(\theta, x) \\ &+ \int_{\mathbb{R}} [e^{\theta \tilde{f}(x,y)} u(\theta, r(x, y)) - u(\theta, x)]\nu(x, dy) \end{aligned} \tag{3.3.1}$$

for $0 \leq x \leq b$ and subject to the boundary conditions

$$u_x(\theta, 0) = -r_1 \theta u(\theta, 0), \qquad u_x(\theta, b) = r_2 \theta u(\theta, b)$$

then $M(\theta, t) = e^{\theta\Lambda(t) - \psi(\theta)t} u(\theta, V(t))$ is a martingale.

Proof. For notational convenience, we define $A(s) = e^{\theta\Lambda(s) - \psi(\theta)s}$. An application of Itô's formula shows:

$$\begin{aligned}
M(\theta,t) - M(\theta,0) = &\int_0^t -\psi(\theta) A(s-) u(\theta, V(s-)) ds \\
&+ \int_0^t \theta A(s-) u(\theta, V(s-)) d\Lambda^c(s) \\
&+ \int_0^t A(s-) u_x(\theta, V(s-)) dV^c(s) \\
&+ \frac{1}{2} \int_0^t A(s-) u_{xx}(\theta, V(s-)) d[V]_s^c \\
&+ \sum_{0<s\leq t} [A(s) u(\theta, V(s)) - A(s-) u(\theta, V(s-))]
\end{aligned}$$

$$\begin{aligned}
M(\theta,t) - M(\theta,0) = &\int_0^t -\psi(\theta) A(s-) u(\theta, V(s-)) ds \\
&+ \int_0^t \theta A(s-) u(\theta, V(s-)) [f(V(s-)) ds + r_1 dL^c(s) + r_2 dU^c(s)] \\
&+ \int_0^t A(s-) u_x(\theta, V(s-)) [\mu(V(s-)) ds + \sigma(V(s-)) dB(s)] \\
&+ \int_0^t A(s-) u_x(\theta, V(s-)) [dL^c(s) - dU^c(s)] \\
&+ \frac{1}{2} \int_0^t A(s-) u_{xx}(\theta, V(s-)) \sigma^2(V(s-)) ds \\
&+ \sum_{0<s\leq t} [A(s-) e^{\theta \tilde{f}(V(s-), \Delta X(s))} u(\theta, V(s)) - A(s-) u(\theta, V(s-))]
\end{aligned}$$

$$\begin{aligned}
M(\theta,t) - M(\theta,0) = &\int_0^t A(s) [(\theta f(V(s)) - \psi(\theta)) u(\theta, V(s))] ds \\
&+ \int_0^t A(s) [\mu(V(s)) u_x(\theta, V(s)) + \frac{1}{2} \sigma^2(V(s)) u_{xx}(\theta, V(s))] ds
\end{aligned}$$

$$
\begin{aligned}
&+ \int_0^t A(s)[\theta r_1 u(\theta,0) + u_x(\theta,0)]dL^c(s) \\
&+ \int_0^t A(s)[\theta r_2 u(\theta,b) - u_x(\theta,b)]dU^c(s) \\
&+ \int_0^t A(s)u_x(\theta,V(s))\sigma(V(s))dB(s) \\
&+ \sum_{0<s\le t} A(s-)[e^{\theta\tilde{f}(V(s-),\Delta X(s))}u(\theta,V(s)) - u(\theta,V(s-))]
\end{aligned}
$$

$$
\begin{aligned}
M(\theta,t) - M(\theta,0) = &\int_0^t A(s)u_x(\theta,V(s))\sigma(V(s))dB(s) \\
&+ \sum_{0<s\le t} A(s-)[e^{\theta\tilde{f}(V(s-),\Delta X(s))}u(\theta,V(s)) - u(\theta,V(s-))] \\
&- \int_0^t A(s-)\int_{\mathbb{R}}[e^{\theta\tilde{f}(V(s-),y)}u(\theta,r(V(s-),y)) \\
&- u(\theta,V(s-))]\nu(x,dy)ds
\end{aligned} \tag{3.3.2}
$$

The last equality uses the fact that $(u(\theta,x),\psi(\theta))$ satisfy the integro-differential equation (3.3.1) and the boundary conditions. For the first integral term in (3.3.2), we are considering only the continuous part of the process V, therefore

$$\lim_{s\to t-} A(s)u_x(\theta,V(s))\sigma(V(s)) = A(t)u_x(\theta,V(t))\sigma(V(t)).$$

This implies that $A(s)u_x(\theta,V(s))\sigma(V(s))$ is a predictable integrand. Furthermore, the integrator is Brownian motion and so by Lemma 2.1.4, the first integral term is a local martingale.

We note that the summation term in (3.3.2) is being subtracted by its compensator and so the two terms define another local martingale. The sum of two local martingales is itself a local martingale and so we may conclude that (3.3.2) is a local martingale. We are left to show that it is a bounded local martingale to complete the proof.

Consider,

$$|M(\theta,t) - M(\theta,0)|$$

$$= \Bigg| \int_0^t A(s) u_x(\theta, V(s)) \sigma(V(s)) dB(s)$$
$$+ \sum_{0<s\leq t} A(s-)[e^{\theta \tilde{f}(V(s-),\Delta X(s))} u(\theta, V(s)) - u(\theta, V(s-))]$$
$$- \int_0^t A(s-) \int_{\mathbb{R}} [e^{\theta \tilde{f}(V(s-),y)} u(\theta, r(V(s-), y)) - u(\theta, V(s-))] \nu(x, dy) ds \Bigg|.$$

We can see that since $u(\theta, x)$ is twice differentiable, both $u(\theta, x)$ and $u_x(\theta, x)$ are continuous on a closed interval and so they must be bounded. Likewise, we have assumed jumps of bounded variation, so $A(s)$ and $e^{\theta \tilde{f}(V(s-),\Delta X(s))}$ must be bounded on $[0, t]$. Since $\sigma(x)$ is a Lipschitz function and $V(s)$ is bounded between 0 and b, then $\sigma(V(s))$ must be bounded. Finally, we recall our assumption that $\int_{\mathbb{R}} e^{\theta \tilde{f}(V(s-),y)} \nu(x, dy) < \infty$.

Putting it all together, we conclude that $M(\theta, t) - M(\theta, 0)$ is a bounded local martingale, ensuring that $M(\theta, t)$ is a martingale. □

We assumed the function $u(\theta, x)$ is positive and we know it is bounded above and below by constants, say $K_1, K_2 \in \mathbb{R}^+$ such that $0 < K_1 \leq u(\theta, x) \leq K_2$. Then by the martingale property $\mathbb{E}[M(\theta, t)] = \mathbb{E}[M(\theta, 0)]$. Therefore,

$$\begin{aligned}
&\mathbb{E}[e^{\theta\Lambda(t) - \psi(\theta)t} u(\theta, V(t))] = \mathbb{E}[e^{\theta\Lambda(0) - \psi(\theta)0} u(\theta, V(0))] = 1 \\
\iff &\mathbb{E}[e^{\theta\Lambda(t)} u(\theta, V(t))] = e^{\psi(\theta)t} \\
\iff &\frac{1}{t} \log \mathbb{E}[e^{\theta\Lambda(t)} u(\theta, V(t))] = \psi(\theta) \\
\iff &\frac{1}{t} \log \mathbb{E}[e^{\theta\Lambda(t)} K_1] \leq \frac{1}{t} \log \mathbb{E}[e^{\theta\Lambda(t)} u(\theta, V(t))] = \psi(\theta) \leq \frac{1}{t} \log \mathbb{E}[e^{\theta\Lambda(t)} K_2] \\
\iff &\frac{1}{t} (\log K_1 + \log \mathbb{E}[e^{\theta\Lambda(t)}]) \leq \psi(\theta) \leq \frac{1}{t} (\log K_2 + \log \mathbb{E}[e^{\theta\Lambda(t)}])
\end{aligned} \tag{3.3.3}$$

Taking limits from both sides as $t \to \infty$, we may establish that

$$\lim_{t\to\infty} \frac{1}{t} \log \mathbb{E}[e^{\theta\Lambda(t)}] = \psi(\theta).$$

Now that the limiting behavior of the cumulant generating function has been established, we may derive the expectation of Λ. To differentiate (3.3.3) with respect to θ, choose a $T > t$. Since $\Lambda(t)$ is a positive non-decreasing function then $|e^{\theta\Lambda(t)} u(\theta, V(t))| \leq |e^{\theta\Lambda(t)} K_2| \leq$

$|e^{\theta\Lambda(T)}K_2| < \infty$. By the dominated convergence theorem, we may establish that

$$\begin{aligned}
&\frac{\partial}{\partial\theta}\mathbb{E}[e^{\theta\Lambda(t)}u(\theta,V(t))] = \frac{\partial}{\partial\theta}e^{\psi(\theta)t} \\
\iff &\mathbb{E}[\Lambda(t)e^{\theta\Lambda(t)}u(\theta,V(t)) + e^{\theta\Lambda(t)}u_\theta(\theta,V(t))] = \psi'(\theta)te^{\psi(\theta)t}.
\end{aligned}$$

Set $\theta = 0$, then

$$\mathbb{E}[\Lambda(t)u(0,V(t)) + u_\theta(0,V(t))] = \psi'(0)te^{\psi(0)t}.$$

For $u(0,x) = 1$, $u_\theta(0,x) = 0$ and noting that $\psi(0) = 0$, we have derived the following,

$$\mathbb{E}[\Lambda(t)] = \psi'(0)t.$$

From this, it is clear that

$$\lim_{t\to\infty}\frac{1}{t}\mathbb{E}[\Lambda(t)] = \lim_{t\to\infty}\frac{1}{t}\psi'(0)t = \psi'(0).$$

Similarly,

$$\begin{aligned}
&\frac{\partial}{\partial\theta}\mathbb{E}[\Lambda(t)e^{\theta\Lambda(t)}u(\theta,V(t)) + e^{\theta\Lambda(t)}u_\theta(\theta,V(t))] = \frac{\partial}{\partial\theta}\psi'(\theta)te^{\psi(\theta)t} \\
\iff &\mathbb{E}[\Lambda(t)^2e^{\theta\Lambda(t)}u(\theta,V(t)) + 2\Lambda(t)e^{\theta\Lambda(t)}u_\theta(\theta,V(t)) + e^{\theta\Lambda(t)}u_{\theta\theta}(\theta,V(t))] \\
&= \psi''(\theta)te^{\psi(\theta)t} + \psi'(\theta)^2t^2e^{\psi(\theta)t}.
\end{aligned}$$

Set $\theta = 0$, then

$$\mathbb{E}[\Lambda(t)^2u(0,V(t)) + 2\Lambda(t)u_\theta(0,V(t)) + u_{\theta\theta}(0,V(t))] = \psi''(0)t + \psi'(0)^2t^2.$$

For $u(0,x) = 1, u_\theta(0,x) = 0, u_{\theta\theta}(0,x) = 0$, we have derived the following

$$E[\Lambda(t)^2] = \psi''(0)t + \psi'(0)^2t^2.$$

Therefore,

$$\begin{aligned} Var(\Lambda(t)) =& E[\Lambda(t)^2] - E[\Lambda(t)]^2 \\ =& \psi''(0)t + \psi'(0)^2t^2 - (\psi'(0)t)^2 \\ =& \psi''(0)t. \end{aligned}$$

Which implies,

$$\lim_{t\to\infty} \frac{1}{t} Var(\Lambda(t)) = \psi''(0).$$

3.3.2 Large Deviations for Λ

To establish a large deviation principle for Λ, we start by computing a good rate function and arrive at the conclusion by means of the Gärtner-Ellis theorem. We recall that by using Theorem 3.3.1, we have already shown $\lim_{t\to\infty} \frac{1}{t} \log \mathbb{E}[e^{\theta\Lambda(t)}] = \psi(\theta)$ and assuming $0 \in \text{int}(\mathcal{D}_\psi)$, we have that $\psi(0) = 0$. We begin with a lemma that shows the Legendre transform of $\psi(\theta)$ is a good rate function.

Lemma 3.3.1. *Let ψ^* denote the Legendre transform of ψ. Suppose there exists a $\theta^* > 0$ for which $\psi(\cdot)$ exists in a neighborhood of θ^* and is continuously differentiable there. Then,*

(1) $\psi^*(a) = \theta^* a - \psi(\theta^*)$, where $a = \psi'(\theta^*)$.

(2) ψ and ψ^* are convex.

(3) ψ^* is a good rate function.

Proof. We split the proof into its three parts:

Proof of (1)

By definition $\psi^*(a) = \sup_{\theta\in\mathbb{R}}[\theta a - \psi(\theta)]$. Taking the derivative with respect to θ and setting it equal to zero,

$$a - \psi'(\theta) = 0 \implies a = \psi'(\theta).$$

So for $\theta^* > 0$,

$$\psi^*(a) = \theta^* a - \psi(\theta^*), \text{ where } a = \psi'(\theta^*).$$

Proof of (2)

First we show that ψ is convex. Define $\varphi_t(\theta) = \frac{1}{t}\log\mathbb{E}[e^{\theta\Lambda(t)}]$, let $x, y \in \mathcal{D}_\psi$ and $\alpha \in [0,1]$. Then,

$$\begin{aligned}\varphi_t(\alpha x + (1-\alpha)y) &= \frac{1}{t}\log\mathbb{E}[e^{(\alpha x+(1-\alpha)y)\Lambda(t)}] \\ &= \frac{1}{t}\log\mathbb{E}[e^{\alpha x\Lambda(t)}e^{(1-\alpha)y\Lambda(t)}]\end{aligned}$$

By Hölder's inequality

$$\begin{aligned}&\leq \frac{1}{t}\log\mathbb{E}[e^{x\Lambda(t)}]^\alpha\mathbb{E}[e^{y\Lambda(t)}]^{1-\alpha} \\ &= \alpha\frac{1}{t}\log\mathbb{E}[e^{x\Lambda(t)}] + (1-\alpha)\frac{1}{t}\mathbb{E}[e^{y\Lambda(t)}] \\ &= \alpha\varphi_t(x) + (1-\alpha)\varphi_t(y)\end{aligned}$$

Since φ_t is convex for all t, then so is ψ.

Now we show that ψ^* is convex. Let $a, b \in \mathcal{D}_{\psi^*}$ and let $\alpha \in [0,1]$. Then,

$$\begin{aligned}\psi^*(\alpha a + (1-\alpha)b) =&(\alpha a + (1-\alpha)b)\theta^* - \psi(\theta^*) \\ =&\alpha a\theta^* + (1-\alpha)b\theta^* - \psi(\theta^*) + \alpha\psi(\theta^*) - \alpha\psi(\theta^*) \\ =&\alpha a\theta^* - \alpha\psi(\theta^*) + (1-\alpha)b\theta^* - (1-\alpha)\psi(\theta^*) \\ =&\alpha\psi^*(a) + (1-\alpha)\psi^*(b)\end{aligned}$$

Therefore, ψ^* is convex.

Proof of (3)

A quick sketch of this proof was provided in Section 2.2.2. Full details may be found in [5, 13].

□

Assuming the conditions on $\psi(\theta)$ are satisfied in the Gärtner-Ellis theorem, then we may immediately claim that the local time of the doubly reflected jump diffusion satisfies a large

deviation principle on $\mathbb{R}$ with rate t and with good rate function ψ^*. That is,

$$\frac{1}{t}\log \mathbb{P}(\Lambda(t) \geq at) \to \psi(\theta^*) - \theta^* a.$$

Finally, we note that the minimum of the rate function $\psi^*(a)$ is at $a = \psi'(0)$. This is the case since $(\psi^*(a))' = 0 \implies \theta^* = 0$ and ψ^* is convex. Using the limit established earlier, we may compute this value by

$$\lim_{t\to\infty} \frac{1}{t}\mathbb{E}[\Lambda(t)] = \psi'(0).$$

3.4 Analytic Examples

This section presents two examples where we solve the integro-differential equation (3.3.1) to find an implicit formula for $\psi(\theta)$. We do this so that in Chapter 4 we have analytic solutions from which to test the simulated solutions. The first example we are interested in is standard Brownian motion and then we consider a simple pure jump process.

3.4.1 Doubly Reflected Brownian Motion

In this example, we establish an implicit equation for $\psi(\theta)$ of the the local time at the lower boundary of a doubly reflected standard Brownian motion. We first find the expression for a Brownian motion with drift and show it reduces to the case we are interested in. In this context the parameter set $\mu(x) = \mu, \sigma(x) = \sigma, \nu(x, dy) = 0, f(x) = 0, \tilde{f}(x, y) = [-(x + y)]^+, r_1 = 1, r_2 = 0$ leads to the differential equation

$$0 = \frac{\sigma^2}{2}u_{xx}(\theta, x) + \mu u_x(\theta, x) - \psi(\theta)u(\theta, x)$$

subject to the boundary conditions

$$\theta u(\theta, 0) = -u_x(\theta, 0), u(\theta, b) = 1, u_x(\theta, b) = 0.$$

This is a linear second order differential equation with constant coefficients and so the

roots of the characteristic equation $\beta^2 + \frac{2\mu}{\sigma^2}\beta - \frac{2\psi(\theta)}{\sigma^2} = 0$ are

$$\beta = \frac{-\frac{2\mu}{\sigma^2} \pm \sqrt{\frac{4\mu^2}{\sigma^4} + 4(\frac{2\psi(\theta)}{\sigma^2})}}{2} = \frac{-\mu \pm \sqrt{\mu^2 + 2\sigma^2\psi(\theta)}}{\sigma^2}$$

The discriminant can be zero, positive or negative. We consider the three cases separately.

Case 1: $\mu^2 + 2\sigma^2\psi(\theta) = 0$. In this case $\beta = -\frac{\mu}{\sigma^2}$, therefore

$$u(\theta, x) = C_1 e^{-\frac{\mu x}{\sigma^2}} + C_2 x e^{-\frac{\mu x}{\sigma^2}} \implies u_x(\theta, x) = -\frac{\mu}{\sigma^2} C_1 e^{-\frac{\mu x}{\sigma^2}} + C_2 e^{-\frac{\mu x}{\sigma^2}} - \frac{\mu}{\sigma^2} C_2 x e^{-\frac{\mu x}{\sigma^2}}.$$

Applying the boundary condition $u_x(\theta, b) = 0$ results in

$$\begin{aligned} u_x(\theta, b) &= -\frac{\mu}{\sigma^2} C_1 e^{-\frac{\mu b}{\sigma^2}} + C_2 e^{-\frac{\mu b}{\sigma^2}} - \frac{\mu}{\sigma^2} C_2 b e^{-\frac{\mu b}{\sigma^2}} = 0 \\ \iff C_1 &= \frac{C_2\left(-e^{-\frac{\mu b}{\sigma^2}} + \frac{\mu}{\sigma^2} b e^{-\frac{\mu b}{\sigma^2}}\right)}{-\frac{\mu}{\sigma^2} e^{-\frac{\mu b}{\sigma^2}}} = \frac{C_2(-1 + \frac{\mu b}{\sigma^2})}{-\frac{\mu}{\sigma^2}} = C_2\left(\frac{\sigma^2}{\mu} - b\right). \end{aligned}$$

Continuing with the boundary condition $u(\theta, b) = 1$ we see that

$$\begin{aligned} u(\theta, b) = C_2\left(\frac{\sigma^2}{\mu} - b\right) e^{-\frac{\mu b}{\sigma^2}} + C_2 b e^{-\frac{\mu b}{\sigma^2}} = 1 &\iff C_2 = \frac{e^{\frac{\mu b}{\sigma^2}}}{\left(\frac{\sigma^2}{\mu} - b\right) + b} = \frac{\mu}{\sigma^2} e^{\frac{\mu b}{\sigma^2}} \\ \implies C_1 = \frac{\mu}{\sigma^2} e^{\frac{\mu b}{\sigma^2}}\left(\frac{\sigma^2}{\mu} - b\right) &= e^{\frac{\mu b}{\sigma^2}}\left(\frac{\sigma^2 - \mu b}{\sigma^2}\right). \end{aligned}$$

Therefore,

$$u(\theta, x) = e^{\frac{\mu(b-x)}{\sigma^2}}\left(\frac{-b\mu + \sigma^2 + \mu x}{\sigma^2}\right) \implies u_x(\theta, x) = e^{\frac{\mu(b-x)}{\sigma^2}}\left(\frac{\mu^2(b-x)}{\sigma^4}\right).$$

Finally, applying the boundary condition $\theta u(\theta, 0) = -u_x(\theta, 0)$ and solving for θ,

$$\theta e^{\frac{\mu b}{\sigma^2}}\left(\frac{-b\mu + \sigma^2}{\sigma^2}\right) = -e^{\frac{\mu b}{\sigma^2}}\left(\frac{\mu^2 b}{\sigma^4}\right) \iff \theta = -\frac{\mu^2 b}{\sigma^2(\sigma^2 - b\mu)}.$$

Case 2: $\mu^2 + 2\sigma^2\psi(\theta) > 0$. For convenience, we will denote $\alpha = \sqrt{\mu^2 + 2\sigma^2\psi(\theta)}$ so that

$\beta_1 = \frac{-\mu+\alpha}{\sigma^2}$ and $\beta_2 = \frac{-\mu-\alpha}{\sigma^2}$. Therefore,

$$u(\theta,x) = C_1 e^{\frac{(\alpha-\mu)x}{\sigma^2}} + C_2 e^{\frac{-(\alpha+\mu)x}{\sigma^2}} \implies u_x(\theta,x) = \frac{C_1(\alpha-\mu)e^{\frac{(\alpha-\mu)x}{\sigma^2}} - C_2(\alpha+\mu)e^{\frac{-(\mu+\alpha)x}{\sigma^2}}}{\sigma^2}.$$

Applying the boundary condition $u_x(\theta,b) = 0$ results in

$$u_x(\theta,b) = \frac{C_1(\alpha-\mu)e^{\frac{(\alpha-\mu)b}{\sigma^2}} - C_2(\alpha+\mu)e^{\frac{-(\mu+\alpha)b}{\sigma^2}}}{\sigma^2} = 0 \iff C_1 = \frac{C_2(\alpha+\mu)e^{-\frac{2\alpha b}{\sigma^2}}}{\alpha-\mu}.$$

Continuing with the boundary condition $u(\theta,b) = 1$ we see that

$$u(\theta,b) = \frac{C_2(\alpha+\mu)e^{-\frac{2\alpha b}{\sigma^2}}}{\alpha-\mu}e^{\frac{(\alpha-\mu)b}{\sigma^2}} + C_2 e^{\frac{-(\alpha+\mu)b}{\sigma^2}} = 1 \iff C_2 = \frac{(\alpha-\mu)e^{-\frac{b(-\alpha-\mu)}{\sigma^2}}}{2\alpha}$$
$$\implies C_1 = \frac{(\alpha+\mu)e^{-\frac{b(\alpha-\mu)}{\sigma^2}}}{2\alpha}.$$

Therefore,

$$u(\theta,x) = \frac{e^{\frac{b(\mu-\alpha)-x(\alpha+\mu)}{\sigma^2}}\left((\alpha-\mu)e^{\frac{2\alpha b}{\sigma^2}} + (\alpha+\mu)e^{\frac{2\alpha x}{\sigma^2}}\right)}{2\alpha}$$

and

$$u_x(\theta,x) = \frac{(\mu-\alpha)(\alpha+\mu)\left(e^{\frac{2\alpha b}{\sigma^2}} - e^{\frac{2\alpha x}{\sigma^2}}\right)e^{\frac{b(\mu-\alpha)-x(\alpha+\mu)}{\sigma^2}}}{2\alpha\sigma^2}$$

. Applying the boundary condition $\theta u(\theta,0) = -u_x(\theta,0)$ results in

$$\theta\left(\frac{e^{\frac{b(\mu-\alpha)}{\sigma^2}}\left((\alpha-\mu)e^{\frac{2\alpha b}{\sigma^2}} + (\alpha+\mu)\right)}{2\alpha}\right) = -\left(\frac{(\mu-\alpha)(\alpha+\mu)\left(e^{\frac{2\alpha b}{\sigma^2}} - 1\right)e^{\frac{b(\mu-\alpha)}{\sigma^2}}}{2\alpha\sigma^2}\right)$$
$$\iff \theta = \frac{(\alpha-\mu)(\alpha+\mu)\left(e^{\frac{2\alpha b}{\sigma^2}} - 1\right)}{\sigma^2\left((\alpha-\mu)e^{\frac{2\alpha b}{\sigma^2}} + (\alpha+\mu)\right)}.$$

Case 3: $\mu^2 + 2\sigma^2\psi(\theta) < 0$. For convenience, we will define $\alpha = \sqrt{-(\mu^2 + 2\sigma^2\psi(\theta))}$ so that $\beta_1 = \frac{-\mu+\alpha i}{\sigma^2}$ and $\beta_2 = \frac{-\mu-\alpha i}{\sigma^2}$. Therefore,

$$u(\theta,x) = e^{-\frac{\mu x}{\sigma^2}}\left(C_1\cos\left(\frac{\alpha x}{\sigma^2}\right) + C_2\sin\left(\frac{\alpha x}{\sigma^2}\right)\right)$$

and

$$u_x(\theta, x) = \frac{e^{-\frac{\mu x}{\sigma^2}} \left((\alpha C_2 - C_1 \mu) \cos\left(\frac{\alpha x}{\sigma^2}\right) - (\alpha C_1 + C_2 \mu) \sin\left(\frac{\alpha x}{\sigma^2}\right) \right)}{\sigma^2}.$$

Applying the boundary condition $u_x(\theta, b) = 0$ results in

$$\begin{aligned} u_x(\theta, b) &= \frac{e^{-\frac{\mu b}{\sigma^2}} \left((\alpha C_2 - C_1 \mu) \cos\left(\frac{\alpha b}{\sigma^2}\right) - (\alpha C_1 + C_2 \mu) \sin\left(\frac{\alpha x}{\sigma^2}\right) \right)}{\sigma^2} = 0 \\ \iff C_1 &= \frac{\alpha C_2 \cos\left(\frac{\alpha b}{\sigma^2}\right) - C_2 \mu \sin\left(\frac{\alpha b}{\sigma^2}\right)}{\mu \cos\left(\frac{\alpha b}{\sigma^2}\right) + \alpha \sin\left(\frac{\alpha b}{\sigma^2}\right)}. \end{aligned}$$

Continuing with the boundary condition $u(\theta, b) = 1$ we see that

$$\begin{aligned} u(\theta, b) &= e^{-\frac{\mu b}{\sigma^2}} \left(\left(\frac{\alpha C_2 \cos\left(\frac{\alpha b}{\sigma^2}\right) - C_2 \mu \sin\left(\frac{\alpha b}{\sigma^2}\right)}{\mu \cos\left(\frac{\alpha b}{\sigma^2}\right) + \alpha \sin\left(\frac{\alpha b}{\sigma^2}\right)} \right) \cos\left(\frac{\alpha b}{\sigma^2}\right) + C_2 \sin\left(\frac{\alpha b}{\sigma^2}\right) \right) = 1 \\ \iff C_2 &= \frac{e^{\frac{b\mu}{\sigma^2}} \left(\mu \cos\left(\frac{\alpha b}{\sigma^2}\right) + \alpha \sin\left(\frac{\alpha b}{\sigma^2}\right) \right)}{\alpha} \implies C_1 = \frac{e^{\frac{b\mu}{\sigma^2}} \left(\alpha \cos\left(\frac{\alpha b}{\sigma^2}\right) - \mu \sin\left(\frac{\alpha b}{\sigma^2}\right) \right)}{\alpha}. \end{aligned}$$

Therefore,

$$u(\theta, x) = \frac{e^{\frac{\mu(b-x)}{\sigma^2}} \left(\alpha \cos\left(\frac{\alpha(b-x)}{\sigma^2}\right) - \mu \sin\left(\frac{\alpha(b-x)}{\sigma^2}\right) \right)}{\alpha}$$

and

$$u_x(\theta, x) = \frac{(\alpha^2 + \mu^2)\, e^{\frac{\mu(b-x)}{\sigma^2}} \sin\left(\frac{\alpha(b-x)}{\sigma^2}\right)}{\alpha \sigma^2}.$$

Finally, applying the boundary condition $\theta u(\theta, 0) = -u_x(\theta, 0)$ results in the expression

$$\begin{aligned} \theta \left(\frac{e^{\frac{\mu b}{\sigma^2}} \left(\alpha \cos\left(\frac{\alpha b}{\sigma^2}\right) - \mu \sin\left(\frac{\alpha b}{\sigma^2}\right) \right)}{\alpha} \right) &= - \left(\frac{(\alpha^2 + \mu^2)\, e^{\frac{\mu b}{\sigma^2}} \sin\left(\frac{\alpha b}{\sigma^2}\right)}{\alpha \sigma^2} \right) \\ \iff \theta &= \frac{(\alpha^2 + \mu^2) \sin\left(\frac{\alpha b}{\sigma^2}\right)}{\sigma^2 \left(\mu \sin\left(\frac{\alpha b}{\sigma^2}\right) - \alpha \cos\left(\frac{\alpha b}{\sigma^2}\right) \right)}. \end{aligned}$$

We consider the particular case of standard Brownian motion with $\mu = 0$ and $\sigma = 1$. In this case $\sqrt{\mu^2 + 2\sigma^2 \psi(\theta)} = \sqrt{2\psi(\theta)}$. For

Case 1:

$\mu^2 + 2\sigma^2 \psi(\theta) = 0$ then $\psi(\theta) = 0$ and $\theta = 0$.

Case 2:

$\mu^2 + 2\sigma^2\psi(\theta) > 0$ then $\psi(\theta) > 0$ and $\theta = \dfrac{2\psi(\theta)\left(e^{2\sqrt{2\psi(\theta)}b} - 1\right)}{\sqrt{2\psi(\theta)}\left(e^{2\sqrt{2\psi(\theta)}b} + 1\right)}$

$= \sqrt{2\psi(\theta)}\tanh\left(b\sqrt{2\psi(\theta)}\right) > 0.$

Case 3:

$\mu^2 + 2\sigma^2\psi(\theta) < 0$ then $\psi(\theta) < 0$ and $\theta = \dfrac{-2\psi(\theta)\sin(b\sqrt{-2\psi(\theta)})}{-\sqrt{-2\psi(\theta)}\cos(b\sqrt{-2\psi(\theta)})}$

$= -\sqrt{-2\psi(\theta)}\tan(b\sqrt{-2\psi(\theta)})$. To ensure it is invertible, we restrict

$-\dfrac{\pi}{2} < b\sqrt{-2\psi(\theta)} < \dfrac{\pi}{2} \implies \dfrac{-\pi^2}{8b^2} < \psi(\theta) < 0 \implies \theta < 0.$

After applying the identity $\tanh(x) = -i\tan(ix)$, we note that this last equality is equal to $-\sqrt{i^2 2\psi(\theta)}\tan(b\sqrt{i^2 2\psi(\theta)}) = \sqrt{2\psi(\theta)}\tanh(b\sqrt{2\psi(\theta)})$.

Therefore, Case 2 and Case 3 are identical and after noting that $\sqrt{2\psi(\theta)}\tanh(b\sqrt{2\psi(\theta)}) = 0$ implies $\psi(\theta) = 0$, given the range of $\psi(\theta) \in (-\frac{\pi^2}{8b^2}, \infty)$, then $\psi(\theta)$ may be solved numerically using the implicit formula

$$\theta = \sqrt{2\psi(\theta)}\tanh(b\sqrt{2\psi(\theta)}).$$

This agrees with the result found in [7].

For the simulations we will carry out in Chapter 4, we set $b = 1$ and solve $\theta = \sqrt{2\psi(\theta)}\tanh(\sqrt{2\psi(\theta)})$.

3.4.2 Doubly Reflected Pure Jump Process

For this example, we are interested in constructing a simple pure jump process that has equal probability of jumping up one and of jumping down one with constant arrival $\lambda(x) = \lambda > 0$. As before, we are considering the local time at the lower boundary. In this context the parameter set $\mu(x) = 0, \sigma(x) = 0, \nu(x,1) = \frac{\lambda}{2}, \nu(x,-1) = \frac{\lambda}{2}, f(x) = 0, \tilde{f}(x,y) = [-(x+y)]^+, r_1 = 1, r_2 = 0$ leads to the recurrence relation

$$0 = -(\lambda + \psi(\theta))u(\theta,x) + \frac{\lambda}{2}\left(e^{\theta[-(x+1)]^+}u(\theta, r(x,1))\right) + \frac{\lambda}{2}\left(e^{\theta[-(x-1)]^+}u(\theta, r(x,-1))\right)$$

subject to the boundary conditions

$$\theta u(\theta,0) = -u_x(\theta,0), u(\theta,b) = 1, u_x(\theta,b) = 0.$$

There are three cases to consider which lead to three different recurrence relations that must be satisfied. When:

$$x = 0 : 0 = -(\lambda + \psi(\theta))u(\theta,0) + \frac{\lambda}{2}u(\theta,1) + \frac{\lambda}{2}e^{\theta}u(\theta,0); \tag{3.4.1}$$

$$x \in [1, b-1] : 0 = -(\lambda + \psi(\theta))u(\theta,x) + \frac{\lambda}{2}u(\theta,x+1) + \frac{\lambda}{2}u(\theta,x-1); \tag{3.4.2}$$

$$x = b : 0 = -(\lambda + \psi(\theta))u(\theta,b) + \frac{\lambda}{2}u(\theta,b) + \frac{\lambda}{2}u(\theta,b-1). \tag{3.4.3}$$

Applying the boundary condition $u(\theta,b) = 1$ to (3.4.3), we see that $u(\theta,b-1)$ must satisfy

$$u(\theta,b-1) = 1 + \frac{2}{\lambda}\psi(\theta).$$

If we let $x = b-1$ in (3.4.2) then we may derive an expression for $u(\theta,b-2)$ as

$$\begin{aligned} 0 &= -(\lambda + \psi(\theta))u(\theta,b-1) + \frac{\lambda}{2}u(\theta,b) + \frac{\lambda}{2}u(\theta,b-2) \\ \iff u(\theta,b-2) &= \frac{\lambda^2 + 6\lambda\psi(\theta) + 4\psi(\theta)^2}{\lambda^2}. \end{aligned}$$

Using (3.4.1), we may derive an expression for $u(\theta,0)$,

$$u(\theta,0) = \frac{u(\theta,1)}{\frac{2}{\lambda}(\lambda + \psi(\theta)) - e^{\theta}}.$$

Similarly, from (3.4.2), we set $x = 1$ then $u(\theta,0)$ must satisfy

$$\begin{aligned} 0 &= -(\lambda + \psi(\theta))u(\theta,1) + \frac{\lambda}{2}u(\theta,2) + \frac{\lambda}{2}u(\theta,0) \\ \iff u(\theta,0) &= \frac{2}{\lambda}(\lambda + \psi(\theta))u(\theta,1) - u(\theta,2). \end{aligned}$$

Setting these two equations for $u(\theta,0)$ equal to each other,

$$\frac{u(\theta,1)}{\frac{2}{\lambda}(\lambda+\psi(\theta))-e^{\theta}}=\frac{2}{\lambda}(\lambda+\psi(\theta))u(\theta,1)-u(\theta,2). \tag{3.4.4}$$

Furthermore, we may solve (3.4.2) by letting $\beta^x=u(\theta,x)$ then

$$\begin{aligned}0&=-(\lambda+\psi(\theta))\beta^x+\frac{\lambda}{2}\beta^{x+1}+\frac{\lambda}{2}\beta^{x-1}\\ \iff 0&=\beta^2-\frac{2}{\lambda}(\lambda+\psi(\theta))\beta+1.\end{aligned}$$

Solving for β,

$$\begin{aligned}\beta=&\frac{\frac{2}{\lambda}(\lambda+\psi(\theta))\pm\sqrt{\frac{4}{\lambda^2}(\lambda+\psi(\theta))^2-4}}{2}\\ =&\left(1+\frac{\psi(\theta)}{\lambda}\right)\pm\sqrt{\frac{\psi(\theta)}{\lambda}\left(\frac{\psi(\theta)}{\lambda}+2\right)}.\end{aligned}$$

We consider the three cases for the discriminant individually.

Case 1: $\frac{\psi(\theta)}{\lambda}\left(\frac{\psi(\theta)}{\lambda}+2\right)=0 \iff \psi(\theta)=0$ or $\psi(\theta)=-2\lambda$ then

$$u(\theta,x)=C_1\left(1+\frac{\psi(\theta)}{\lambda}\right)^x+C_2x\left(1+\frac{\psi(\theta)}{\lambda}\right)^x.$$

Solving

$$\begin{aligned}u(\theta,b-1)&=C_1\left(1+\frac{\psi(\theta)}{\lambda}\right)^{b-1}+C_2(b-1)\left(1+\frac{\psi(\theta)}{\lambda}\right)^{b-1}=1+\frac{2}{\lambda}\psi(\theta)\\ u(\theta,b-2)&=C_1\left(1+\frac{\psi(\theta)}{\lambda}\right)^{b-2}+C_2(b-2)\left(1+\frac{\psi(\theta)}{\lambda}\right)^{b-2}=\frac{\lambda^2+6\lambda\psi(\theta)+4\psi(\theta)^2}{\lambda^2}\end{aligned}$$

for C_1 and C_2, we find that

$$\begin{aligned}u(\theta,x)=&\frac{\left(\frac{\lambda+\psi(\theta)}{\lambda}\right)^{-b+x+1}(\lambda^2\psi(\theta)(5b-5x-3)+10\lambda\psi(\theta)^2(b-x-1))}{\lambda^3}\\ &+\frac{\left(\frac{\lambda+\psi(\theta)}{\lambda}\right)^{-b+x+1}(4\psi(\theta)^3(b-x-1)+\lambda^3)}{\lambda^3}.\end{aligned}$$

Now that we have an equation for $u(\theta, x)$, we may use it to solve (3.4) and find that $\theta = \log(\frac{A}{B})$ where

$$\begin{aligned}
A =&(5b+6)\lambda^4\psi(\theta) + 10(3b-1)\lambda^3\psi(\theta)^2 + 2(27b-23)\lambda^2\psi(\theta)^3 + 36(b-1)\lambda\psi(\theta)^4 \\
&+ 8(b-1)\psi(\theta)^5 + \lambda^5 \\
B =&\lambda(\lambda+\psi(\theta))\left((5b-3)\lambda^2\psi(\theta) + 10(b-1)\lambda\psi(\theta)^2 + 4(b-1)\psi(\theta)^3 + \lambda^3\right).
\end{aligned}$$

Case 2: $\frac{\psi(\theta)}{\lambda}\left(\frac{\psi(\theta)}{\lambda}+2\right) > 0 \iff \psi(\theta) > 0$ or $\psi(\theta) < -2\lambda$ then

$$\begin{aligned}
u(\theta, x) =&C_1\left(\left(1+\frac{\psi(\theta)}{\lambda}\right) + \sqrt{\frac{\psi(\theta)}{\lambda}\left(\frac{\psi(\theta)}{\lambda}+2\right)}\right)^x \\
&+ C_2\left(\left(1+\frac{\psi(\theta)}{\lambda}\right) - \sqrt{\frac{\psi(\theta)}{\lambda}\left(\frac{\psi(\theta)}{\lambda}+2\right)}\right)^x.
\end{aligned}$$

Solving

$$\begin{aligned}
u(\theta, b-1) =&C_1\left(\left(1+\frac{\psi(\theta)}{\lambda}\right) + \sqrt{\frac{\psi(\theta)}{\lambda}\left(\frac{\psi(\theta)}{\lambda}+2\right)}\right)^{b-1} \\
&+ C_2\left(\left(1+\frac{\psi(\theta)}{\lambda}\right) - \sqrt{\frac{\psi(\theta)}{\lambda}\left(\frac{\psi(\theta)}{\lambda}+2\right)}\right)^{b-1} \\
=&1 + \frac{2}{\lambda}\psi(\theta) \\
u(\theta, b-2) =&C_1\left(\left(1+\frac{\psi(\theta)}{\lambda}\right) + \sqrt{\frac{\psi(\theta)}{\lambda}\left(\frac{\psi(\theta)}{\lambda}+2\right)}\right)^{b-2} \\
&+ C_2\left(\left(1+\frac{\psi(\theta)}{\lambda}\right) - \sqrt{\frac{\psi(\theta)}{\lambda}\left(\frac{\psi(\theta)}{\lambda}+2\right)}\right)^{b-2} \\
=&\frac{\lambda^2 + 6\lambda\psi(\theta) + 4\psi(\theta)^2}{\lambda^2}
\end{aligned}$$

for C_1 and C_2, we find that

$$
\begin{aligned}
u(\theta,x) =& \frac{1}{2}\left(-\sqrt{\frac{\psi(\theta)(2\lambda+\psi(\theta))}{\lambda^2}}+\frac{\psi(\theta)}{\lambda}+1\right)^{x-b} \\
&+\frac{1}{2}\left(\sqrt{\frac{\psi(\theta)(2\lambda+\psi(\theta))}{\lambda^2}}+\frac{\psi(\theta)}{\lambda}+1\right)^{x-b} \\
&+\frac{\psi(\theta)}{2}\left(\frac{\left(-\sqrt{\frac{\psi(\theta)(2\lambda+\psi(\theta))}{\lambda^2}}+\frac{\psi(\theta)}{\lambda}+1\right)^{x-b}}{\lambda\sqrt{\frac{\psi(\theta)(2\lambda+\psi(\theta))}{\lambda^2}}}\right) \\
&-\frac{\psi(\theta)}{2}\left(\frac{\left(\sqrt{\frac{\psi(\theta)i(2\lambda+\psi(\theta))}{\lambda^2}}+\frac{\psi(\theta)}{\lambda}+1\right)^{x-b}}{\lambda\sqrt{\frac{\psi(\theta)(2\lambda+\psi(\theta))}{\lambda^2}}}\right).
\end{aligned}
$$

Now that we have an equation for $u(\theta,x)$, we may use it to solve (3.4) and find that $\theta=\log(\frac{A}{B})$ where

$$
\begin{aligned}
A =& -2\psi(\theta)^2\left(-\sqrt{\frac{\psi(\theta)(2\lambda+\psi(\theta))}{\lambda^2}}+\frac{\psi(\theta)}{\lambda}+1\right)^{b} \\
&+2\psi(\theta)^2\left(\sqrt{\frac{\psi(\theta)(2\lambda+\psi(\theta))}{\lambda^2}}+\frac{\psi(\theta)}{\lambda}+1\right)^{b} \\
&+\lambda^2\sqrt{\frac{\psi(\theta)(2\lambda+\psi(\theta))}{\lambda^2}}\left(-\sqrt{\frac{\psi(\theta)(2\lambda+\psi(\theta))}{\lambda^2}}+\frac{\psi(\theta)}{\lambda}+1\right)^{b} \\
&+\lambda^2\sqrt{\frac{\psi(\theta)(2\lambda+\psi(\theta))}{\lambda^2}}\left(\sqrt{\frac{\psi(\theta)(2\lambda+\psi(\theta))}{\lambda^2}}+\frac{\psi(\theta)}{\lambda}+1\right)^{b} \\
&+\lambda\psi(\theta)\left((2\sqrt{\frac{\psi(\theta)(2\lambda+\psi(\theta))}{\lambda^2}}\left(-\sqrt{\frac{\psi(\theta)(2\lambda+\psi(\theta))}{\lambda^2}}+\frac{\psi(\theta)}{\lambda}+1\right)^{b}\right. \\
&-3\left(-\sqrt{\frac{\psi(\theta)(2\lambda+\psi(\theta))}{\lambda^2}}+\frac{\psi(\theta)}{\lambda}+1\right)^{b} \\
&+2\sqrt{\frac{\psi(\theta)(2\lambda+\psi(\theta))}{\lambda^2}}\left(\sqrt{\frac{\psi(\theta)(2\lambda+\psi(\theta))}{\lambda^2}}+\frac{\psi(\theta)}{\lambda}+1\right)^{b}
\end{aligned}
$$

$$
\begin{aligned}
&+3\left(\sqrt{\frac{\psi(\theta)(2\lambda+\psi(\theta))}{\lambda^2}}+\frac{\psi(\theta)}{\lambda}+1\right)^b\Bigg)\\
B=&\lambda\left(\lambda\sqrt{\frac{\psi(\theta)(2\lambda+\psi(\theta))}{\lambda^2}}\left(-\sqrt{\frac{\psi(\theta)(2\lambda+\psi(\theta))}{\lambda^2}}+\frac{\psi(\theta)}{\lambda}+1\right)^b\right.\\
&+\lambda\sqrt{\frac{\psi(\theta)(2\lambda+\psi(\theta))}{\lambda^2}}\left(\sqrt{\frac{\psi(\theta)(2\lambda+\psi(\theta))}{\lambda^2}}+\frac{\psi(\theta)}{\lambda}+1\right)^b\\
&-\psi(\theta)\left(-\sqrt{\frac{\psi(\theta)(2\lambda+\psi(\theta))}{\lambda^2}}+\frac{\psi(\theta)}{\lambda}+1\right)^b\\
&\left.+\psi(\theta)\left(\sqrt{\frac{\psi(\theta)(2\lambda+\psi(\theta))}{\lambda^2}}+\frac{\psi(\theta)}{\lambda}+1\right)^b\right).
\end{aligned}
$$

Case 3: $\frac{\psi(\theta)}{\lambda}\left(\frac{\psi(\theta)}{\lambda}+2\right)>0 \iff -2\lambda<\psi(\theta)<0$ then

$$
\begin{aligned}
u(\theta,x)=&\tilde{C_1}\left(\left(1+\frac{\psi(\theta)}{\lambda}\right)+i\sqrt{-\frac{\psi(\theta)}{\lambda}\left(\frac{\psi(\theta)}{\lambda}+2\right)}\right)^x\\
&+\tilde{C_2}\left(\left(1+\frac{\psi(\theta)}{\lambda}\right)-i\sqrt{-\frac{\psi(\theta)}{\lambda}\left(\frac{\psi(\theta)}{\lambda}+2\right)}\right)^x.
\end{aligned}
$$

We then convert to trigonometric form and apply De Moivre's theorem,

$$u(\theta,x)=C_1\cos(\varphi x)+C_2\sin(\varphi x)$$

where φ solves $\cos(\varphi)=\left(1+\frac{\psi(\theta)}{\lambda}\right)$ and $\sin(\varphi)=\sqrt{-\frac{\psi(\theta)}{\lambda}\left(\frac{\psi(\theta)}{\lambda}+2\right)}$. Solving

$$
\begin{aligned}
u(\theta,b-1)&=C_1\cos(\varphi(b-1))+C_2\sin(\varphi(b-1))=1+\frac{2}{\lambda}\psi(\theta)\\
u(\theta,b-2)&=C_1\cos(\varphi(b-2))+C_2\sin(\varphi(b-2))=\frac{\lambda^2+6\lambda\psi(\theta)+4\psi(\theta)^2}{\lambda^2}
\end{aligned}
$$

for C_1 and C_2, we find that

$$u(\theta,x)=-\frac{\csc(\varphi)\lambda(\lambda+2\psi(\theta))\sin(\varphi(b-x-2))}{\lambda^2}$$

$$+\frac{\csc(\varphi)\left(\lambda^2+6\lambda\psi(\theta)+4\psi(\theta)^2\right)\sin(\varphi(b-x-1))}{\lambda^2}.$$

Now that we have an equation for $u(\theta,x)$, we may use it to solve (3.4) and find that $\theta=\log(\frac{A}{B})$ where

$$\begin{aligned}
A =&2\lambda^2\left(\lambda^2+3\lambda\psi(\theta)+2\psi(\theta)^2\right)\sin((b-4)\varphi)\\
&-\lambda\left(5\lambda^3+28\lambda^2\psi(\theta)+40\lambda\psi(\theta)^2+16\psi(\theta)^3\right)\sin((b-3)\varphi)\\
&+\left(3\lambda^4+26\lambda^3\psi(\theta)+64\lambda^2\psi(\theta)^2+56\lambda\psi(\theta)^3+16\psi(\theta)^4\right)\sin((b-2)\varphi)\\
B =&\lambda(-\lambda\left(3\lambda^2+12\lambda\psi(\theta)+8\psi(\theta)^2\right)\sin((b-3)\varphi)+\lambda^2(\lambda+2\psi(\theta))\sin((b-4)\varphi)\\
&+2\left(\lambda^3+7\lambda^2\psi(\theta)+10\lambda\psi(\theta)^2+4\psi(\theta)^3\right)\sin((b-2)\varphi))
\end{aligned}$$

For the purpose of the simulations, we will set $\lambda=50$ and $b=3$ which reduces our three cases to:

Case 1:

$$\theta=\log\left(\frac{16\psi(\theta)^5+3600\psi(\theta)^4+290000\psi(\theta)^3+10000000\psi(\theta)^2}{50(\psi(\theta)+50)\left(8\psi(\theta)^3+1000\psi(\theta)^2+30000\psi(\theta)+125000\right)}\right.$$
$$\left.+\frac{131250000\psi(\theta)+312500000}{50(\psi(\theta)+50)\left(8\psi(\theta)^3+1000\psi(\theta)^2+30000\psi(\theta)+125000\right)}\right)$$

Case 2:

$$\theta=\log\left(\frac{\psi(\theta)^4+175\psi(\theta)^3+9375\psi(\theta)^2+156250\psi(\theta)+390625}{25\left(\psi(\theta)^3+125\psi(\theta)^2+3750\psi(\theta)+15625\right)}\right)$$

Case 3:

$$\theta=\log\left(\frac{\psi(\theta)^4+175\psi(\theta)^3+9375\psi(\theta)^2+156250\psi(\theta)+390625}{25\left(\psi(\theta)^3+125\psi(\theta)^2+3750\psi(\theta)+15625\right)}\right)$$

As can be seen, Case 2 and Case 3 reduce to the same equation and if $\psi(\theta)=0$ then so is θ. If we set $\psi(\theta)=0$ in Case 1, then $\theta=0$ and if we set $\psi(\theta)=-100$, $\theta=\log(\frac{9}{7})+i\pi\notin\mathbb{R}$ and so -100 is not in the range of $\psi(\theta)$.

To summarize, we may solve for $\psi(\theta)$ implicitly in the equation

$$\theta=\log\left(\frac{\psi(\theta)^4+175\psi(\theta)^3+9375\psi(\theta)^2+156250\psi(\theta)+390625}{25\left(\psi(\theta)^3+125\psi(\theta)^2+3750\psi(\theta)+15625\right)}\right).$$

Chapter 4

Simulation and Numerics

4.1 Algorithms

Unlike the two examples proposed in Chapter 3, some models are too computationally intractable to have closed form solutions. In this section, we present the main algorithms used to put the theory of the previous chapter into practice. First we implement a Monte Carlo scheme based on the previous results and then we numerically solve the integro-differential equation (3.3.1). The former method requires that we simulate many paths of the reflected jump diffusion, which we introduce first by slightly modifying an algorithm for simulating jump diffusions shown in [9].

4.1.1 Reflected Jump Diffusion Path Simulation

The challenge with simulating a jump diffusion is that the jump intensity may depend on the position of the process right before the jump. As such, attempting to simulate the continuous part and the jump parts separately is futile. One way to work around this is to apply a stochastic time change so that the new process will have the same intensity as a Poisson process with unit intensity.

Following the work in [9], we let $\mathcal{E}_n$ and Z_n be i.i.d. sequences of standard exponentials and $\rho-$distributed random variables, respectively. We define a new process $\tilde{X}$ with $\tilde{X}_0 = x_0$

and an increasing sequence of jump times $0 = \tau_0 < \tau_1 < \tau_2 < ...$ such that

$$\tilde{X}(t) = \tilde{X}(\tau_n) + \int_{\tau_n}^{t} \mu(V(s))ds + \int_{\tau_n}^{t} \sigma(V(s))dW(s)$$

for $t \in [\tau_n, \tau_{n+1})$, with

$$\tau_{n+1} = \inf\left\{t > \tau_n : \int_{\tau_n}^{t} \lambda(V(s))ds \geq \mathcal{E}_{n+1}\right\}$$

and with jump update

$$\tilde{X}(\tau_{n+1}) = \tilde{X}(\tau_{n+1-}) + \gamma(V(\tau_{n+1-}), Z_{n+1}).$$

Finally, we define the process $A(t) = \int_0^t \lambda(V(s))ds$.

Essentially, our new process $\tilde{X}$ is defined recursively in such a way that we consider the process as a diffusion with the same parameters of our original jump diffusion up to a jump and repeat throughout. τ is defined as the stochastic change of time, where the intensity of the original process X is scaled to match that of a Poisson process. If we observe $\tilde{X}$ at the times τ_n then the time change has constant intensity $\lambda = 1$.

It is immediately clear that between jump times, X and $\tilde{X}$ have the same distribution as it has the same drift and volatility. It can be shown that $(X(t))_{t\geq 0}$ and $(\tilde{X}(t))_{t\geq 0}$ are in fact equal in distribution [9]. So we may use $\tilde{X}$ to simulate for X.

In order to update the reflected process V between jumps, that is on $[\tau_n, \tau_{n+1})$, we need to first update U and L by checking if a jump over a boundary happens and whether there have been any continuous crossings. Therefore, define

$$\begin{aligned}
L(t) &= L(\tau_n) + [a - (V(\tau_{n-}) + \Delta\tilde{X}(\tau_n))]^+ + \int_{\tau_n}^{t} dL^c(s), \\
U(t) &= U(\tau_n) + [(V(\tau_{n-}) + \Delta\tilde{X}(\tau_n)) - b]^+ + \int_{\tau_n}^{t} dU^c(s), \text{ and} \\
V(t) &= V(\tau_n) + \int_{\tau_n}^{t} d\tilde{X}(s) + \int_{\tau_n}^{t} dL(s) - \int_{\tau_n}^{t} dU(s)
\end{aligned}$$

where a and b are the lower and upper boundaries, respectively.

With this, we may apply the Euler-Maruyama discretization by setting $h = \frac{T}{N}$ where T is the total time interval and N is the total number of steps. We use the superscript h to denote the discretized path of the process and subscript i to denote the current interval step. The usual approximation is given by

$$\begin{aligned} X^h_{t_{i+1-}} &= X^h_{t_i} + \mu(V^h_{t_i})(t_{i+1} - t_i) + \sigma(V^h_{t_i})(W_{t_{i+1}} - W_{t_i}) \\ A^h_{t_{i+1}} &= A^h_{t_i} + \lambda(V^h_{t_i})(t_{i+1} - t_i) \end{aligned}$$

at the discretization times t_i and

$$\begin{aligned} X^h_t &= X^h_{t_i} + \mu(V^h_{t_i})(t - t_i) + \sigma(V^h_{t_i})(W_t - W_{t_i}) \\ A^h_t &= A^h_{t_i} + \lambda(V^h_{t_i})(t - t_i) \end{aligned}$$

between discretization times where $t \in [t_i, t_{i+1})$. We note that for the nth approximate jump time and $\eta^h_n = \inf\{t_i : A^h_{t_i} + \lambda(V^h_{t_i})\left(\left(\left\lfloor \frac{t_i}{h} \right\rfloor + 1\right) h - t_i\right) > E_n\}$, the last discretization time before the jump,

$$\begin{aligned} \tau^h_n =& \inf\{t : A^h_t \geq E_n\} \\ =& \inf\{t : A^h_{t_i} + \lambda(V^h_{t_i})(t - t_i) \geq E_n\} \\ =& \inf\{t_i : A^h_{t_i} + \lambda(V^h_{t_i})\left(\left(\left\lfloor \frac{t_i}{h} \right\rfloor + 1\right) h - t_i\right) > E_n\} \\ &+ \inf\{t - t_{\eta^h_n} : A^h_{\eta^h_n} + \lambda(V^h_{\eta^h_n})(t - t_{\eta^h_n}) = E_n\} \\ =& \eta^h_n + \frac{E_n - A^h_{\eta^h_n}}{\lambda(V^h_{\eta^h_n})} \end{aligned}$$

where the second to last equality follows since A^h_t is linearly increasing.

Finally, the jump update takes the form,

$$X^h_{\tau^h_n} = X^h_{\tau^h_n -} + \gamma(V^h_{\tau^h_n -}, Z_n).$$

We may follow the same discretization scheme for the processes used to reflect $\tilde{X}$. At each interval step t_{i+1}, we verify whether $V^h_{t_{i+1}}$ would cross either an upper or lower boundary

and update $L^h_{t_{i+1}}$ and $U^h_{t_{i+1}}$ accordingly to ensure that when $V^h_{t_{i+1}}$ is updated, it stays within its boundaries,

$$\begin{aligned}
L^h_{t_{i+1}} &= L^h_{t_i} + \max[0, a - ((X^h_{t_{i+1}} - X^h_{t_i}) + V^h_{t_i})] \\
U^h_{t_{i+1}} &= U^h_{t_i} + \max[0, ((X^h_{t_{i+1}} - X^h_{t_i}) + V^h_{t_i}) - b] \\
V^h_{t_{i+1}} &= V^h_{t_i} + (X^h_{t_{i+1}} - X^h_{t_i}) + (L^h_{t_{i+1}} - L^h_{t_i}) - (U^h_{t_{i+1}} - U^h_{t_i}).
\end{aligned}$$

Likewise, if a jump occurs between interval steps at $t \in [t_i, t_{i+1})$,

$$\begin{aligned}
L^h_t &= L^h_{t_i} + \max[0, a - ((X^h_t - X^h_{t_i}) + V^h_{t_i})] \\
U^h_t &= U^h_{t_i} + \max[0, ((X^h_t - X^h_{t_i}) + V^h_{t_i}) - b] \\
V^h_t &= V^h_{t_i} + (X^h_t - X^h_{t_i}) + (L^h_t - L^h_{t_i}) - (U^h_t - U^h_{t_i}).
\end{aligned}$$

Pseudo-Code

Let $\mathcal{N}$ be a standard normal random variable and let $\mathcal{E}$ be a standard exponential random variable. The input parameters are: T for the total time, N for the number of interval steps, x_0 for the starting value of $\tilde{X}$, v_0 for the starting value of V, a for the lower boundary and b for the upper boundary. The particular implementation for this thesis may be found in the appendix.

procedure PATHSIM$V(T, N, x_0, v_0, a, b)$
  Set $h \leftarrow \frac{T}{N}$
  Initialize $i = n = s \leftarrow 0, X^h_s \leftarrow x_0, V^h_s \leftarrow v_0, A^h_s = L^h_s = U^h_s \leftarrow 0, E = \mathcal{E}$
  while $s \neq T$ **do**
    Compute $A^h_{\text{temp}} = A^h_s + \lambda(V^h_s)((i+1)h - s)$
    if $A^h_{\text{temp}} \geq E$ **then** ▷ jump between s and $(i+h)h$
      Compute $\tau^h_n = s + \frac{E - A^h_s}{\lambda(V^h_s)}$
      Compute $X^h_{\tau^h_{n-}} = X^h_s + \mu(V^h_s)(\tau^h_n - s) + \sigma(V^h_s)\sqrt{\tau^h_n - s}\mathcal{N}$
      Compute $X^h_{\tau^h_n} = X^h_{\tau^h_{n-}} + \gamma(V^h_{\tau^h_{n-}}, Z_n)$
      Compute $L^h_{\tau^h_n} = L^h_s + \max[0, a - ((X^h_{\tau^h_n} - X^h_{\tau^h_{n-}}) + V_{\tau^h_{n-}})]$

11: **Compute** $U^h_{\tau^h_n} = U^h_s + \max[0, ((X^h_{\tau^h_n} - X^h_{\tau^h_{n-}}) + V_{\tau^h_{n-}}) - b]$

12: **Compute** $V^h_{\tau^h_n} = V^h_s + (X^h_{\tau^h_n} - X^h_{\tau^h_{n-}}) + (L^h_{\tau^h_n} - L^h_s) - (U^h_{\tau^h_n} - U^h_s)$

13: **Set** $s \leftarrow \tau^h_n, A^h_s \leftarrow E, n \leftarrow n+1, E \leftarrow E + \mathcal{E}$

14: **else** ▷ no jump between s and $(i+h)h$

15: **Compute** $X^h_{(i+1)h} = X^h_s + \mu(V^h_s)((i+1)h - s) + \sigma(V^h_s)\sqrt{(i+1)h - s}\mathcal{N}$

16: **Set** $s \leftarrow (i+1)h, A^h_s \leftarrow A^h_{\text{temp}}, i \leftarrow i+1$

17: **Compute** $L^h_s = L^h_{(i-1)h} + \max[0, a - ((X^h_s - X^h_{(i-1)h}) + V^h_{(i-1)h})]$

18: **Compute** $U^h_s = U^h_{(i-1)h} + \max[0, ((X^h_s - X^h_{(i-1)h}) + V^h_{(i-1)h}) - b]$

19: **Compute** $V^h_s = V^h_{(i-1)h} + (X^h_s - X^h_{(i-1)h}) + (L^h_s - L^h_{(i-1)h}) - (U^h_s - U^h_{(i-1)h})$

4.1.2 Simulation Methods for $\psi(\theta)$

We consider the first of our algorithms for approximating $\psi(\theta)$ for given values of θ. Recall the result from Chapter 3, $\lim_{t\to\infty} \frac{1}{t}\log \mathbb{E}[e^{\theta\Lambda(t)}] = \psi(\theta)$. Our objective will be to numerically simulate this limit and in the process approximate $\psi(\theta)$.

The Monte Carlo method allows us to evaluate $\mathbb{E}[e^{\theta\Lambda(t)}]$ by repeatedly sampling $\Lambda(t)$ from simulations of $V(t)$ and taking an appropriate average. For k samples of $\Lambda(t)$, where the i^{th} sample is denoted by $\Lambda_i(t)$, and by letting c be the maximal $\theta\Lambda_i(t)$, we see that

$$\begin{aligned}
\lim_{t\to\infty} \frac{1}{t}\log \mathbb{E}[e^{\theta\Lambda(t)}] = \psi(\theta) &\iff \frac{1}{t}\log \mathbb{E}[e^{\theta\Lambda(t)}] = \psi(\theta) + o(t) \\
&\iff \frac{1}{t}\log \mathbb{E}[\frac{e^c}{e^c}e^{\theta\Lambda(t)}] = \psi(\theta) + o(t) \\
&\iff \frac{c}{t} + \frac{1}{t}\log \mathbb{E}[e^{\theta\Lambda(t)-c}] = \psi(\theta) + o(t) \\
&\implies \frac{c}{t} + \frac{1}{t}\log \frac{1}{k}\sum_{i=1}^{k}[e^{\theta\Lambda_i(t)-c}] \approx \psi(\theta).
\end{aligned}$$

While running the simulation in practice, we will be increasing the value of t which will cause samples of $\Lambda_i(t)$ to grow relatively large. We introduce c so as to avoid the finite capacity of the computer from returning a value of infinity when the answer should not be infinite.

This method of approximating $\psi(\theta)$ will inevitably give rise to two types of errors, the

estimation error from the Monte Carlo estimate of the expectation and the truncation error resulting from having to choose a fixed value for t. Since any errors in the estimation of $\Lambda_i(t)$ are being exponentiated, we would expect that for larger values of θ, the estimate will increasingly diverge from its true value.

Pseudo-Code

Let T, N, x_0, v_0, a, b be as above. Let k be the desired number of simulations of $\Lambda(t)$ and let $\bar{\theta} = (\theta^1, \theta^2, ...\theta^l)$. This method requires that the path simulation algorithm from the previous subsection, *PathSimV*, return the value of the local time at the last iteration step and it stores this value in a variable L.

1: **procedure** PsiThetaMC($T, N, x_0, v_0, a, b, k, \bar{\theta}$)
2: **Initialize** $L_T = (L_T^1 = 0, L_T^2 = 0, ..., L_T^k = 0)$
3: **for** i in $1 : k$ **do**
4: **Compute** $L_T^i \leftarrow$ PathSimV(T, N, x_0, v_0, a, b)
5: **Initialize** $\psi(\bar{\theta})$
6: **for** j in $1 : l$ **do**
7: **Compute** $c \leftarrow \max[\theta^j L_T]$
8: **Compute** $\psi(\theta^j) = \frac{c}{T} + \frac{1}{T}\log\left(\frac{1}{k}\sum_{i=1}^{k} e^{\theta^j L_T^i - c}\right)$
9: **return** $\psi(\bar{\theta})$

Before moving on to numerically solving the integro-differential equation, we present two modifications to this algorithm. If implemented as suggested, the following algorithms produce inferior results to the aforementioned algorithm. However, it is believed that with more work, these algorithms may produce reasonable results.

An immediate way to improve on using the limit definition above would be to arrive at an equation for $\psi(\theta)$ by solving for $u(\theta, x)$. We recall $M(\theta, t) = e^{\theta\Lambda(t) - \psi(\theta)t}u(\theta, V(t))$ is a martingale so that $\mathbb{E}[M(\theta, t)] = \mathbb{E}[M(\theta, 0)] = 1$. Then by conditioning

$$\begin{aligned} &\mathbb{E}[e^{\theta\Lambda(t) - \psi(\theta)t}u(\theta, V(t))] = 1 \\ \iff &\mathbb{E}[\mathbb{E}[e^{\theta\Lambda(t) - \psi(\theta)t}u(\theta, V(t))]|V(t) = x] = \mathbb{E}[1|V(t) = x] \end{aligned}$$

$$\iff u(\theta,x)\mathbb{E}[e^{\theta\Lambda(t)}|V(t)=x]=e^{\psi(\theta)t}$$
$$\iff \frac{1}{t}\log u(\theta,x)+\frac{1}{t}\log\mathbb{E}[e^{\theta\Lambda(t)}|V(t)=x]=\psi(\theta)$$

Now we only need one boundary point to solve for $\psi(\theta)$. We will continue with the lower boundary local time, then $r_1=1$ and $r_2=0$ which gives us the boundary point $u(\theta,b)=1$. This point is ideal as it does not require estimating $u_x(\theta,x)$ which will involve a truncation error from the finite difference scheme chosen. Therefore,

$$\psi(\theta)=\frac{1}{t}\log\mathbb{E}[e^{\theta\Lambda(t)}|V(t)=b]$$
$$\implies \psi(\theta)\approx\frac{1}{t}\log\frac{1}{k}\sum_{i=1}^{k}[e^{\theta\Lambda_i(t)}|V_i(t)=b]$$

We omit the pseudo-code as it is identical to the previous code with one difference. When the reflected jump diffusion is simulated, rather than returning every value of $\Lambda_i(t)$, we only return those for which $V_i(t)=b$ and reject all other paths. Naturally, such a method is quite slow.

This method of solving for $\psi(\theta)$ numerically has the advantage of only introducing the estimation error from the Monte Carlo simulation of the expected value. Unfortunately, since we are approximating an integral of an exponential function, small errors in estimating $\Lambda_i(t)$ are exponentiated and produce large errors in the final estimate. One possible workaround would be to use Laplace's method which involves applying a formula to approximate integrals of exponential functions.

To work around the issue of computational speed, we offer another way to possibly simulate solutions for $\psi(\theta)$. This may be done by applying Doob's Optional Sampling theorem to obtain an expression for $u(\theta,x)$ and then through the same boundary condition as above, solve for $\psi(\theta)$. We begin by noting that since $M(\theta,t)$ is always positive and by the dominated convergence theorem

$$\begin{aligned}\mathbb{E}\left[\left|\lim_{t\to\infty}M(\theta,t)\right|\right]=&\mathbb{E}\left[\left|\lim_{t\to\infty}e^{\theta\Lambda(t)-\psi(\theta)t}u(\theta,V(\theta))\right|\right]\\=&\mathbb{E}\left[\lim_{t\to\infty}e^{\theta\Lambda(t)-\psi(\theta)t}u(\theta,V(\theta))\right]\end{aligned}$$

$$= \lim_{t\to\infty} \mathbb{E}\left[e^{\theta\Lambda(t)-\psi(\theta)t}u(\theta, V(\theta))\right]$$
$$= \lim_{t\to\infty} \mathbb{E}\left[M(\theta, 0)\right] = 1 < \infty.$$

For $t \leq s, \mathbb{E}[\lim_{s\to\infty} M(\theta, s)|\mathcal{F}_t] = \lim_{s\to\infty} \mathbb{E}[M(\theta, s)|\mathcal{F}_t] = \lim_{s\to\infty} M(\theta, t) = M(\theta, t)$. Therefore, $M(\theta, t)$ is closed by $M(\theta, \infty)$. Define $\tau_x = \inf\{t : V(t) = x\}$ then by Doob's Optional Sampling theorem

$$\begin{aligned}
&\mathbb{E}[M(\theta, \tau_x)|\mathcal{F}_0] = M(\theta, 0) = 1 \\
\iff &\mathbb{E}[e^{\theta\Lambda(\tau_x)-\psi(\theta)\tau_x}u(\theta, V(\tau_x))|\mathcal{F}_0] = 1 \\
\iff &u(\theta, x) = \frac{1}{\mathbb{E}[e^{\theta\Lambda(\tau_x)-\psi(\theta)\tau_x}|\mathcal{F}_0]}
\end{aligned}$$

Applying the boundary condition $u(\theta, b) = 1$, we see that

$$\begin{aligned}
u(\theta, b) = &\frac{1}{\mathbb{E}[e^{\theta\Lambda(\tau_b)-\psi(\theta)\tau_b}|\mathcal{F}_0]} = 1 \\
\iff &\mathbb{E}[e^{\theta\Lambda(\tau_b)-\psi(\theta)\tau_b}|\mathcal{F}_0] = 1.
\end{aligned}$$

In a similar way to above, we will simulate $\Lambda(\tau_b)$ and τ_b, k times and consider the Monte Carlo estimate to approximate the expectation. Then we find $\psi(\theta)$ as the unique root of the equation

$$\frac{1}{k}\sum_{i=1}^{k} e^{\theta\Lambda_i(\tau_b)-\psi(\theta)\tau_{i,b}} = 1.$$

This method of using the solution to the integro-differential equation has the advantage that one simulation run can stop at the first instance of $V(t) = b$, making it computationally faster for the same choice of step size and number of simulations. However, we are now estimating two quantities in the exponential function which results in an even larger error.

We provide the pseudo-code below but due to the large errors, we do not pursue these methods further. In the next section we numerically solve the integro-differential equation which is both computationally faster and more precise than using Monte Carlo methods.

Pseudo-Code

Let $T, N, x_0, v_0, a, b, k, \bar{\theta}$ be as above. This method requires that the path simulation algorithm from 4.1.1, *PathSimV*, return two values. The first is the stopping time at $V(t) = b$ which we store in a variable R_1 and the second value is the corresponding local time which we store in a variable R_2.

1: **procedure** PsiTheta2($T, N, x_0, v_0, a, b, k, \bar{\theta}$)
2: **Initialize** $\tau_b = (\tau_b^1 = 0, ...\tau_b^k = 0)$ and $L_b = (L_b^1 = 0, ...L_b^k = 0)$
3: **for** i in $1 : k$ **do**
4: **Return** R_1 and R_2 from PathSimV(T, N, x_0, v_0, a, b)
5: **Set** $\tau_b^i \leftarrow R_1$, $L_b^i \leftarrow R_2$
6: **Initialize** $\psi(\bar{\theta})$
7: **for** j in $1 : l$ **do**
8: **Solve for** x **in** $1 = \frac{1}{k}\sum_{i=1}^{k} e^{\theta^j L_b^i - x\tau_b^i}$
9: **Set** $\psi(\theta^j) \leftarrow x$
10: **return** $\psi(\bar{\theta})$

4.1.3 Numerical Methods for $\psi(\theta)$

In order to numerically solve the integro-differential equation, we discretize the equation from Section 3.3.1 using finite differences and solve the corresponding eigenvalue problem. Recall from Chapter 3 that

$$\begin{aligned} 0 =& \mu(x)u_x(\theta, x) + \frac{1}{2}\sigma^2(x)u_{xx}(\theta, x) + (\theta f(x) - \psi(\theta))u(\theta, x) \\ &+ \int_{\mathbb{R}} [e^{\theta \tilde{f}(x,y)} u(\theta, r(x, y)) - u(\theta, x)]\nu(x, dy) \end{aligned}$$

for $0 \leq x \leq b$ and subject to the boundary conditions

$$u_x(\theta, 0) = -r_1\theta u(\theta, 0), \qquad u_x(\theta, b) = r_2\theta u(\theta, b).$$

We begin by choosing the number of steps, N, from which we define $h = \frac{b}{N}$, $x_i = ih$

where $i = 0, 1, 2, .., N$, and $u_i = u(\theta, x_i)$. In what follows, all finite difference formulas chosen are of second order accuracy. We first approximate the first and second derivatives using the centered difference formulas, which are easily derived from Taylor's expansion and may be found in [4],

$$u_x(\theta, x_i) \approx \frac{u_{i+1} - u_{i-1}}{2h}, \qquad u_{xx}(\theta, x_i) \approx \frac{u_{i+1} - 2u_i + u_{i-1}}{h^2}.$$

Since we do not have prior knowledge of the measure $\nu(x, dy)$, we apply Monte Carlo estimation to approximate the integral term. Recall $\nu(x, dy)$ is of the form $\lambda(x)\rho(dy)$ and so we simulate k trials of $y_j \sim \rho(dy)$ where $j = 1, 2, ..., k$ and compute

$$\frac{1}{k}\sum_{j=1}^{k} e^{\theta \tilde{f}(x_i, y_j)} u_l - u_i$$

where l refers to the corresponding step that $r(x_i, y_j)$ falls within the discretization scheme; that is, $l \leq r(x_i, y_j) < l + 1$ for $l = 0, 1, 2, ..., N$.

Now consider the upper and lower boundary conditions to derive expressions for u_0 and u_N which are then substituted into the numerical scheme. The first boundary condition is $u_x(\theta, 0) = -r_1\theta u(\theta, 0)$, then the three-point forward difference formula gives

$$-\frac{3}{2}u_0 + 2u_1 - \frac{1}{2}u_2 = -r_1\theta u_0 \iff u_0 = \frac{u_2 - 4u_1}{2r_1\theta - 3},$$

where $r_1\theta \neq \frac{3}{2}$.

Also,

$$\begin{aligned}
u_x(\theta, x_0) =& \frac{-\frac{3}{2}u_0 + 2u_1 - \frac{1}{2}u_2}{h} = a_1u_1 + a_2u_2 \\
=& \left(\frac{2}{h} + \frac{6}{h(-3 + 2hr_1\theta)}\right) u_1 + \left(-\frac{1}{2h} - \frac{3}{2h(-3 + 2hr_1\theta)}\right) u_2 \\
u_x(\theta, x_1) =& \frac{-u_0 + u_2}{2h} = a_3u_1 + a_4u_2 \\
=& \left(\frac{2}{h(-3 + 2r_1\theta)}\right) u_1 + \left(\frac{1}{2h} - \frac{1}{2h(-3 + 2r_1\theta)}\right) u_2 \\
u_{xx}(\theta, x_0) =& \frac{2u_0 - 5u_1 + 4u_2 - u_3}{h^2} = b_1u_1 + b_2u_2 + b_3u_3
\end{aligned}$$

$$
\begin{aligned}
&= \left(\frac{-5}{h^2} - \frac{8}{h^2(-3+2hr_1\theta)}\right) u_1 + \left(\frac{4}{h^2} + \frac{2}{h^2(-3+2hr_1\theta)}\right) u_2 \\
&\quad + \left(-\frac{1}{h^2}\right) u_3 \\
u_{xx}(\theta, x_1) =& \frac{u_0 - 2u_1 + u_2}{h^2} = b_4 u_1 + b_5 u_2 \\
&= \left(-\frac{2}{h^2} - \frac{4}{h^2(-3+2hr_1\theta)}\right) u_1 + \left(\frac{1}{h^2} + \frac{1}{h^2(-3+2hr_1\theta)}\right) u_2
\end{aligned}
$$

Likewise, for the second boundary condition $u_x(\theta, b) = r_2\theta u(\theta, b)$, the backward difference formula gives

$$
\frac{3}{2}u_N - 2u_{N-1} + \frac{1}{2}u_{N-2} = r_2\theta u_N \iff u_N = \frac{u_{N-2} - 4u_{N-1}}{2r_2\theta - 3}
$$

where $r_2\theta \neq \frac{3}{2}$.

Also,

$$
\begin{aligned}
u_x(\theta, x_{N-1}) =& \frac{-u_{N-2} + u_N}{2h} = a_5 u_{N-2} + a_6 u_{N-1} \\
&= \left(-\frac{1}{2h} + \frac{1}{2h(-3+2r_2\theta)}\right) u_{N-2} + \left(-\frac{2}{h(-3+2r_2\theta)}\right) u_{N-1} \\
u_x(\theta, x_N) =& \frac{\frac{3}{2}u_N - 2u_{N-1} + \frac{1}{2}u_{N-2}}{h} = a_7 u_{N-2} + a_8 u_{N-1} \\
&= \left(\frac{1}{2h} + \frac{3}{2h(-3+2hr_2\theta)}\right) u_{N-2} + \left(-\frac{2}{h} - \frac{6}{h(-3+2hr_2\theta)}\right) u_{N-1} \\
u_{xx}(\theta, x_{N-1}) =& \frac{u_N - 2u_{N-1} + u_{N-2}}{h^2} = b_6 u_{N-2} + b_7 u_{N-1} \\
&= \left(\frac{1}{h^2} + \frac{1}{h^2(-3+2hr_2\theta)}\right) u_{N-2} + \left(-\frac{2}{h^2} - \frac{4}{h^2(-3+2hr_2\theta)}\right) u_{N-1} \\
u_{xx}(\theta, x_N) =& \frac{2u_N - 5u_{N-1} + 4u_{N-2} - u_{N-3}}{h^2} = b_8 u_{N-3} + b_9 u_{N-2} + b_{10} u_{N-1} \\
&= \left(-\frac{1}{h^2}\right) u_{N-3} + \left(\frac{4}{h^2} + \frac{2}{h^2(-3+2hr_2\theta)}\right) u_{N-2} \\
&\quad + \left(\frac{-5}{h^2} - \frac{8}{h^2(-3+2hr_2\theta)}\right) u_{N-1}
\end{aligned}
$$

Putting it all together, we must solve the following system of equations,

$$
\mu(x_0) \left(\left(\frac{2}{h} + \frac{6}{h(-3+2hr_1\theta)}\right) u_1 + \left(-\frac{1}{2h} - \frac{3}{2h(-3+2hr_1\theta)}\right) u_2 \right)
$$

$$
\begin{aligned}
&+\frac{1}{2}\sigma^2(x_0)\left(\left(\frac{-5}{h^2}-\frac{8}{h^2(-3+2hr_1\theta)}\right)u_1+\left(\frac{4}{h^2}+\frac{2}{h^2(-3+2hr_1\theta)}\right)u_2\right.\\
&\left.+\left(-\frac{1}{h^2}\right)u_3\right)+\theta f(x_0)\frac{u_2-4u_1}{2r_1\theta-3}+\frac{\lambda(x_0)}{k}\sum_{j=1}^{k}\left[e^{\theta\tilde{f}(x_i,y_j)}u_l-\frac{u_2-4u_1}{2r_1\theta-3}\right]=\psi(\theta)u_0,\\
&\mu(x_1)\left(\left(\frac{2}{h(-3+2r_1\theta)}\right)u_1+\left(\frac{1}{2h}-\frac{1}{2h(-3+2r_1\theta)}\right)u_2\right)\\
&+\frac{1}{2}\sigma^2(x_1)\left(\left(-\frac{2}{h^2}-\frac{4}{h^2(-3+2hr_1\theta)}\right)u_1+\left(\frac{1}{h^2}+\frac{1}{h^2(-3+2hr_1\theta)}\right)u_2\right)\\
&+\theta f(x_1)u_1+\frac{\lambda(x_1)}{k}\sum_{j=1}^{k}\left[e^{\theta\tilde{f}(x_i,y_j)}u_l-u_1\right]=\psi(\theta)u_1,\\
&\mu(x_i)\frac{u_{i+1}-u_{i-1}}{2h}+\frac{1}{2}\sigma^2(x_i)\frac{u_{i+1}-2u_i+u_{i-1}}{h^2}+\theta f(x_i)u_i+\frac{\lambda(x_i)}{k}\sum_{j=1}^{k}\left[e^{\theta\tilde{f}(x_i,y_j)}u_l-u_i\right]\\
&=\psi(\theta)u_i\qquad\text{for each } i=2,3,...,N-2,\\
&\mu(x_{N-1})\left(\left(-\frac{1}{2h}+\frac{1}{2h(-3+2r_2\theta)}\right)u_{N-2}+\left(-\frac{2}{h(-3+2r_2\theta)}\right)u_{N-1}\right)\\
&+\frac{1}{2}\sigma^2(x_{N-1})\left(\left(\frac{1}{h^2}+\frac{1}{h^2(-3+2hr_2\theta)}\right)u_{N-2}+\left(-\frac{2}{h^2}-\frac{4}{h^2(-3+2hr_2\theta)}\right)u_{N-1}\right)\\
&+\theta f(x_{N-1})u_{N-1}+\frac{\lambda(x_{N-1})}{k}\sum_{j=1}^{k}\left[e^{\theta\tilde{f}(x_i,y_j)}u_l-u_{N-1}\right]=\psi(\theta)u_{N-1},\\
&\mu(x_N)\left(\left(\frac{1}{2h}+\frac{3}{2h(-3+2hr_2\theta)}\right)u_{N-2}+\left(-\frac{2}{h}-\frac{6}{h(-3+2hr_2\theta)}\right)u_{N-1}\right)\\
&+\frac{1}{2}\sigma^2(x_N)\left(\left(-\frac{1}{h^2}\right)u_{N-3}+\left(\frac{4}{h^2}+\frac{2}{h^2(-3+2hr_2\theta)}\right)u_{N-2}\right.\\
&\left.+\left(\frac{-5}{h^2}-\frac{8}{h^2(-3+2hr_2\theta)}\right)u_{N-1}\right)+\theta f(x_N)\frac{u_{N-2}-4u_{N-1}}{2r_2\theta-3}\\
&+\frac{\lambda(x_N)}{k}\sum_{j=1}^{k}\left[e^{\theta\tilde{f}(x_i,y_j)}u_l-\frac{u_{N-2}-4u_{N-1}}{2r_2\theta-3}\right]=\psi(\theta)u_N.
\end{aligned}
$$

It is more convenient to view this in matrix form as the eigenvalue problem $\mathbf{A}u=\psi(\theta)u$, where u is the eigenvector corresponding to the eigenvalue $\psi(\theta)$ and $\mathbf{A}$ is the matrix generated from all the coefficient terms. Using boldface to denote a matrix, let

$$\mathbf{A}=\boldsymbol{\mu}\cdot\boldsymbol{u_x}+\boldsymbol{\sigma}\cdot\boldsymbol{u_{xx}}+\boldsymbol{f}\cdot\boldsymbol{u}+\boldsymbol{\lambda}\cdot(\boldsymbol{B}-\boldsymbol{u})$$

or explicitly, $\mathbf{A}$ is the $(N+1)\times(N+1)$ matrix equal to

$$\begin{bmatrix} \mu(x_0) & 0 & 0 & \dots & 0 \\ 0 & \mu(x_1) & 0 & \dots & 0 \\ \vdots & \ddots & \ddots & \ddots & \vdots \\ 0 & \dots & 0 & \mu(x_{N-1}) & 0 \\ 0 & \dots & 0 & 0 & \mu(x_N) \end{bmatrix} \begin{bmatrix} 0 & a_1 & a_2 & 0 & \dots & 0 & 0 & 0 & 0 \\ 0 & a_3 & a_4 & 0 & \dots & 0 & 0 & 0 & 0 \\ 0 & -\frac{1}{2h} & 0 & \frac{1}{2h} & \dots & 0 & 0 & 0 & 0 \\ \vdots & \ddots & \ddots & \ddots & \ddots & \ddots & \ddots & \ddots & \vdots \\ 0 & 0 & 0 & 0 & \dots & -\frac{1}{2h} & 0 & \frac{1}{2h} & 0 \\ 0 & 0 & 0 & 0 & \dots & 0 & a_5 & a_6 & 0 \\ 0 & 0 & 0 & 0 & \dots & 0 & a_7 & a_8 & 0 \end{bmatrix}$$

$$+ \begin{bmatrix} \frac{\sigma^2(x_0)}{2} & 0 & 0 & \dots & 0 \\ 0 & \frac{\sigma^2(x_1)}{2} & 0 & \dots & 0 \\ \vdots & \ddots & \ddots & \ddots & \vdots \\ 0 & \dots & 0 & \frac{\sigma^2(x_{N-1})}{2} & 0 \\ 0 & \dots & 0 & 0 & \frac{\sigma^2(x_N)}{2} \end{bmatrix} \begin{bmatrix} 0 & b_1 & b_2 & b_3 & \dots & 0 & 0 & 0 & 0 \\ 0 & b_4 & b_5 & 0 & \dots & 0 & 0 & 0 & 0 \\ 0 & -\frac{1}{h^2} & -\frac{2}{h^2} & \frac{1}{h^2} & \dots & 0 & 0 & 0 & 0 \\ \vdots & \ddots & \ddots & \ddots & \ddots & \ddots & \ddots & \ddots & \vdots \\ 0 & 0 & 0 & 0 & \dots & -\frac{1}{h^2} & -\frac{2}{h^2} & \frac{1}{h^2} & 0 \\ 0 & 0 & 0 & 0 & \dots & 0 & b_6 & b_7 & 0 \\ 0 & 0 & 0 & 0 & \dots & b_8 & b_9 & b_{10} & 0 \end{bmatrix}$$

$$+ \begin{bmatrix} \theta f(x_0) & 0 & 0 & \dots & 0 \\ 0 & \theta f(x_1) & 0 & \dots & 0 \\ \vdots & \ddots & \ddots & \ddots & \vdots \\ 0 & \dots & 0 & \theta f(x_{N-1}) & 0 \\ 0 & \dots & 0 & 0 & \theta f(x_N) \end{bmatrix} \begin{bmatrix} 0 & -\frac{4}{2r_1\theta-3} & \frac{1}{2r_1\theta-3} & \dots & 0 \\ 0 & 1 & 0 & \dots & 0 \\ \vdots & \ddots & \ddots & \ddots & \vdots \\ 0 & \dots & 0 & 1 & 0 \\ 0 & \dots & \frac{1}{2r_2\theta-3} & -\frac{4}{2r_2\theta-3} & 0 \end{bmatrix}$$

$$+ \begin{bmatrix} \lambda(x_0) & 0 & 0 & \dots & 0 \\ 0 & \lambda(x_1) & 0 & \dots & 0 \\ \vdots & \ddots & \ddots & \ddots & \vdots \\ 0 & \dots & 0 & \lambda(x_{N-1}) & 0 \\ 0 & \dots & 0 & 0 & \lambda(x_N) \end{bmatrix} \left(\mathbf{B} - \begin{bmatrix} 0 & -\frac{4}{2r_1\theta-3} & \frac{1}{2r_1\theta-3} & \dots & 0 \\ 0 & 1 & 0 & \dots & 0 \\ \vdots & \ddots & \ddots & \ddots & \vdots \\ 0 & \dots & 0 & 1 & 0 \\ 0 & \dots & \frac{1}{2r_2\theta-3} & -\frac{4}{2r_2\theta-3} & 0 \end{bmatrix} \right)$$

so that

$$\mathbf{A}\begin{bmatrix} u_0 \\ u_1 \\ \vdots \\ u_{N-1} \\ u_N \end{bmatrix} = \begin{bmatrix} \psi(\theta) & 0 & 0 & \dots & 0 \\ 0 & \psi(\theta) & 0 & \dots & 0 \\ \vdots & \ddots & \ddots & \ddots & \vdots \\ 0 & \dots & 0 & \psi(\theta) & 0 \\ 0 & \dots & 0 & 0 & \psi(\theta) \end{bmatrix} \begin{bmatrix} u_0 \\ u_1 \\ \vdots \\ u_{N-1} \\ u_N \end{bmatrix}.$$

The matrix $\mathbf{B}$ is randomly generated as follows. For each i, simulate $y_j \sim \rho(dy)$, $j = 1, 2, ..., k$. Denote l as $l \leq r(x_i, y_j) < l + 1$ and construct $\boldsymbol{B}_{temp}$, a $k \times N + 1$ matrix, by considering the following cases:

Case 1: if $l = 0$, assign $\boldsymbol{B}^{j,1}_{temp} = -\dfrac{4e^{\theta \tilde{f}(x_i,y_j)}}{2hr_1\theta - 3}$ and $\boldsymbol{B}^{j,2}_{temp} = \dfrac{e^{\theta \tilde{f}(x_i,y_j)}}{2hr_1\theta - 3}$.

Case 2: if $l = N$, assign $\boldsymbol{B}^{j,N-1}_{temp} = -\dfrac{4e^{\theta \tilde{f}(x_i,y_j)}}{2hr_2\theta - 3}$ and $\boldsymbol{B}^{j,N-2}_{temp} = \dfrac{e^{\theta \tilde{f}(x_i,y_j)}}{2hr_2\theta - 3}$.

Case 3: if $0 < l < N$, assign $\boldsymbol{B}^{j,l}_{temp} = e^{\theta \tilde{f}(x_i,y_j)}$.

Finally, average each column vector of $\boldsymbol{B}_{temp}$ to get $\mathbf{B}^{i,\cdot} = \frac{1}{k}\sum_{j=1}^{k} \boldsymbol{B}^{j,\cdot}_{temp}$.

Once the matrix $\mathbf{A}$ has been computed, we use the eigen() function in R to compute the eigenvalues and eigenvectors of the system, disregarding the eigenvalues from the first and last columns, as these will always be zero. In order to isolate the desired eigenvalue from the generated list of $N-1$ values, we recall the assumption that $u(\theta, x)$ is a positive function and so we search for eigenvectors with exclusively positive values. Empirically, while running the simulations, this eigenvector has always been unique and its existence appears to depend on an appropriate choice of step size. Further research is needed to make this precise. However, it has been possible to consistently identify the correct eigenvalue by searching for either all positive or all negative eigenvectors for any choice of step size.

Pseudo-Code

Let b be the upper boundary, N the number of steps from 0 to b, r_1 and r_2 as described in Section 3.1, k the desired number of trials and let $\bar{\theta} = (\theta^1, \theta^2, ..., \theta^j, ..., \theta^l)$ be the vector of θ values for which to compute $\psi(\theta)$. In the following pseudo-code, when we state: **Set** *a*

matrix, we are referring to the scheme used from the corresponding matrices in this section.

1: **procedure** NUMERICALPSITHETA($N, k, r_1, r_2, b, \bar{\theta}$)
2: **Set** $h \leftarrow \frac{b}{N}$, $x_i \leftarrow ih$ for $i = 0, 1, 2, ..., N$
3: **Initialize** $\psi(\bar{\theta})$
4: **for** each $\bar{\theta}$ **do**
5: **Set** $(N+1) \times (N+1)$*matrices* $\boldsymbol{\mu}$, $\boldsymbol{\sigma}$, $\boldsymbol{f}$, $\boldsymbol{\lambda}$,$\boldsymbol{u}$, $\boldsymbol{u_x}$, $\boldsymbol{u_{xx}}$ and $\mathbf{B}$
6: **Compute** $\mathbf{A} = \boldsymbol{\mu} \cdot \boldsymbol{u_x} + \boldsymbol{\sigma} \cdot \boldsymbol{u_{xx}} + \boldsymbol{f} \cdot \boldsymbol{u} + \boldsymbol{\lambda} \cdot (\boldsymbol{B} - \boldsymbol{u})$
7: **Compute** eigenvectors of $\mathbf{A}$
8: **Set** m $\leftarrow$ index of unique positive eigenvector
9: **Set** $\psi(\theta^j) \leftarrow m^{th}$ eigenvalue of $\mathbf{A}$
10: **return** $\psi(\bar{\theta})$

4.2 Algorithm Verification

We numerically verify the algorithms proposed against the analytic solutions found in Section 3.4. To remain consistent with the rest of the thesis, all computations will be for the local time at the lower boundary $L(t)$.

4.2.1 Doubly Reflected Brownian Motion

Recall from Section 3.4.1, we analytically computed $\theta = \sqrt{2\psi(\theta)}\tanh(\sqrt{2\psi(\theta)})$ for standard Brownian motion with parameter $b = 1$. The first test we would like to carry out is to check whether the algorithm to simulate the paths of a reflected jump diffusion result in an empirical mean for $L(t)$ that converges to the exact value of $\mathbb{E}[L(t)]$. To do this we compare the two cases $t = 1$ and $t = 10$ with $N = 400$, by increasing k from 1 to 160000 and verify $\lim_{t\to\infty} \frac{1}{t}\mathbb{E}[L(t)] = \psi'(0)$. The green line represents the true value of $\psi'(0) = 0.5$ which was computed by numerical differentiation.

As is evident from Figure 4.1, increasing the number of trials will cause the empirical mean to converge, but more importantly, increasing the time interval will cause the empirical mean to converge to the true expected value. This is due to the error from approximating

the limit being $o(t)$ which tends to zero as t increases.

Likewise, we can plot the variances of $L(t)$ for increasing values of N and k, where $k = N^2$ and see that they converge as well. The blue, black and green lines in Figure 4.2 represent variances for $t = 1$, $t = 10$ and the true variance respectively. The true variance was computed to be 0.3329.

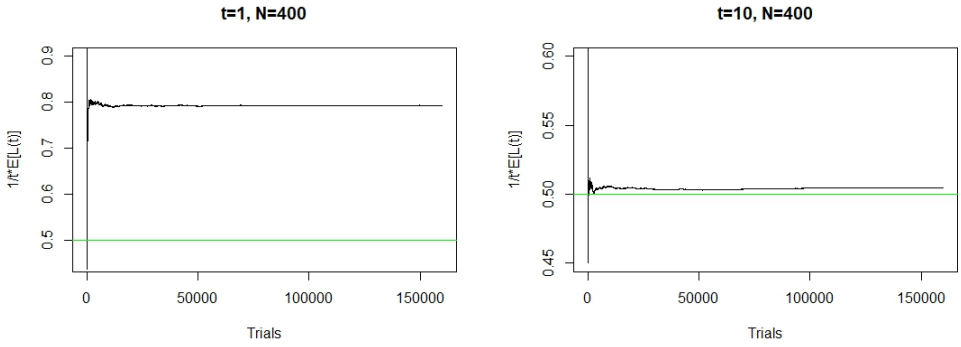

Figure 4.1: Reflected Brownian Motion Path Simulation: Convergence of empirical mean to true mean (green overlay). Left: T=1, N=400. Right: T=10, N=400.

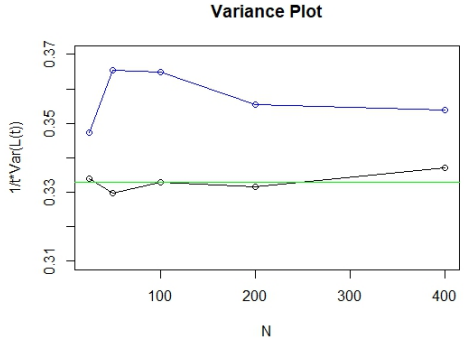

Figure 4.2: Reflected Brownian Motion Path Simulation: Variance plot. Blue: T=1. Black: T=10. Green: exact variance.

Now we move on to compute the errors between the estimated $\psi(\theta)$ by its limit definition for $N = 100$ and 10000 trials and the analytically computed $\psi(\theta)$. Figure 4.3 shows the numerically exact value for $\psi(\theta)$. Figures 4.4 and 4.5 show plots of the estimated $\psi(\theta)$ with a green overlay line representing the exact value for $\psi(\theta)$ for $T = 1$ and $T = 10$, respectively, and the difference between the two values.

The equality $\lim_{t\to\infty} \frac{1}{t} \log \mathbb{E}[e^{\theta\Lambda(t)}] = \psi(\theta)$ holds only as t tends to infinity. The error in

comparing an estimate of $\frac{1}{t}\log\mathbb{E}[e^{\theta\Lambda(t)}]$ and $\psi(\theta)$ comes from having to choose a fixed value for t which allows for there to be a difference between the two quantities as long as this difference grows slower than t. To compound this, each sample of $\Lambda(t)$ will vary by a certain amount which is expected to converge in the mean as the sample size is increased. However, the small errors in the exponential function are expected cause the overall errors to become large quickly, especially if they are being multiplied by an increasing value of θ. So as is expected, the error grows as we move further away from $\theta = 0$.

Furthermore, we also notice that as t increases from $T = 1$ to $T = 10$, the estimate becomes more precise near $\theta = 0$ and less so for larger values of θ. This happens since as we increase t, there is a larger variability around which values $\Lambda(t)$ can take and again, this error is exponentiated. This can be mitigated by making the estimate more precise, that is taking larger values for N and k, as can be seen in Figure 4.6 where we keep $T = 10$ but increase $N = 400$, $k = 160000$.

$\psi(\theta)$ computed analytically:

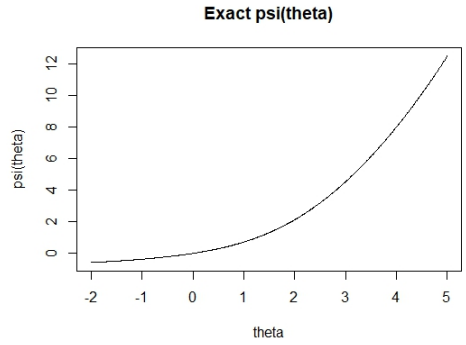

Figure 4.3: Reflected Brownian Motion Path Simulation: Analytic $\psi(\theta)$

$\psi(\theta)$ computed by limiting behavior:

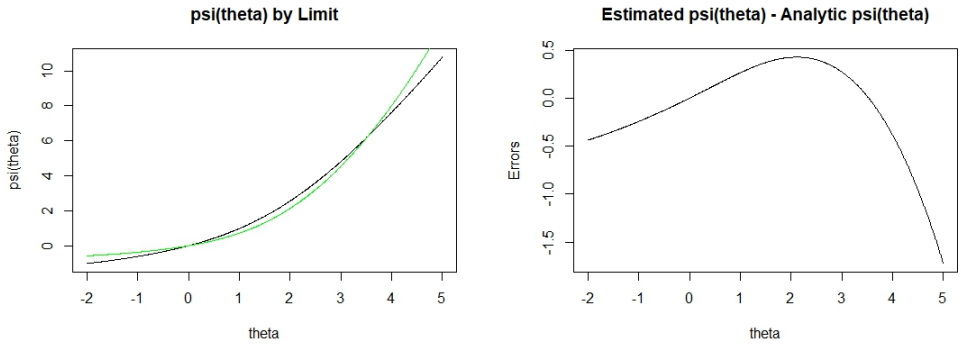

Figure 4.4: Reflected Brownian Motion: Left: Estimated $\psi(\theta)$ by limit with green analytic overlay. Right: Difference between exact and estimated $\psi(\theta)$. $T = 1, N = 100, k = 10000$.

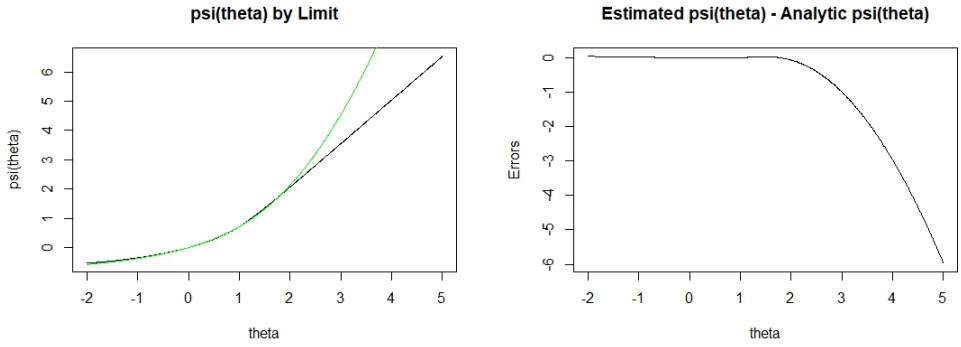

Figure 4.5: Reflected Brownian Motion: Left: Estimated $\psi(\theta)$ by limit with green analytic overlay. Right: Difference between exact and estimated $\psi(\theta)$. $T = 10, N = 100, k = 10000$.

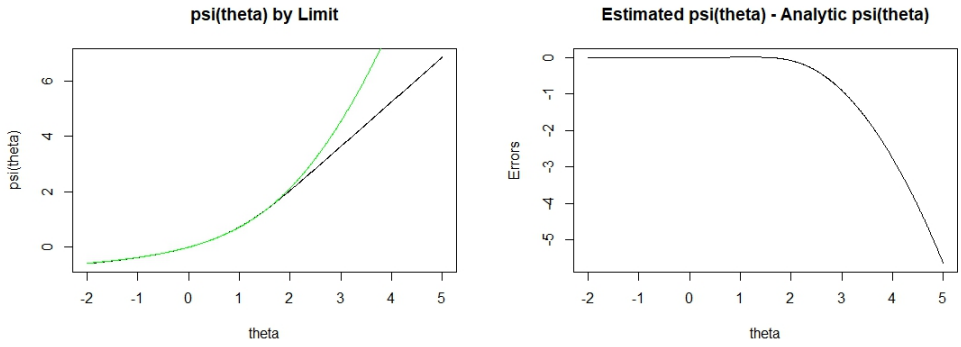

Figure 4.6: Reflected Brownian Motion: Left: Estimated $\psi(\theta)$ by limit with green analytic overlay. Right: Difference between exact and estimated $\psi(\theta)$. $T = 10, N = 400, k = 160000$.

Similarly to above, we will now compare the estimate of $\psi(\theta)$ that was found by numerically solving the integro-differential equation to the analytic solution for $\psi(\theta)$. In Figure 4.7 and Figure 4.8 respectively, we present plots for $N = 10$ and $N = 100$, with the green line still representing the true value of $\psi(\theta)$.

We can see a considerable improvement in the precision of the estimate from solving the integro-differential equation as opposed to using a Monte Carlo estimate. As expected, increasing the step size from $N = 10$ to $N = 100$ improved the precision of the estimate. We note that using finite differences results in both a round-off error and a truncation error which increase inversely for changes in the step size. Therefore, improvements to the precision beyond a certain optimal choice of N are not expected. Lastly, we note that the errors increase for larger θ and this is due to the order of accuracy chosen for the model, which is further evidenced by the fact that the errors for $N = 10$ and $N = 100$ are proportional to each other.

$\psi(\theta)$ computed by solving the IDE:

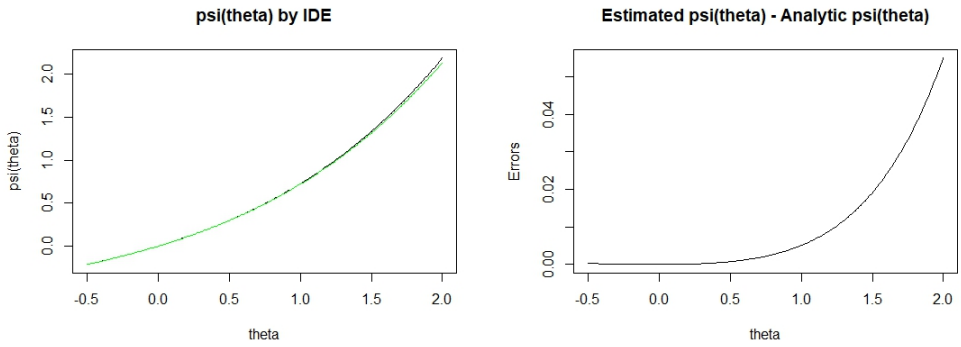

Figure 4.7: Reflected Brownian Motion: Left: Estimated $\psi(\theta)$ by IDE with green analytic overlay. Right: Difference between exact and estimated $\psi(\theta)$. $N = 10$, $k = 10000$.

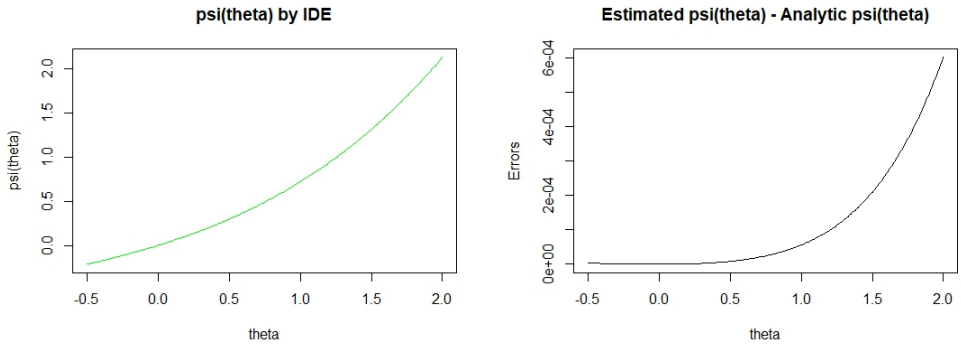

Figure 4.8: Reflected Brownian Motion: Left: Estimated $\psi(\theta)$ by IDE with green analytic overlay. Right: Difference between exact and estimated $\psi(\theta)$. $N = 100$, $k = 10000$.

To further illustrate the differences between the errors of the Monte Carlo estimate and those from solving the integro-differential equation, we present a table for select values of θ below. The parameters chosen for the Monte Carlo estimate are $T = 10, N = 100, k = 10000$ and for the integro-differential equation, $N = 100$, $k = 10000$.

θ	Analytic $\psi(\theta)$	Monte Carlo $\psi(\theta)$		IDE $\psi(\theta)$	
	Exact	Estimate	Absolute Error	Estimate	Absolute Error
-0.5	-0.21338162	-0.20270337	0.01067825	-0.213378326	0.000003294
-0.1	-0.04837694	-0.04620514	0.0021718	-0.048376750	0.00000019
0.1	0.05171196	0.04953719	0.00217477	0.051712189	0.000000229
0.25	0.1361446	0.1307937	0.0053509	0.136146270	0.00000167
0.5	0.29776223	0.28824002	0.00952221	0.297770605	0.000008375
1	0.71961442	0.72229774	0.00268332	0.719670359	0.000055939
2	2.13281081	2.06865321	0.0641576	2.133413301	0.000602491

Table 4.1: Reflected Brownian Motion: Numerical comparison of two algorithms for estimating $\psi(\theta)$. Parameter values for MC estimate are $T = 10, N = 100, k = 10000$ and for IDE estimate are $N = 100, k = 10000$.

Recall that $\frac{1}{t}\log \mathbb{P}(\Lambda(t) \geq at) \to \psi(\theta^*) - \theta^* a$ where $a = \psi'(\theta)$. Using this, we may numerically estimate the rate function, $\psi^*(a)$, and subsequently compute $\mathbb{P}(L(t) \geq at) \approx e^{-t\psi^*(a)}$ for various values of $\theta > 0$. We present these numerical results in three tables: Table 4.2 lists the results derived from analytically computing $\psi(\theta)$, Table 4.3 from the Monte Carlo estimate of $\psi(\theta)$ and from the IDE estimate of $\psi(\theta)$. We choose $t = 10$ and continue with the same parameter values as above. In Figure 4.9 we plot the rate function to show that it is in fact convex and the minimum is achieved exactly where the theory would suggest,

that is at $\psi'(0) = 0.5$ and we illustrate the exponential decay of the probabilities.

θ	$a = \psi'(\theta)$	$\psi^*(a)$	$\mathbb{P}(L(t) \geq at)$
0	0.5	0	1
0.1	0.5347	0.0018	0.9826
0.25	0.5922	0.0119	0.8877
0.5	0.7043	0.0544	0.5804
1	1	0.2804	0.0606
2	1.8828	1.6327	0

Table 4.2: Reflected Brownian Motion: Numerical large deviations result using analytic $\psi(\theta)$. $t = 10$.

θ	$a = \psi'(\theta)$	$\psi^*(a)$	$\mathbb{P}(L(t) \geq at)$
0	0.4782	0	1
0.1	0.513	0.0018	0.9825
0.25	0.5718	0.0122	0.8855
0.5	0.6936	0.0586	0.5566
1	1.0724	0.3501	0.0302
2	1.4677	0.8666	0.0002

θ	$a = \psi'(\theta)$	$\psi^*(a)$	$\mathbb{P}(L(t) \geq at)$
0	0.5	0	1
0.1	0.5347	0.0018	0.9826
0.25	0.5922	0.0119	0.8877
0.5	0.7044	0.0544	0.5803
1	1.0002	0.2805	0.0605
2	1.8788	1.6241	0

Table 4.3: Reflected Brownian Motion: Numerical large deviations result using: Left: Monte Carlo estimate of $\psi(\theta)$. Right: IDE estimate of $\psi(\theta)$. $t = 10$.

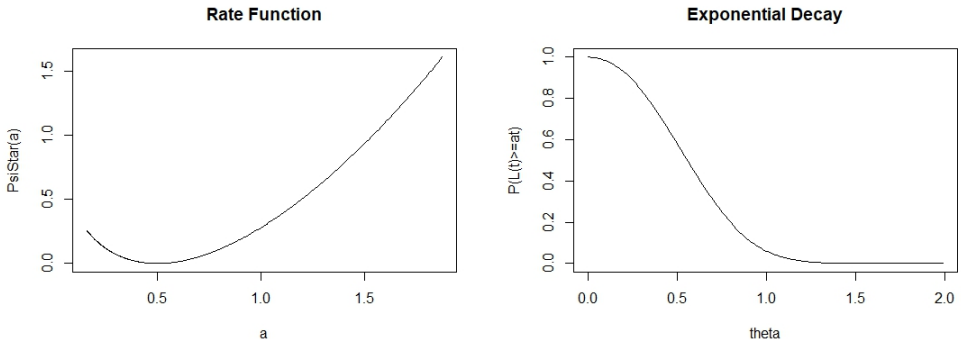

Figure 4.9: Reflected Brownian Motion: Left: Plot of the convex rate function, minimum at 0.5. Right: Plot of the exponential decay of the probabilities.

4.2.2 Doubly Reflected Pure Jump Process

We now repeat the same checks as in the previous section for the simple pure jump process from Section 3.4.2. Since the discussion remains the same, we simply provide the plots with captions describing the choice of parameters. Recall from Section 3.4.2, we analytically computed $\theta = \log\left(\frac{\psi(\theta)^4+175\psi(\theta)^3+9375\psi(\theta)^2+156250\psi(\theta)+390625}{25(\psi(\theta)^3+125\psi(\theta)^2+3750\psi(\theta)+15625)}\right)$ for a pure jump process with parameter $b = 3$ and constant arrival function $\lambda = 50$. In this case $\mathbb{E}[L(t)] = 6.25$ and $Var(L(t)) = 17.1875$.

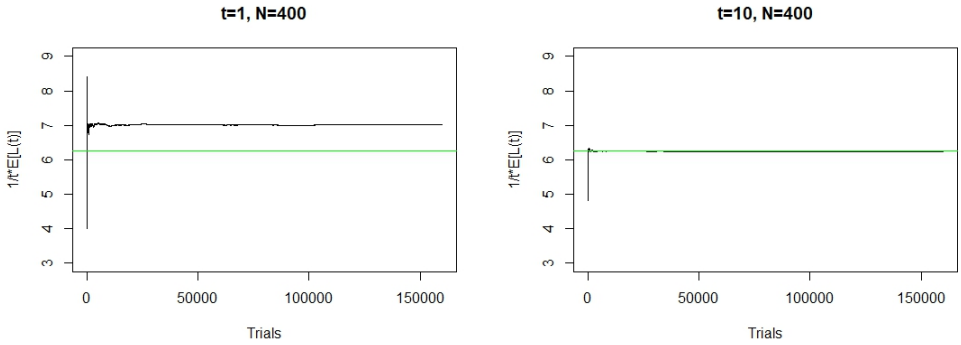

Figure 4.10: Reflected Pure Jump Process: Convergence of empirical mean to true mean (green overlay). Left: T=1, N=400. Right: T=10, N=400.

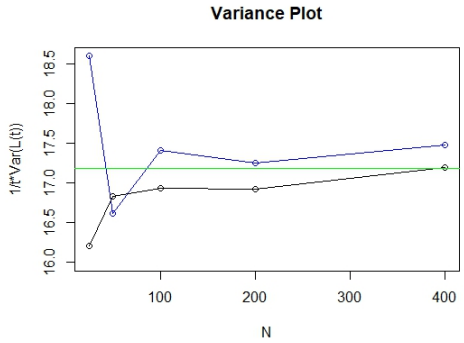

Figure 4.11: Reflected Pure Jump Process: Variance plot. Blue: T=1. Black: T=10. Green: exact variance.

$\psi(\theta)$ computed analytically:

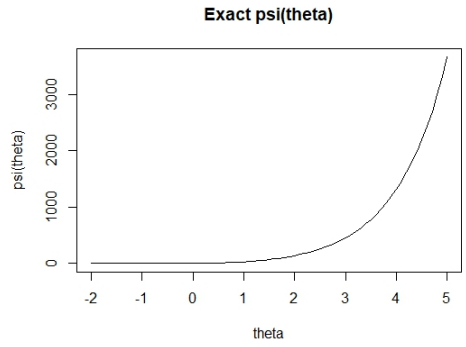

Figure 4.12: Reflected Pure Jump Process: Analytic $\psi(\theta)$

$\psi(\theta)$ computed by limiting behavior:

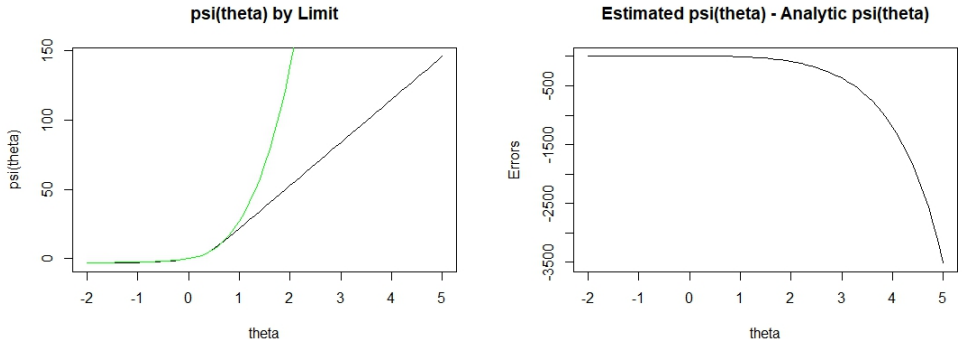

Figure 4.13: Reflected Pure Jump Process: Left: Estimated $\psi(\theta)$ by limit with green analytic overlay. Right: Difference between exact and estimated $\psi(\theta)$. $T = 1, N = 100, k = 10000$.

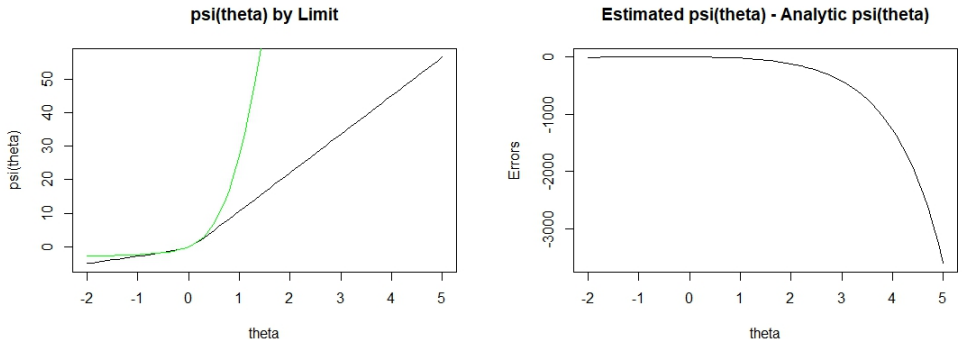

Figure 4.14: Reflected Pure Jump Process: Left: Estimated $\psi(\theta)$ by limit with green analytic overlay. Right: Difference between exact and estimated $\psi(\theta)$.$T = 10, N = 100, k = 10000$.

$\psi(\theta)$ computed by solving the IDE:

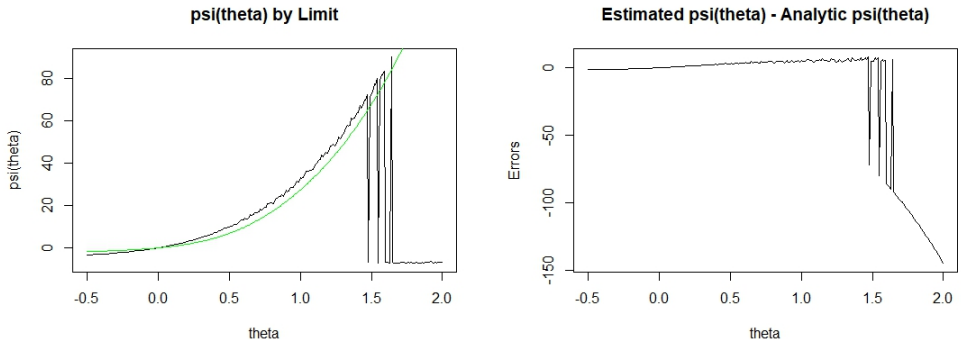

Figure 4.15: Reflected Pure Jump Process: Left: Estimated $\psi(\theta)$ by IDE with green analytic overlay. Right: Difference between exact and estimated $\psi(\theta)$. $N = 10, k = 10000$.

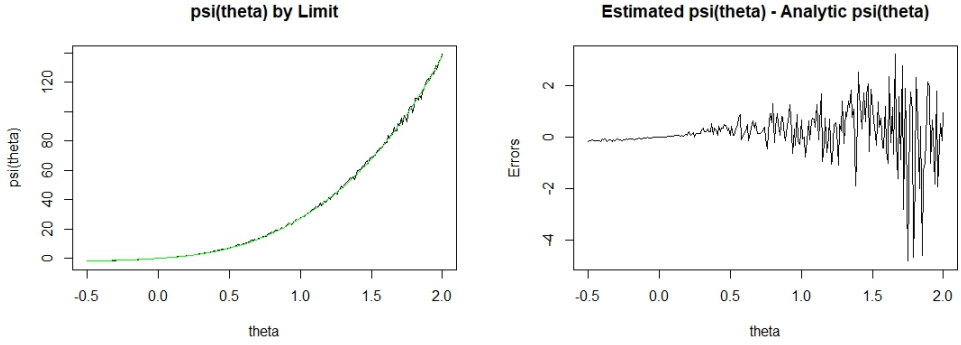

Figure 4.16: Reflected Pure Jump Process: Left: Estimated $\psi(\theta)$ by IDE with green analytic overlay. Right: Difference between exact and estimated $\psi(\theta)$. $N = 100, k = 10000$.

We note that the instability for increasing values of θ arises because of the way we calculated the integral part of the integro-differential equation. When designing the algorithm for general use, we do not know the measure $\nu(x, dy)$ and so the only method we are aware of to handle such generality is to approximate it by Monte Carlo methods. Then the same issues that were present in computing $\psi(\theta)$ by its limit definition are present here, namely the growing error of the exponential term with increasing θ and the variability of the Monte Carlo estimate. Having said this, this algorithm performs considerably better for large values of θ and follows the exact value of $\psi(\theta)$ consistently throughout.

θ	Analytic $\psi(\theta)$	Monte Carlo $\psi(\theta)$		IDE $\psi(\theta)$	
	Exact	Estimate	Absolute Error	Estimate	Absolute Error
-0.5	-1.7745581	-1.7756343	0.0010762	-1.786109	0.0115509
-0.1	-0.5476136	-0.5247709	0.0228427	-0.5579613	0.0103477
0.05	0.3351856	0.3229893	0.0121963	0.328563	0.0066226
0.1	0.7209206	0.6941261	0.0267945	0.718304	0.0026166
0.15	1.165823	1.1173521	0.0484709	1.187411	0.021588
0.2	1.679614	1.5897722	0.0898418	1.680787	0.001173
0.25	2.272985	2.0999454	0.1730396	2.302708	0.029723

Table 4.4: Reflected Pure Jump Process: Numerical comparison of two algorithms for estimating $\psi(\theta)$. Parameter values for MC estimate are $T = 10, N = 100, k = 10000$ and for IDE estimate are $N = 500$, $k = 50000$.

θ	$a = \psi'(\theta)$	$\psi^*(a)$	$\mathbb{P}(L(t) \geq at)$
0	6.25	0	1
0.05	7.1834	0.024	0.7867
0.1	8.277	0.1068	0.3438
0.15	9.5541	0.2673	0.069
0.2	11.0361	0.5276	0.051
0.25	12.7399	0.912	0.0001

Table 4.5: Reflected Pure Jump Process: Numerical large deviations result using Analytic $\psi(\theta)$. $t = 10$.

θ	$a = \psi'(\theta)$	$\psi^*(a)$	$\mathbb{P}(L(t) \geq at)$
0	6.0173	0	1
0.05	6.9235	0.0232	0.793
0.1	7.9381	0.0997	0.369
0.15	8.9816	0.2299	0.1004
0.2	9.871	0.3844	0.0214
0.25	10.486	0.5216	0.0054

θ	$a = \psi'(\theta)$	$\psi^*(a)$	$\mathbb{P}(L(t) \geq at)$
0	6.3166	0	1
0.05	7.2035	0.0316	0.729
0.1	8.3576	0.1175	0.309
0.15	9.4243	0.2262	0.1041
0.2	10.243	0.3678	0.0253
0.25	13.5507	1.085	0

Table 4.6: Reflected Pure Jump Process: Numerical large deviation result using: Left: Monte Carlo estimate of $\psi(\theta)$. Right: Using IDE estimate of $\psi(\theta)$. $t = 10$.

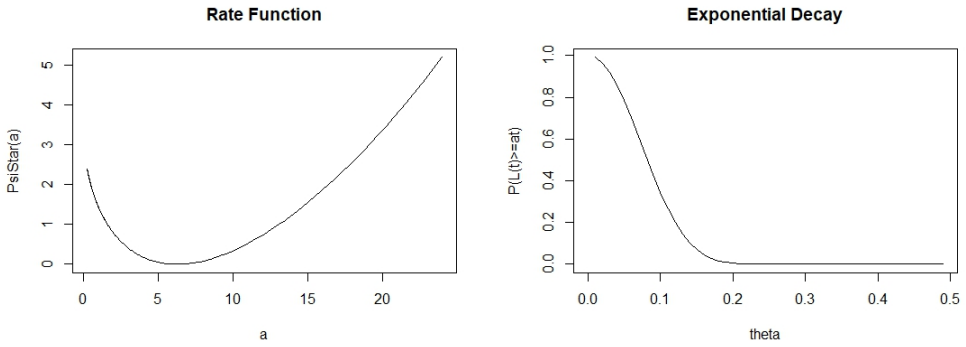

Figure 4.17: Reflected Pure Jump Process: Left: Plot of the convex rate function, minimum at 6.25. Right: Plot of the exponential decay of the probabilities.

Chapter 5

Conclusion

5.1 Concluding Remarks

In [11] a large deviation result for the local time was established for reflected diffusions and in [1] the same was accomplished for reflected Lévy processes. In this thesis, we extended those results to the reflected jump diffusion setting. By way of Itô's formula, we derived an integro-differential equation with appropriate boundary conditions from which the limit of the cumulant generating function was found. This limit allowed for the Gärtner-Ellis theorem to be applied which established the result.

The theory was practically implemented in a simulation study. We first described how to simulate a path of a reflected jump diffusion and then derived algorithms to approximate $\psi(\theta)$ in two ways, first by approximating the limit and then by numerically solving the integro-differential equation. The algorithms' decimal precision was then tested against the analytically computed results for standard Brownian motion and a simple pure jump process with constant coefficients.

Further research can still be done to improve the algorithms. Namely Laplace's method could be attempted to improve the Monte Carlo simulations and a deeper study of the behavior of the eigenvectors would certainly help in developing a more efficient numerical scheme for the solution of the integro-differential equation. Having said this, we look forward to seeing the real world practical applications of this theory and continuing this research into related areas of applied probability.

Appendix A

Appendix

A.1 R Code

A.1.1 Reflected Jump Diffusion

```
############ Path Simulation - Reflected Jump Diffusion ############

#########################################################USER INPUT FUNCTIONS
mu = function (V){return(0)}
sigma = function (V){return(0)}
lambda = function (V){return(0)}
gamma = function (V, Z){return(0)}
rho = function (V){return(0)}
#########################################################################

PathSimV = function(T, N, x0, v0, a, b){
  h = T / N
  i = 0; s = 0; j = 1
  A = 0
  E = rexp(1)

  X = L = U = V = vector()
  X[1] = x0; V[1] = v0
  L[1] = U[1] = 0
```

```
20
21    while(s!=T){
22
23      Atemp = A + lambda(V[j])*((i+1)*h-s)
24
25      if(Atemp >= E){ #jump between s and (i+1)h
26
27        tau = s + (E - A)/(lambda(V[j]))
28        X[j] = X[j] + mu(V[j])*(tau - s) + sigma(V[j])*sqrt(tau - s)*rnorm(1)
29        deltaX = gamma(V[j], rho(V[j]))
30        X[j] = X[j] + deltaX
31
32        deltaL = max(0, a - (deltaX + V[j]))
33        deltaU = max(0, (deltaX + V[j]) - b)
34        L[j] = L[j] + deltaL
35        U[j] = U[j] + deltaU
36        V[j] = V[j] + deltaX + deltaL - deltaU
37
38        s = tau; A = E; E = E + rexp(1)
39
40      } else { #no jump between s and (i+1)h
41
42        X[j+1] = X[j] + mu(V[j])*((i+1)*h - s) + sigma(V[j])*sqrt((i+1)*h - s)*
              rnorm(1)
43        s = (i+1)*h; A = Atemp; i = i + 1; j = j + 1
44
45        L[j] = L[j-1] + max(0, a - ((X[j] - X[j-1]) + V[j-1]))
46        U[j] = U[j-1] + max(0, (X[j] - X[j-1]) + V[j-1] - b)
47        V[j] = V[j-1] + (X[j]-X[j-1]) + (L[j]-L[j-1]) - (U[j]-U[j-1])
48
49      }
50    }
51    #return(L[N+1])
52  }
```

A.1.2 $\psi(\theta)$ by Limit of CGF

```
########## Psi Theta by Limit of CGF ##########
PsiThetaMC = function(T, N, x0, v0, a, b, k, thetaVec){
  L = vector()
  for(i in 1:k){ L[i] = PathSimV(T, T*N, x0, v0, a, b) }
  psiTheta = vector()
  for(i in 1:length(thetaVec)){
    maxThetaL = max(thetaVec[i]*L)
    psiTheta[i] = 1/T*maxThetaL + 1/T*log(mean(exp(thetaVec[i]*L-maxThetaL)))
  } return(psiTheta)
}
```

A.1.3 $\psi(\theta)$ by DOS theorem

```
########## Psi Theta by DOS theorem ##########
PsiThetaDOS = function(T, N, x0, v0, a, b, k, thetaVec){
  taub=lb=vector()
  for(i in 1:k){
    temp=PathSimV(T, T*N, x0, v0, a, b)
    while(is.null(temp)){temp=PathSimV(T, T*N, x0, v0, a, b)}
    taub[i] = temp[1]
    lb[i] = temp[2]
  }
  psiTheta = vector()
  for(j in 1:length(thetaVec)){
    f=function(x) -1+mean(exp(thetaVec[j]*lb-x*taub))
    psiTheta[j]=uniroot(f,c(0,1), tol=.Machine$double.eps*10, extendInt = "yes
        ")$root
  } return(psiTheta)
}
```

A.1.4 $\psi(\theta)$ by IDE numerics

```
########## Eigenvalue - IDE ##########

#####################################################USER INPUT FUNCTIONS
mu = function (V){return(0)}
sigma = function (V){return(0)}
lambda = function (V){return(0)}
gamma = function (V, Y){return(0)}
rho = function (V){return(0)}
f = function (V){return(0)}
f_tilde = function(V, Y){return(0)}
#########################################################################
numericalPsiTheta = function(N,k,r1,r2,b,thetaVec){
h=b/N
x = seq(from=0, to=b, by=h)
counter = 0
psiTheta = vector()
for(theta in thetaVec){
  counter = counter + 1
  muMatrix = matrix(0L, nrow=length(x), ncol=length(x))
  for(i in 1:length(x)){ muMatrix[i,i]=mu(x[i]) }
  sigmaMatrix = matrix(0L, nrow=length(x), ncol=length(x))
  for(i in 1:length(x)){ sigmaMatrix[i,i]=sigma(x[i])^2/2 }
  fMatrix = matrix(0L, nrow=length(x), ncol=length(x))
  for(i in 1:length(x)){ fMatrix[i,i]=theta*f(x[i]) }
  lambdaMatrix = matrix(0L, nrow=length(x), ncol=length(x))
  for(i in 1:length(x)){ lambdaMatrix[i,i]=lambda(x[i]) }
  u = matrix(0L, nrow=length(x), ncol=length(x))
  u[1,2]=-4/(2*r1*theta-3)
  u[1,3]=1/(2*r1*theta-3)
  u[length(x),(length(x)-1)]=-4/(2*r2*theta-3)
  u[length(x),(length(x)-2)]=1/(2*r2*theta-3)
  for(i in 2:(length(x)-1)){
    u[i,i]=1
  }
```

```
  ux = matrix(0L, nrow=length(x), ncol=length(x))
  ux[1,2]=2/h+6/(h*(-3+2*h*r1*theta))
  ux[1,3]=-1/(2*h)-3/(2*h*(-3+2*h*r1*theta))
  ux[2,2]=2/(h*(-3+2*h*r1*theta))
  ux[2,3]=1/(2*h)-1/(2*h*(-3+2*h*r1*theta))
  ux[length(x)-1,length(x)-1]=-2/(h*(-3+2*h*r2*theta))
  ux[length(x)-1,length(x)-2]=-1/(2*h)+1/(2*h*(-3+2*h*r2*theta))
  ux[length(x),(length(x)-1)]=-2/h-6/(h*(-3+2*h*r2*theta))
  ux[length(x),(length(x)-2)]=1/(2*h)+3/(2*h*(-3+2*h*r2*theta))
  for(i in 3:(length(x)-2)){
    ux[i,i-1]=-1/(2*h)
    ux[i,i+1]=1/(2*h)
  }
  uxx = matrix(0L, nrow=length(x), ncol=length(x))
  uxx[1,2]=-5/h^2-8/(h^2*(-3+2*h*r1*theta))
  uxx[1,3]=4/h^2+2/(h^2*(-3+2*h*r1*theta))
  uxx[1,4]=-1/h^2
  uxx[2,2]=-2/h^2-4/(h^2*(-3+2*h*r1*theta))
  uxx[2,3]=1/h^2+1/(h^2*(-3+2*h*r1*theta))
  uxx[length(x)-1,length(x)-1]=-2/h^2-4/(h^2*(-3+2*h*r2*theta))
  uxx[length(x)-1,length(x)-2]=1/h^2+1/(h^2*(-3+2*h*r2*theta))
  uxx[length(x),(length(x)-1)]=-5/h^2-8/(h^2*(-3+2*h*r2*theta))
  uxx[length(x),(length(x)-2)]=4/h^2+2/(h^2*(-3+2*h*r2*theta))
  uxx[length(x),(length(x)-3)]=-1/h^2
  for(i in 3:(length(x)-2)){
    uxx[i,i-1]=1/h^2
    uxx[i,i]=-2/h^2
    uxx[i,i+1]=1/h^2
  }
  B = matrix(0L, nrow=length(x), ncol=length(x))
  for(i in 1:length(x)){
    tempB = matrix(0L, nrow=k, ncol=length(x))
    for(j in 1:k){
      y=rho(x[i])
      if(x[i]+y<0){
        tempB[j,2]=tempB[j,2]-4*exp(theta*f_tilde(x[i],y))/(-3+2*h*r1*theta)
```

```
71            tempB[j,3]=tempB[j,3]+exp(theta*f_tilde(x[i],y))/(-3+2*h*r1*theta)
72          }else if(x[i]+y>b){
73            tempB[j,(length(x)-1)]=tempB[j,(length(x)-1)]-4*exp(theta*f_tilde(x[i
                ],y))/(-3+2*h*r2*theta)
74            tempB[j,(length(x)-2)]=tempB[j,(length(x)-2)]+exp(theta*f_tilde(x[i],y
                ))/(-3+2*h*r2*theta)
75          }else{
76            if(y==0){
77              if(i==1){
78                tempB[j,2]=tempB[j,2]-4*exp(theta*f_tilde(x[i],y))/(-3+2*h*r1*
                    theta)
79                tempB[j,3]=tempB[j,3]+exp(theta*f_tilde(x[i],y))/(-3+2*h*r1*theta)
80              }else if(i == length(x)){
81                tempB[j,(length(x)-1)]=tempB[j,(length(x)-1)]-4*exp(theta*f_tilde(
                    x[i],y))/(-3+2*h*r2*theta)
82                tempB[j,(length(x)-2)]=tempB[j,(length(x)-2)]+exp(theta*f_tilde(x[
                    i],y))/(-3+2*h*r2*theta)
83              }else{
84                tempB[j,i]=exp(theta*f_tilde(x[i],y))
85              }
86            }else if(y<0){
87              if(ceiling((N+1)*(x[i]+y)/b)==1){
88                tempB[j,2]=tempB[j,2]-4*exp(theta*f_tilde(x[i],y))/(-3+2*h*r1*
                    theta)
89                tempB[j,3]=tempB[j,3]+exp(theta*f_tilde(x[i],y))/(-3+2*h*r1*theta)
90              }else{
91                tempB[j,ceiling((N+1)*(x[i]+y)/b)]=exp(theta*f_tilde(x[i],y))
92              }
93            }else{
94              if(floor((N+1)*(x[i]+y)/b)==length(x)){
95                tempB[j,(length(x)-1)]=tempB[j,(length(x)-1)]-4*exp(theta*f_tilde(
                    x[i],y))/(-3+2*h*r2*theta)
96                tempB[j,(length(x)-2)]=tempB[j,(length(x)-2)]+exp(theta*f_tilde(x[
                    i],y))/(-3+2*h*r2*theta)
97              }else{
98                tempB[j,floor((N+1)*(x[i]+y)/b)]=exp(theta*f_tilde(x[i],y))
```

```
99              }
100           }
101         }
102       }
103       for(l in 1:length(x)){
104         B[i,l]=mean(tempB[,l])
105       }
106     }
107     A=muMatrix%*%ux+sigmaMatrix%*%uxx+fMatrix%*%u+lambdaMatrix%*%(B-u)
108     A = A[2:(length(x)-1),2:(length(x)-1)]
109     EVec=eigen(A)$vectors
110     EVal=eigen(A)$values
111     i = length(x)-1
112     ct1=0
113     ct2=0
114     while(ct1 != (length(x)-2)&& ct2 != (length(x)-2)){
115       i=i-1
116       ct1=0
117       ct2=0
118       for(j in 1:(length(x)-2)){
119         if(Re(EVec[j,i])>0&&abs(Im(EVec[j,i]))<0.0001){
120           ct1=ct1+1
121         }
122         if(Re(EVec[j,i])<0&&abs(Im(EVec[j,i]))<0.0001){
123           ct2=ct2+1
124         }
125       }
126     }
127     psiTheta[counter] = Re(EVal[i])
128     } return(psiTheta)
129 }
```

References

[1] L. N. Andersen et al. "Lévy Processes with Two-Sided Reflection". In: *Lévy Matters V: Functionals of Lévy Processes*. Cham: Springer International Publishing, 2015, pp. 67–182. DOI: 10.1007/978-3-319-23138-9_2.

[2] J. Bertoin. *Lévy Processes*. Cambridge Tracts in Mathematics. Cambridge University Press, 1998. ISBN: 9780521646321.

[3] S. Boyd and L. Vandenberghe. *Convex Optimization*. Cambridge University Press, 2004. ISBN: 9780521833783.

[4] R.L. Burden and J.D. Faires. *Numerical Analysis*. Cengage Learning, 2010. ISBN: 9780538733519.

[5] A. Dembo and O. Zeitouni. *Large Deviations Techniques and Applications*. Applications of mathematics. Springer, 1998. ISBN: 9780387984063.

[6] R. S. Ellis. "Large Deviations for a General Class of Random Vectors". In: *Ann. Probab.* 12.1 (Feb. 1984), pp. 1–12. DOI: 10.1214/aop/1176993370.

[7] M. Forde, R. Kumar, and H. Zhang. "Large deviations for the boundary local time of doubly reflected Brownian motion". English. In: *Statistics & Probability Letters* 96 (Jan. 2015), pp. 262–268. ISSN: 0167-7152. DOI: 10.1016/j.spl.2014.09.004.

[8] J. Gärtner. "On Large Deviations from the Invariant Measure". In: *Theory of Probability & Its Applications* 22.1 (1977), pp. 24–39. DOI: 10.1137/1122003.

[9] K. Giesecke et al. "Numerical Solution of Jump-Diffusion SDEs". In: (Mar. 2018). DOI: http://dx.doi.org/10.2139/ssrn.2298701.

[10] P. Glasserman and M. Merener. "Convergence of a Discretization Scheme for Jump-Diffusion Processes with State-Dependent Intensities". In: *Proceedings: Mathematical, Physical and Engineering Sciences* 460.2041 (2004), pp. 111–127. ISSN: 13645021.

[11] P. W. Glynn and R. J. Wang. "Central Limit Theorems and Large Deviations for Additive Functionals of Reflecting Diffusion Processes". In: *ArXiv e-prints* (July 2013). arXiv: 1307.1574 [math.PR].

[12] G. Grimmett and D. Stirzaker. *Probability and Random Processes*. Probability and Random Processes. OUP Oxford, 2001. ISBN: 9780198572220.

[13] F. den Hollander. *Large Deviations*. Fields Institute monographs. American Mathematical Society, 2008. ISBN: 9780821844359.

[14] P.E. Kloeden and E. Platen. *Numerical Solution of Stochastic Differential Equations*. Stochastic Modelling and Applied Probability. Springer Berlin Heidelberg, 2011. ISBN: 9783540540625.

[15] A. E. Kyprianou. *Introductory lectures on fluctuations of Lévy processes with applications*. Universitext. Springer-Verlag Berlin Heidelberg, 2006. DOI: 10.1007/978-3-540-31343-4.

[16] P. Lévy. *Processus stochastiques et mouvement brownien*. Paris, 1965.

[17] P. L. Lions and A. S. Sznitman. "Stochastic differential equations with reflecting boundary conditions". In: *Communications on Pure and Applied Mathematics* 37.4 (), pp. 511–537. DOI: 10.1002/cpa.3160370408.

[18] B. Øksendal. *Stochastic Differential Equations: An Introduction with Applications*. Hochschultext / Universitext. Springer, 2003. ISBN: 9783540047582.

[19] B. Øksendal and A. Sulem. *Applied Stochastic Control of Jump Diffusions*. Universitext. Springer Berlin Heidelberg, 2007. ISBN: 9783540698265.

[20] P. E. Protter. *Stochastic Integration and Differential Equations*. Second. Stochastic Modelling and Applied Probability. Germany: Springer-Verlag Berlin Heidelberg, 2004. DOI: 10.1007/978-3-662-10061-5.

[21] S.M. Ross. *Simulation*. Elsevier Science, 2012. ISBN: 9780124158252.

[22] H.L. Royden and P. Fitzpatrick. *Real Analysis*. Prentice Hall, 2010. ISBN: 9780131437470.

[23] A. V. Skorokhod. "Stochastic Equations for Diffusion Processes in a Bounded Region". In: *Theory of Probability & Its Applications* 6.3 (1961), pp. 264–274. DOI: 10.1137/1106035.

[24] A. V. Skorokhod. "Stochastic Equations for Diffusion Processes in a Bounded Region. II". In: *Theory of Probability & Its Applications* 7.1 (1962), pp. 3–23. DOI: 10.1137/1107002.

[25] S. R. S. Varadhan. "Asymptotic probabilities and differential equations". In: *Communications on Pure and Applied Mathematics* 19.3 (1966), pp. 261–286. DOI: 10.1002/cpa.3160190303.

[26] L. Zhang and C. Jiang. "Stationary distribution of reflected O–U process with two-sided barriers". In: *Statistics & Probability Letters* 79.2 (2009), pp. 177–181. ISSN: 0167-7152. DOI: https://doi.org/10.1016/j.spl.2008.07.035.

[27] X. Zhang and P. W. Glynn. "On the dynamics of a finite buffer queue conditioned on the amount of loss". In: *Queueing Systems* 67.2 (Feb. 2011), pp. 91–110. ISSN: 1572-9443. DOI: 10.1007/s11134-010-9204-z.